

Chandra News

Published by the Chandra X-ray Center (CXC)

Issue number 14

Chandra and Constellation-X Home in on the Event Horizon, Black Hole Spin and the Kerr Metric: The Journey from Astrophysics to Physics

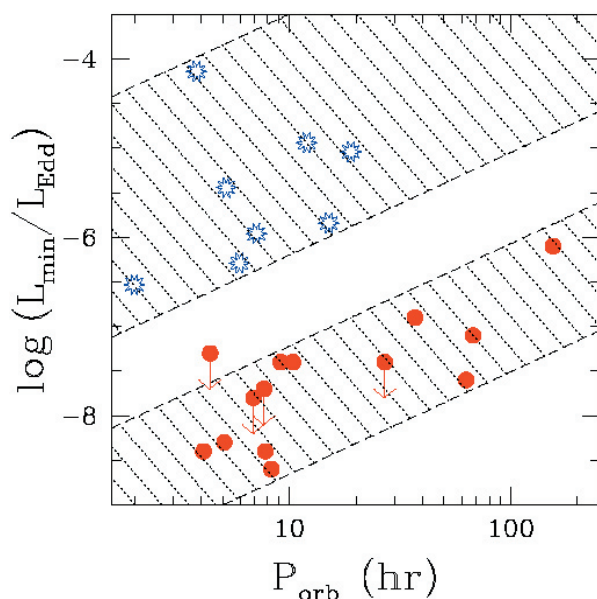


FIGURE 1: Eddington-scaled luminosities of black-hole (red circles) and neutron-star (blue stars) X-ray transients in quiescence. The diagonal hatched areas delineate the regions occupied by the two classes of sources and indicate the dependency on orbital period.

Astrophysical black holes have the potential to revolutionize classical black hole physics. After all, the only black holes we know, or may ever know, are astrophysical black holes. But how can we make this journey from astrophysics to physics? In fact, it is well underway (e.g., see §8 in Remillard & McClintock 2006), and *Chandra* is making leading contributions by (1) providing strong evidence for the existence of the event horizon — the defining property of a black hole, and by (2) measuring both the *spin* and mass of an eclipsing stellar black hole in M33. Meanwhile, *Constellation-X* promises to deliver the ultimate prize, namely, a quantitative test of the Kerr metric. One of

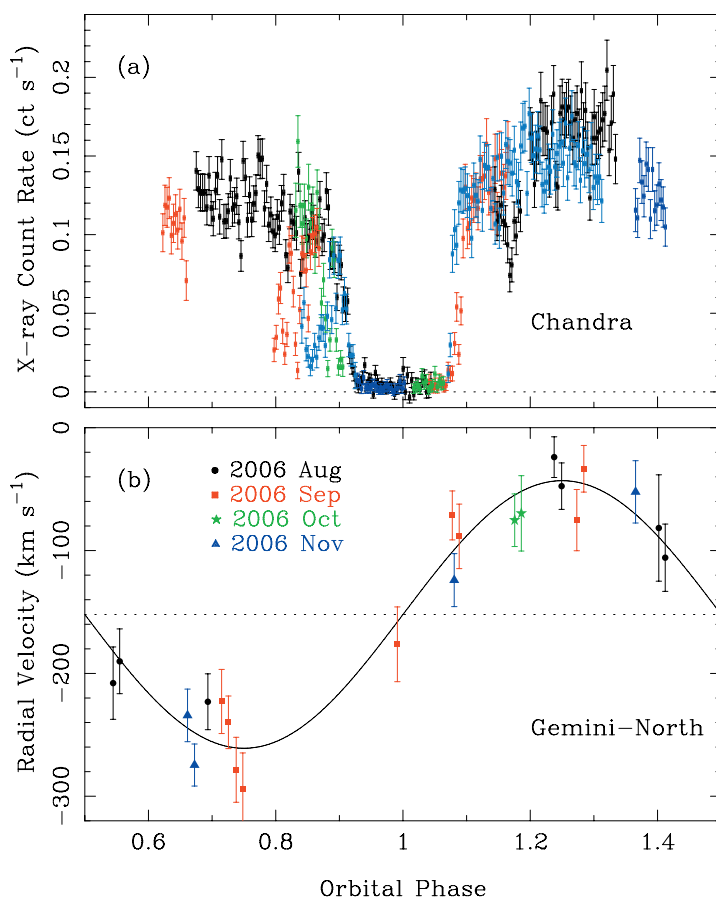


FIGURE 2: (a). ACIS X-ray eclipse light curve of the black hole binary X-7. The different colors correspond to different observation epochs. (b). Radial velocity curve of X-7's O-star companion.

the most remarkable predictions of black hole physics is that two numbers specifying mass and spin suffice to provide a complete and absolutely exact description of the space-time surrounding a stationary rotating black hole. Testing this prediction is the most important contribution that astrophysics can make to black hole physics.

CONTENTS			
<i>Chandra</i> and <i>Constellation-X</i> Home in on the Event Horizon, Black Hole Spin and the Kerr Metric	1	Useful <i>Chandra</i> Web Addresses	30
Project Scientist's Report	6	<i>Chandra</i> Data Processing	31
Project Manager's Report	6	The <i>Chandra</i> Automated Processing System	31
Instruments: ACIS	8	The <i>Chandra</i> X-ray Observatory Calibration Database	33
Instruments: HRC	11	<i>Chandra</i> Data Archive Operations	35
Instruments: HETG	13	CIAO: <i>Chandra</i> 's Data Analysis System	36
Instruments: LETG	16	Status of the <i>Chandra</i> Source Catalog Project	38
<i>Chandra</i> Important Dates 2007	19	<i>Chandra</i> Data Archive	40
<i>Chandra</i> Calibration	20	Absolute Time Calibration for the <i>Chandra</i> X-ray Observatory	41
Cross-Calibrating <i>Chandra</i> and XMM-Newton	21	The Results of the Cycle 8 Peer Review	43
CXC 2006 Press Releases	23	<i>Chandra</i> -Related Meetings Planned for the Next Year	45
<i>Chandra</i> Fellows for 2007	23	Monte-Carlo Processes ...	47
Running <i>Chandra</i>	24	<i>Chandra</i> Education and Public Outreach	48
<i>Chandra</i> Flight Operations Software Tools Improve Mission Execution	24	Constellation X-ray Mission Update	51
The <i>Chandra</i> X-Ray Observatory Mission Planning Process	25	Mission Planning under Bill Forman	52
<i>Chandra</i> , Hardware and Systems	27	HelpDesk	53
<i>Chandra</i> Monitoring and Trends Analysis	27	<i>Chandra</i> Users' Committee Membership List	53
A Historical Fluence Analysis ...	29	X-ray Grating Spectroscopy Workshop	54
Eight Years of Science with <i>Chandra</i>	30	Mz 3, BD+30°3639, Hen 3-1475 and NGC 7027	55
X-ray Astronomy School	30	CXC Contact Personnel	55
<i>Chandra</i> Calibration Workshop	30		

Black Holes are Black: *Chandra* Points to the Phantom Horizon

Presently, some 20 X-ray binary black hole candidates have well-determined masses which exceed the theoretical maximum mass of a neutron star. This is taken to be a sign that the objects are black holes. But do they really have event horizons?

The first test for the presence of the event horizon was carried out by Narayan, Garcia & McClintock (1997) using archival X-ray data. However, one had to wait for *Chandra* before one could claim definitive evidence. Figure 1 is a plot of Eddington-scaled X-ray luminosities of neutron-star and black-hole X-ray binaries in their quiescent or ultralow mass accretion rate (\dot{M}) state. The horizontal axis shows the orbital period, which according to binary mass transfer models is a predictor of \dot{M} (Menou et al. 1999). The contrast between the neutron-star and black-hole candidates is dramatic. At every orbital period, black hole candidates

have Eddington-scaled luminosities that are lower than neutron stars by two to three orders of magnitude. Even if we do not scale by the Eddington limit, the difference is still nearly two orders of magnitude.

The explanation for this result is that accretion in these quiescent systems occurs via a radiatively inefficient mode (advection-dominated accretion), as confirmed through spectral studies. Therefore, the disk luminosity $L_{\text{disk}} \ll \dot{M} c^2$ and most of the binding energy that is released as gas falls into the potential well is retained in the gas as thermal energy. In the case of an accreting neutron star, this energy is eventually radiated from the stellar surface, and so an external observer still sees the full accretion luminosity $\sim 0.2\dot{M} c^2$. In the case of a black hole, however, the superheated gas falls through the event horizon, carrying all its thermal energy with it. The observer therefore sees only the disk luminosity L_{disk} , which is extremely small. This argument was originally presented by Narayan & Yi (1995) and was the basis of their prediction that, in the pres-

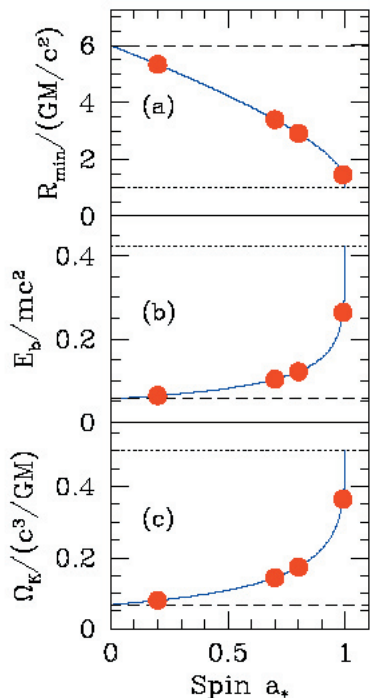


FIGURE 3: Behavior of three key dimensionless quantities (see text for definitions) that depend only on the black hole spin parameter a_* . The filled circles correspond to nominal estimates of the spins of (from left to right) LMC X-3, GRO J1655-40, 4U1543-47 and GRS1915+105 (McClintock et al. 2006). The horizontal dashed and dotted lines corresponds to $a_* = 0$ and $a_* = 1$, respectively. In panel a, $GM/c^2 = 15 \text{ km}$ for $M = 10M_\odot$.

ence of advection-dominated accretion, there should be a large luminosity difference between compact objects with surfaces and those with event horizons. Convincing confirmation of their prediction is provided by Figure 1, which is an updated version of a similar figure that appeared first in Garcia et al. (2001; see also McClintock et al. 2004). *Chandra*, which supplied most of the data shown in this figure, is by far the best telescope for this work because of its low background.

In addition to the above test, which is based on luminosity, one could also consider spectral information. There are strong theoretical reasons to expect the radiation emitted by the surface of a compact star to be thermal. Therefore, if the tiny luminosity seen in quiescent black holes is from the stellar surface, one would expect the spectrum to be thermal (as it is, for instance, in most quiescent neutron stars). Observations with *Chandra* of the quiescent black hole X-ray binary XTE J1118+480 show, however, that the radiation comes out almost entirely in a power-law component, confirming that this object does not have a surface (McClintock et al. 2004)

The Spin and Mass of the First Eclipsing Black Hole, M33 X-7

The *Chandra* Legacy observations of M33 revealed the first eclipsing black hole X-ray binary, which was dubbed X-7 (Figure 2a; Pietsch et al. 2006). At a distance of 810 kpc, X-7 lies at 100 times the distance of a typical Galactic X-ray binary. Despite this great distance, *Chandra* pinpointed the location of X-7's O-type optical counterpart, which has a probable mass of about $50M_\odot$. This massive star's large velocity amplitude, $K = 110 \pm 7 \text{ km s}^{-1}$ (Figure 2b; Orosz et al. 2007), implies an estimated black hole mass of $10\text{-}15 M_\odot$.

Once precise values of black hole mass and orbital inclination have been determined, the 1.4 Msec of *Chandra* data will be used further to estimate the spin of X-7 by fitting its X-ray continuum spectrum to a model of an accretion disk that includes all relativistic effects. Recently, the spins of four stellar black holes have been estimated in this way (McClintock et al. 2006).

As mentioned above, an astrophysical black hole

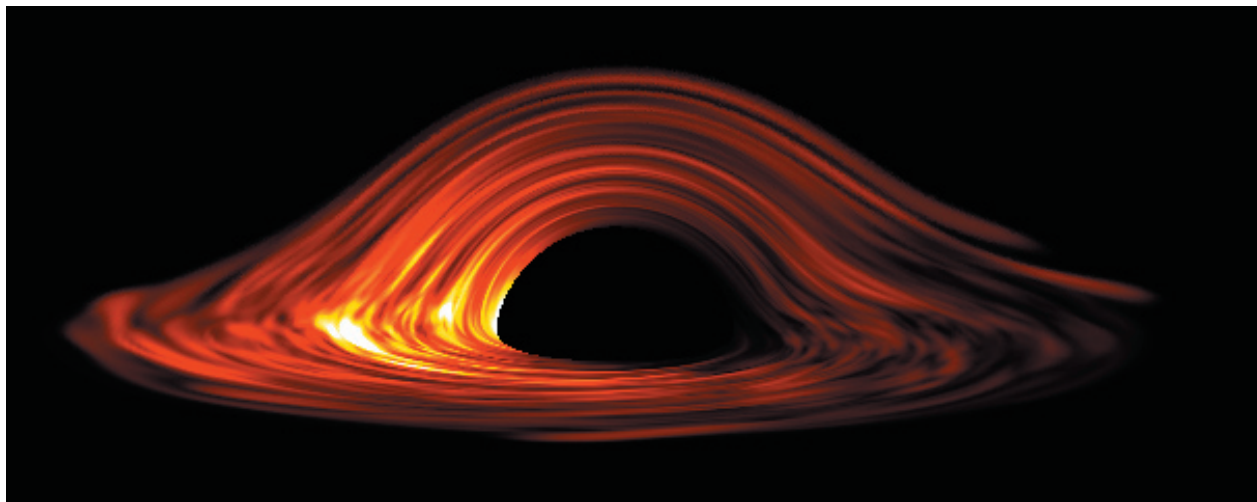


FIGURE 4: Simulated accretion disk image showing strong non-axisymmetric structure (from simulations of Armitage & Reynolds 2003).

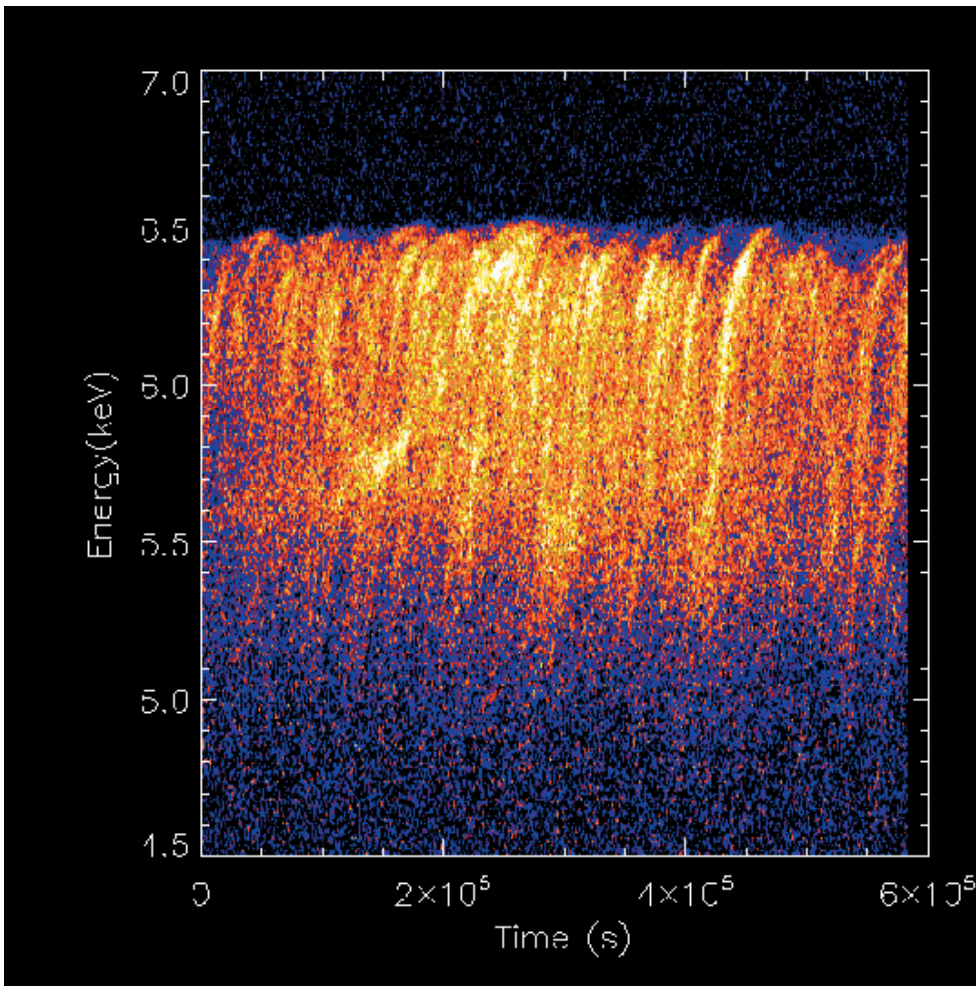


FIGURE 5: Simulated Constellation-X observation of iron line variability from the simulation shown in Fig. 4 assuming a disk inclination of 20 degrees and a black hole with mass $M=3\times 10^7 M_{\odot}$. The 2-10 keV flux is assumed to be $F=5\times 10^{-11} \text{ erg s}^{-1} \text{ cm}^{-2}$, characteristic of a bright AGN.

is completely defined by just two numbers: its mass and its dimensionless spin. The latter parameter, called a_* , is limited to the range 0 (non-spinning hole) to 1 (maximally spinning hole). A further remarkable prediction of general relativity (GR) is the existence of a smallest radius R_{\min} for a particle orbiting a black hole. As shown in Figure 3a, R_{\min} depends only on the mass and spin of the black hole, decreasing from 90 km to 15 km as the spin increases from 0 to 1 (for $M = 10 M_{\odot}$). The inner edge of the accretion disk that encircles the black hole is truncated at this innermost stable circular orbit. Thus, by fitting the disk spectrum and thereby measuring the radius of the inner edge of the disk, one can obtain an estimate of spin. Three dimensionless quantities of interest are plotted in Figure 3 versus the spin parameter a_* : (a) the radius of the innermost orbit R_{\min} , (b) the binding energy per unit mass at R_{\min} , and (c) the Keplerian frequency at R_{\min} (McClintock et al. 2006). Also shown in the figure are the nominal values of these quantities for four black holes.

The black hole mass of M33 X-7 will soon be available (Orosz et al., in preparation), and it will be precise because the X-ray eclipse duration and known distance are strong constraints, which are not available for Galactic black hole binaries. Meanwhile, a preliminary analysis of all the *Chandra* ACIS data shows that it will be possible to obtain a secure estimate of spin because the source was in the required thermal state.

It is a testimony to the power of *Chandra* and a wonder to think that we will soon know the mass and spin — i.e., a complete description in GR — of this tiny and distant black hole.

Do Black Holes Manifest the Kerr Metric? Testing the Kerr Metric with Constellation-X

General Relativity makes a clear and robust prediction: The space-time structure around an isolated black hole is described by the so-called Kerr metric. The

studies discussed above assume the validity of GR and the Kerr metric in seeking evidence for the event horizon or estimating black hole spin. Although not discussed here, spin is also being estimated via studies of the time-averaged profile of the Fe line (e.g., Brenneman & Reynolds 2006; Miller et al. 2004), which will be observed for hundreds of AGN by *Constellation-X*. The dynamical tests of the Fe line that we now discuss are entirely different and aim at providing a quantitative X-ray test of the Kerr metric itself. *Constellation-X* will achieve this goal by examining rapid variability of the broad iron line.

There are two possible origins of iron line variability that can be used to probe the metric. We expect the pattern of line emission across the disk to be highly non-axisymmetric due to non-axisymmetric reconnection/flaring events in the irradiating corona, as well as geometric corrugations and/or patchy ionization of the disk surface itself (see Figure 4). Orbital motion of the disk combined with the asymmetry in the line

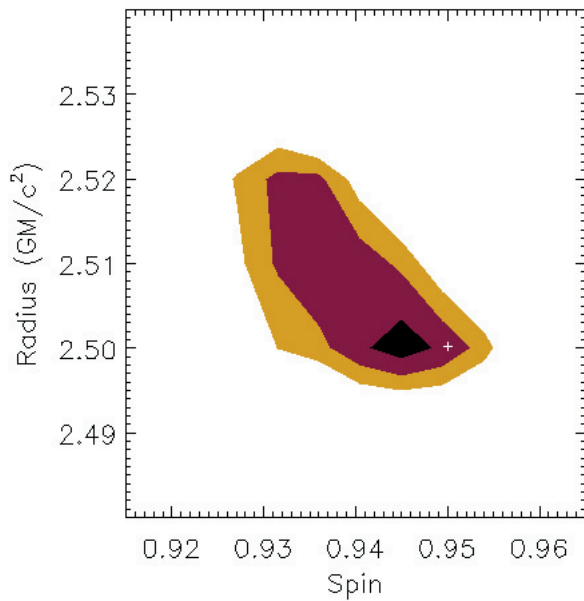


FIGURE 6: 1, 2, and 3- σ confidence contours for the constraints on spin and radius for a simulated *Constellation-X* observation of a single hot spot containing 10% of the total iron line flux.

emission pattern will induce characteristic variability of the iron line profile. Figure 5 shows a *Constellation-X* simulation of line variability due to orbiting coronal hotspots, and Figure 6 shows the confidence contours on black hole spin and hot spot radius that result from fitting the simulated energy-time track with a library of theoretical tracks. The superb constraints highlight the power of iron line variability and suggest the following experiment for quantitatively testing the Kerr metric. By fitting many observed tracks with templates that assume GR, one can determine the mass, spin and radius for each track. GR then fails if the inferred black hole spins and masses measured at different radii are not consistent.

A second kind of iron line variability accessible to *Constellation-X* is associated with the light echo of very rapid X-ray flares across the inner accretion disk. As well as the “normal” outward-going X-ray echo (which produces a progressively narrowing iron line), an inward-moving echo is created by photon propagation through the curved space-time close to the black hole. This purely relativistic branch of the echo (which eventually freezes at the event horizon) produces a characteristic redward moving bump in the iron line profile (Reynolds et al. 1999). Comparing observed reverberation signals with predictions from GR gives a powerful probe of photon dynamics close to a black hole and has the potential to falsify the Kerr metric.

References

- Armitage, P. J., & Reynolds, C. S. 2003, MNRAS, 341, 1041
- Brenneman, L. W., & Reynolds, C. S. 2006, ApJ, 652, 1028
- Garcia, M. R., McClintock, J. E., Narayan, R., Callanan, P., Barret, D., & Murray, S. S. 2001, ApJ, 553, L47
- McClintock, J. E., Narayan, R., & Rybicki, G. B. 2004, ApJ, 615, 402
- McClintock, J. E., Shafee, R., Narayan, R., Remillard, R. A., Davis, S. W., & Li, L.-X. 2006, ApJ, 652, 518
- Menou, K., Esin, A. A., Narayan, R., Garcia, M. R., Lasota, J. P., & McClintock, J. E. 1999, ApJ, 520, 276
- Miller, J. M., Fabian, A. C., Reynolds, C. S., Nowak, M. A., Homan, J., Freyberg, M.J., Ehle, M., Belloni, T., Wijnands, R., van der Klis, M., Charles, P.A., Lewin, W. H. G. 2004, ApJ, 606, L131
- Narayan, R., Garcia, M. R., & McClintock, J. E. 1997, ApJ, 478, L79
- Narayan, R., & Yi, I. 1995, ApJ, 452, 710
- Orosz, J. A., McClintock, J. E., Bailyn, C. D., Remillard, R. A., Pietsch, W., & Narayan, R. 2007, ATEL #977
- Pietsch, W., Haberl, F., Sasaki, M., Gaetz, T. J., Plucinsky, P. P., Ghavamian, P., Long, K. S., & Pannuti, T. G. 2006, ApJ, 646, 420
- Remillard, R. A., & McClintock, J. E. 2006, ARAA, 44, 49
- Reynolds, C. S., Young, A. J., Begelman, M. C., & Fabian, A. C. 1999, ApJ, 514, 164

Jeff McClintock, Ramesh Narayan,
Chris Reynolds, Michael Garcia,
Jerome Orosz, Wolfgang Pietsch
& Manuel Torres

Project Scientist's Report

Congratulations to the entire *Chandra* Team, including the hundreds of Guest Observers! We're now into the eighth year of highly productive *Chandra* operations. NASA's planning now projects *Chandra* operations through 2014. We hope and expect that this successful mission will continue beyond that projection.

Chandra Project Science continues to support activities addressing radiation damage to and molecular contamination of the ACIS instrument. Based upon current trends, neither of these is life limiting; however, each will progressively impact science performance throughout the mission. A more serious limitation on science operations and (perhaps) mission life is the continuing increase in component temperatures, due to degradation of *Chandra*'s thermal blankets. We applaud the efforts of the mission planning team in dealing with the increasingly more demanding constraints due (primarily) to thermal issues.

Within X-ray astronomy, *Chandra* has pioneered the definition and allocation of large (LP) and very large (VLP) projects, which require more observing time than typical Guest Observer (GO) projects. In this spirit, the CXC and Project Science this past year sought community response to the idea of an extremely large project (ELPs) program, which would allow projects that cannot be accomplished within the time allocated for a GO, LP, or VLP. If scientifically justified, one ELP — with 3-5 Ms total exposure — could be selected every 3 years. The proposed ELP program does not impact the GO program; it would affect the LP and VLP programs only once every 3 years. Please visit cxc.harvard.edu/proposer/elp.html for more details.

We invite you to read SPIE paper 6271:07 (2006), "The role of Project Science in the *Chandra* X-ray Observatory". This is a retrospective look at the *Chandra* X-ray Observatory — see Advanced X-ray Astrophysics Facility (AXAF) — from the perspective of Project Science. We presented this paper in the conference Modeling, Systems Engineering, and Project Management for Astronomy II, at the SPIE symposium Astronomical Telescopes 2006. The paper first briefly describes the *Chandra* X-ray Observatory, chronicles the *Chandra* Program from mission formulation to operations, and acknowledges the many contributing organizations.

Next the paper discusses the *Chandra*-AXAF project-science function — distributed amongst MSFC, SAO, and instrument-team scientists — and project-science activities, especially those performed by MSFC Project Science. The paper concludes with a summary of some factors that we believe contribute to the success of a large scientific project — teamwork amongst all elements of the project and amongst all project cultures, a distributed project-science function that encouraged both cooperation and constructive criticism, and an involvement of scientists in all aspects of the project. You may access this and other selected papers by members of *Chandra* Project Science at www.wastro.msfc.nasa.gov/research/papers.html.

In closing, we want to recognize the other present and past members of *Chandra* Project Science at MSFC — Drs. Robert A. Austin, Charles R. Bower, Roger W. Bussard, Ronald F. Elsner, Marshall K. Joy, Jeffery J. Kolodziejczak, Brian D. Ramsey, Martin E. Sulkanen, Douglas A. Swartz, Allyn F. Tennant, Alton C. Williams, & Galen X. Zirnstein, and Mr. Darell Engelhaupt.

Martin C. Weisskopf, Project Scientist
Stephen L. O'Dell, Deputy Project Scientist

CXC Project Manager's Report

Chandra passed its seven year milestone in July 2006 with continued excellent operational and scientific performance. Telescope time remained in very high demand, with significant oversubscription in the Cycle 8 peer review held in June. The observing program transitioned on schedule in December from Cycle 7 to Cycle 8 and we look forward to the Cycle 9 peer review in June. The competition for *Chandra* Fellows positions was also fierce this year, with a record 104 applicants for the 5 new awards.

The CXC mission planning staff continued to devote much effort to minimizing the effects of rising spacecraft temperatures on the scheduled efficiency. The temperature increase is due in large part to the degradation of layers of silvarized teflon multilayer insulation that provide *Chandra*'s passive thermal control.

During 2005 a number of competing thermal

constraints have resulted in an increased number of observations having to be split into multiple short duration segments. This allows the spacecraft to cool at preferred attitudes but results in a decreased observing efficiency (down ~4% in the last year) and an increase in the complexity of data reduction for observers. The efficiency improved following the relaxation of a thermal constraint associated with the EPHIN (Electron Proton Helium Instrument) radiation detector. The maximum allowed temperature limit was raised from 96°F to 110°F in December 2005 following a study that showed that the instrument can operate safely up to 120°F. The constraint change provided welcome relief to the mission planning team. Overall the average observing efficiency in the last year was 64% compared with the maximum possible of ~70%.

Operational highlights have included responding to 9 fast turn-around observing requests that required the mission planning and flight teams to reschedule and interrupt the on-board command loads. The year was a quiet one with respect to interruptions due to high levels of solar activity, with only 4 stoppages, with 3 of them in December. *Chandra* passed through the summer 2006 and winter 2007 eclipse seasons with nominal power and thermal performance, and handled lunar eclipses in August and October without incident. Perhaps most importantly, the mission continued without a major anomaly or safe mode transition this year.

A number of flight software patches were uplinked. Two patches were uplinked in July to add on-board monitoring of selected propulsion line and valve temperatures. The patches added a new monitor and replaced 21 of the Liquid Apogee Engine temperature readings (unused since the ascent phase of the mission) with 21 -Z side propulsion line and valve temperatures. *Chandra* has experienced decreased thermal margins as the mission has proceeded. The new on-board monitor mitigates the risk of a frozen propulsion line by ensuring a transition to normal sun mode in the event that temperatures fall below a safe trigger threshold.

The on-board gyro scale-factor and alignment matrix was updated in December. Following the patch uplink, a series of test maneuvers executed from the daily load showed that the performance of the pointing system matched model predictions extremely well.

As anticipated, the number of 'warm' pixels in the Aspect Camera Assembly's CCD detector has gradually increased during the mission. Ultimately, this trend will constrain our flexibility to choose guide stars

for spacecraft pointing and aspect reconstruction. To reduce the number of warm pixels, mission engineers lowered the ACA's temperature during the latter part of 2006 to -19°C, from its previous value of -15°C. The number of warm pixels decreased as expected. Because -19°C is the lowest temperature at which the ACA can be controlled, we anticipate the number of pixels to rise gradually through the remainder of the mission. However, projections indicate that the effect will not have an operational impact until well after 15 years of operations.

Both focal plane instruments have continued to operate well and have experienced no major problems. ACIS's Back End Processor rebooted as a result of the execution of the spacecraft's radiation safing software while a bias map was being computed. The event resulted in a reversion to the launch version of the ACIS flight software; the current version was uplinked without impact. ACIS has continued to show an increased warming trend (along with the overall spacecraft) and it was decided to ask observers to identify chips that could be turned off during observations. Each chip provides approximately 5°C of additional margin. The strategy has increased the mission planning team flexibility.

A test was conducted in August of the HRC +Y shutter select function. During the test, three select/deselect cycles were run and confirmed full functionality of the relay. The test verified that after two years without use, the +Y shutter has not been affected by the same failure mode as the -Y shutter.

All systems at the *Chandra* Operations Control Center continued to perform well in supporting flight operations. The ground system software content has remained relatively stable, with an upgrade to improve mission planning efficiency. A new voice communications system was installed at the OCC during the fall, while the OCC's network infrastructure was upgraded significantly in January to resolve component end-of-support issues and improve the network's design and fault tolerance. The interface with the Deep Space Network for command up-link and data down-link continued very smoothly, and the OCC team supported the transition to new DSN systems, a new Central Data Recorder at JPL, and a new DSN scheduling system.

Chandra data processing and distribution to observers continued smoothly, with the average time from observation to data delivery averaging less than 3 days. The *Chandra* archive holdings grew by 0.3 TB to

4.4 TB (compressed) and now consist of 15.5 million files.

The third full re-processing of the *Chandra* archive, which began in February, is now more than 70% complete. The re-processed data, which incorporate the most recent instrument calibrations, are being made available incrementally through the *Chandra* data archive. The reprocessing is expected to be complete in the summer. Work is progressing on the *Chandra* source catalog, with a science review held in February providing a sound overview of the requirements. An initial version of the catalog is expected to be released later this year.

The Science Data System team released software updates in support of the Cycle 8 observation proposal submission deadline (March) and Peer Review (June), and for the Cycle 9 Call for Proposals (December). Software was released in September to support the use of optional ACIS chip configurations driven by the thermal limitations mentioned above.

Sixteen *Chandra* press releases and 48 image releases were issued last year. The Education and Public Outreach team also held a NASA Media Teleconference in November that announced a new result on dark matter. The team broke new ground by starting to release *Chandra* podcasts through the CXC website. These have proven very popular by providing a convenient way to obtain *Chandra* science highlights and educational material.

We look forward to the next year of continued smooth operations and exciting science results, and to celebrating eight years of the mission at the “8 Years of Science with *Chandra*” symposium to be held 22-23 October 2007 in Huntsville, Alabama. We also anticipate concurrent observations with GLAST following its launch in November and wish our colleagues well as they work toward launch.

Roger Brissenden

Instruments: ACIS

ACIS Update for Cycles 8 and 9

[1] Selection of Optional CCDs:

Because of changes in the *Chandra* thermal environment, the ACIS Power Supply and Mechanism Controller (PSMC) has been steadily warming over the course of the mission. Under current thermal conditions and assuming an initial PSMC temperature of less than +30C, observations at pitch angles less than 60 degrees which are longer than ~50 ks and which consume maximum power within ACIS (6 CCDs clocking) are likely to approach or exceed the Yellow High thermal limit for the PSMC. Figure 7 shows a series of observations from March 2006. Two ACIS PSMC temperatures are plotted in green and blue, the pitch angle of the spacecraft labeled “SAA Angle” is plotted in red, and the Yellow High limit for these values is plotted in yellow. The plot shows several observations with *Chandra*, as indicated by the times when the pitch angle is flat and mostly constant. Notice the time when the pitch angle decreases to 46 degrees, the PSMC temperatures rise quickly once the spacecraft is in this orientation. The side A temperature comes very close to the Yellow High limit. Figure 8 displays the range of pitch angles for which there are limitations on the time the spacecraft can spend in that orientation. The range of pitch angles which are of concern for the ACIS PSMC is 45-60 degrees.

To counter this, all observers are now being asked to review their CCD selections and determine which, if any, of their CCDs can be turned off to prevent the PSMC from approaching its thermal limits. The RPS forms and OBSCAT now allow for 6 CCDs with at least one required (marked as YES) and up to 5 optional CCDs (marked as OPT1-OPT5). When the observation is being planned in a short-term schedule, the Flight mission planning team may turn off one or more of the optional CCDs starting with OPT1 and proceeding through OPT2 to OPT5, if necessary, to protect the PSMC. Please review your CCD selection and determine which CCDs are not required to achieve your science goals. Efforts will be made to avoid turning off optional CCDs unless needed to protect the PSMC.

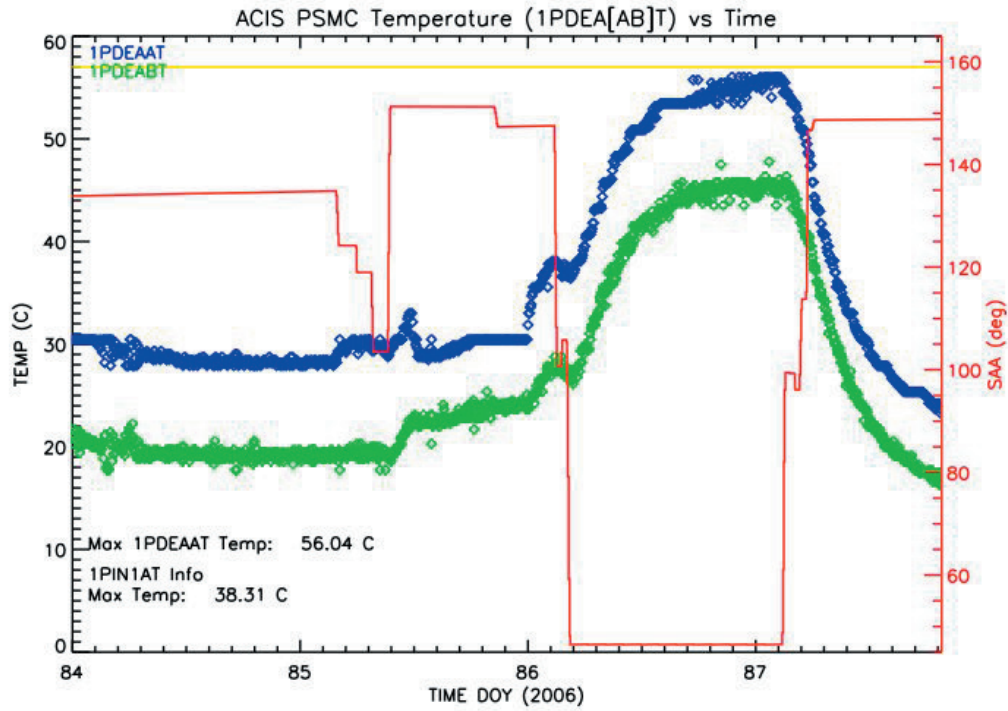


FIGURE 7: The ACIS PSMC temperatures 1PDEAAT/1PDEABT over a 4 day period from March 2006. The PSMC temperatures are indicated by the green and blue data points and the spacecraft pitch angle is indicated by the red line labeled “SAA Angle”. Note how the PSMC temperatures increase on DOY 86 when the pitch angle is ~46 degrees.

Current Temperature Dependencies vs Sun Pitch

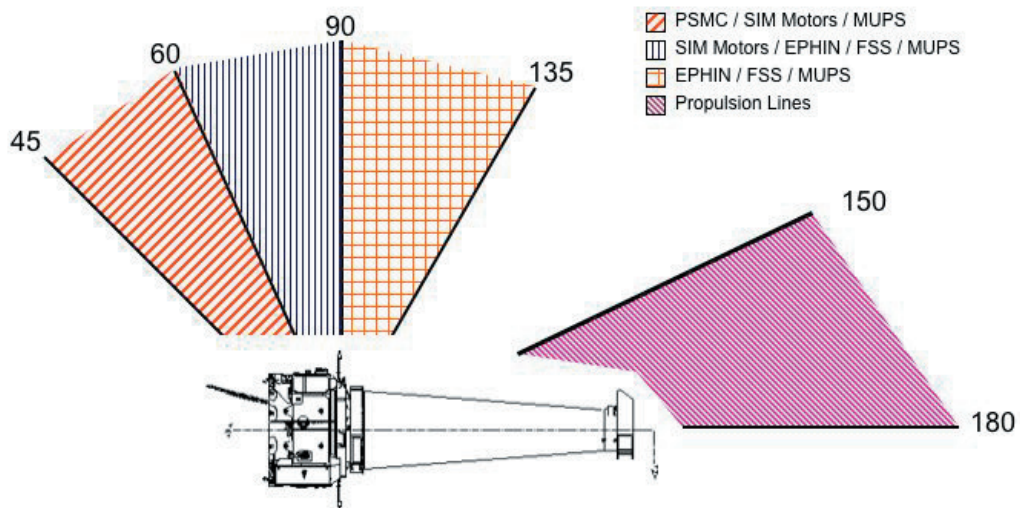


FIGURE 8: Diagram of the range of pitch angles for which the durations of observations may be limited with Chandra. The affected subsystem is indicated for each range. Pitch angles of less than 60 degrees are a concern for ACIS.

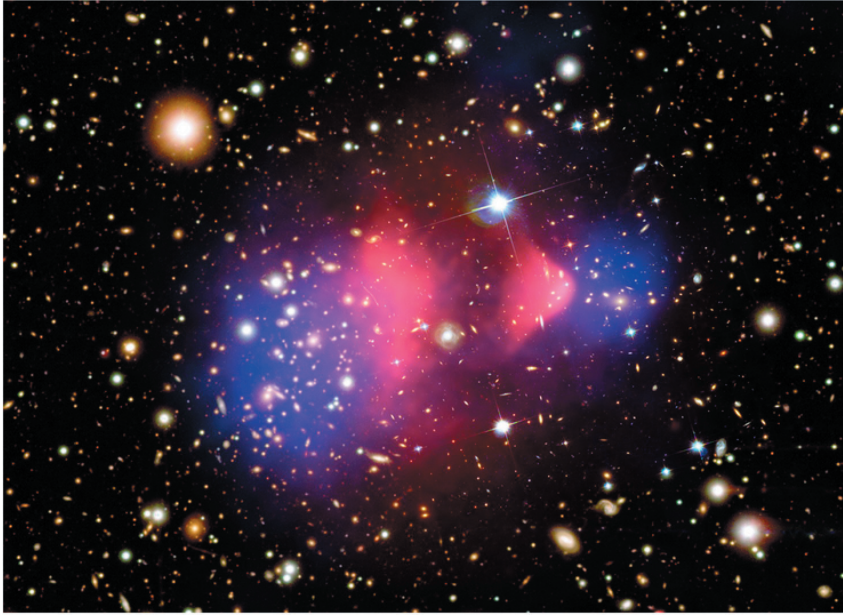


FIGURE 9: Composite image of the “bullet cluster”. See text on next page for discussion.

[2] Updated Energy to PHA Conversion

In cycle 8, a new energy to PHA conversion will be used for observations with energy filters. Two sets of conversions will be used, depending on the aimpoint of the observation. Observations with ACIS-S at the aimpoint will use a conversion tailored for the back-illuminated (BI) CCDs and those with ACIS-I at the aimpoint will use front-illuminated (FI) CCD specific conversions. The BI and FI specific conversions are more accurate for each type of CCD than the conversion used in previous AOs. The assumption is that it is desirable to have the most accurate gain conversion for the CCD on which the HRMA aimpoint falls. The

new conversion is ONLY used for creating the command loads to the instrument which define which PHA values should be included in the telemetry stream and which should be rejected. This change does NOT affect the computation of the energy of an X-ray event contained in the calibrated events files produced by the CXC.

However, in the interest of scheduling efficiency we will tend to avoid splitting observations.

If no optional CCDs are selected, six CCDs are being clocked and the observation MUST be scheduled at a pitch angle less than 60 degrees, then the observation is likely to be split into two (or more) observations.

If no optional CCDs are selected, six CCDs are being clocked and the observation is not constrained in such a way as to prohibit it, the observation is likely to be scheduled at a time for which the pitch angle is greater than 60 degrees. If the observation is assigned a time in the Long Term Schedule for which the pitch angle is smaller than 60 degrees, the observation may be rescheduled for a later date when the pitch angle is larger based on the detailed scheduling of the time slot for that observation.

While these restrictions apply to all observations, those most likely to be affected are those for which the approved observing time is larger than 25 ks and at least five required CCDs. Note that even if your observation is very short, it may occur in a sequence of observations at bad pitch angles, and it is therefore important that you consider whether any chips are optional unless your target is at an ecliptic latitude greater than 60 degrees.

For examples of common selections of optional CCDs, GOs are encouraged to consult Section 6.1.19 of the Proposers’ Guide.

The observer should be aware that for observations which mix CCD type (i.e. BI and FI CCDs on), the selected conversion (based on aimpoint as above), will apply to all selected CCDs. This will not affect the observation if the low energy threshold for the energy filter (the “Event filter: Lower” parameter) is 0.5 keV or less as the use of either conversion at these energies results in essentially no difference in the accepted events. However, above 0.5 keV, the conversions are significantly different. Observations which apply an energy filter with a low energy threshold greater than 0.5 keV will automatically be assigned spatial windows that allow the FI CCDs to use the FI conversion and the BI CCDs to use the BI conversion regardless of aimpoint.

If the reader desires more detail on this, they are encouraged to consult the following web page: http://cxc.harvard.edu/acis/memos/acis_gain/web/compare.html and to send questions to the CXC.

Paul Plucinsky

Figure 9. Three views of the merging cluster of galaxies 1E0657-56, a.k.a. the “bullet cluster.” Encoded in pink is an X-ray image from the 500 ks ACIS exposure, with a prominent “bullet” subcluster visible at right.

In X-rays, we see the hot intergalactic gas, the dominant visible matter component in galaxy clusters. It is overlaid on an optical image, which shows two concentrations of galaxies belonging to the merging subclusters.

Galaxies contribute only a small fraction to the total mass of the cluster, much less than the gas. Encoded in blue is a map of the total projected mass derived using the gravitational lensing technique (Clowe et al. 2006, ApJ, 648, L109).

The two peaks of the total mass are clearly offset from the two peaks of the visible mass (i.e., the hot gas). This shows that there is something else in the cluster, much more massive than the most massive visible mass component. That something else is dark matter.

This observation provided the first direct and unambiguous proof of its existence, ruling out a competing possibility that what we thought of as “dark matter” may in fact be a manifestation of non-Newtonian gravity on large linear scales (e.g., Milgrom 1983, ApJ, 270, 365). The separation of visible and dark matter, observed for the first time, is caused by a violent merger, which we were lucky to observe at exactly the right time.

Maxim Markevitch

Instruments: HRC

The HRC continues to operate smoothly with no major problems or anomalies. The ongoing monitoring of the HRC gain shows a small decrease as a result of extracted charge, but the need for any increase in the MCP high voltage to offset the loss of gain is several years away. In fact, the gain appears to be stabilizing and it may hold steady for many years or even decades at the present rate of charge extraction. Continued monitoring of the HRC X-ray and UV sensitivities shows no change in instrument performance. The move of the HRC laboratory from Porter Square, Cambridge, to our new facility in Cambridge Discovery Park was completed during the last year. The lab is now up and run-

ning and supports on-going HRC flight operations. In short, it has been a smooth, routine year for HRC as the flight instrument continues to function well.

A variety of science observations, both GO and GTO, have been made over the past year with the HRC-I, the HRC-S in timing mode, and the HRC-S/LETG combination. We present some science highlights from the last year, including an HRC-I observation of relativistic flow in the jets of SS433, and the HRC-S timing of the pulsar PSR J1357-6429.

An underlying relativistic flow in the jets of SS433?

In recent years, evidence has come to light for unseen, highly-relativistic flows in the Galactic neutron star X-ray binaries Scorpius X-1 (Fomalont et al., 2000) and Circinus X-1 (Fender et al., 2004). An underlying flow propagating outwards at high speed energizes the mildly-relativistic radio-emitting regions further downstream in the flow, lighting them up via shock heating. Tentative evidence for this phenomenon was also seen in simultaneous *Chandra* and VLA observations of the powerful, super-Eddington jet source SS433. ACIS images showed X-ray jets cospatial with the radio emission, which evolved on timescales of a few days at angular separations of 10^{17} cm from the center of the system (Migliari et al., 2005). The implied velocity of the underlying flow was $\geq 0.5c$. The X-ray spectra implied reheating of the jet material to high ($>10^7$ K) temperatures by thermalization of the jet kinetic energy, creating a hybrid plasma dominated by a population of thermally-emitting particles with a small ($\sim 1\%$) synchrotron-emitting high-energy tail.

A team led by Drs. S. Migliari and J. Miller-Jones, and including Drs. R. Fender, M. van der Klis, and J. Tomsick, proposed for linked *Chandra* HRC X-ray and VLA radio observations, in order to simultaneously study the thermal and non-thermal emitting populations with the high spatial resolution afforded by the HRC and the VLA. The rapid readout rate of the HRC would also prevent pile-up from the X-ray bright core from hindering the detection of any resolved jets. Four 10-ks observations were made over the course of 8 days, aiming to track the evolution of the emitting jet knots. They showed that while the well-known radio jets were present, tracing out the familiar corkscrew pattern owing to the precession of the twin beams, no extended X-ray emission was visible. The source was unresolved with the HRC (see Fig. 10 compared with an earlier

ACIS-S observation Fig. 11), suggesting that any underlying relativistic flow is not persistent, and that the non-thermal population has a longer lifetime than any thermally-emitting population. An increase in the X-ray count rate over the course of the four epochs, in line with the measured radio flux of the core, suggests that a new phase of activity and jet heating might have been beginning at this time. Analysis of these data are still ongoing.

Pulsar J1357-6429

The young and energetic pulsar PSR J1357-6429, discovered recently at radio frequencies, was the prime target during two CXO observations performed on November 18 and 19, 2005 by Drs. Lucien Kuiper and Mariano Mendez. The HRC-S in imaging mode was used as focal plane instrument to allow high-precision imaging and timing. In the combined exposure of 33 ks for the first time X-rays were detected from PSR J1357-

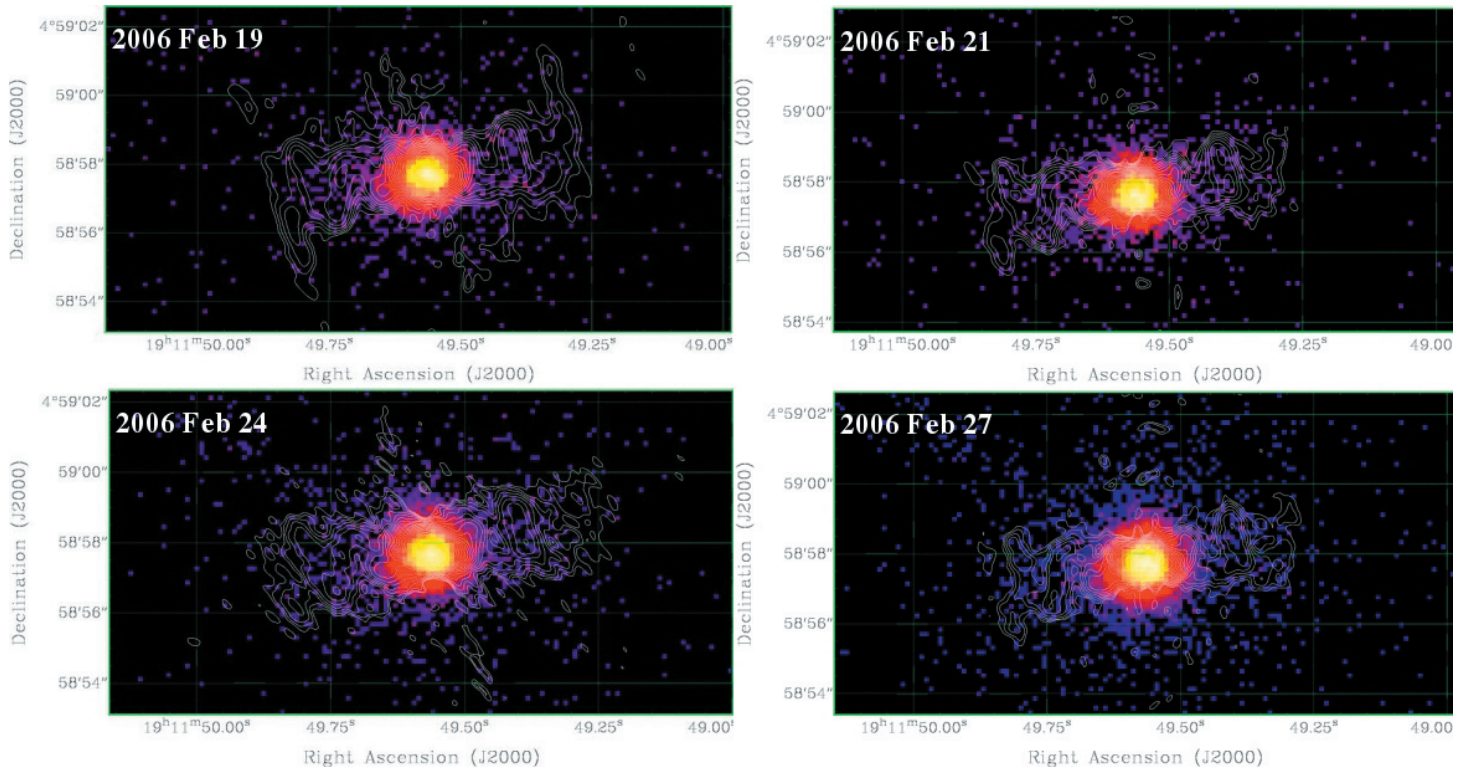


FIGURE 10: Montage of the four epochs of observation of SS433. Shown in each case is a colormap of the HRC image, with VLA radio contours superposed. There is no evidence for any extension of the X-ray emission along the radio jets.

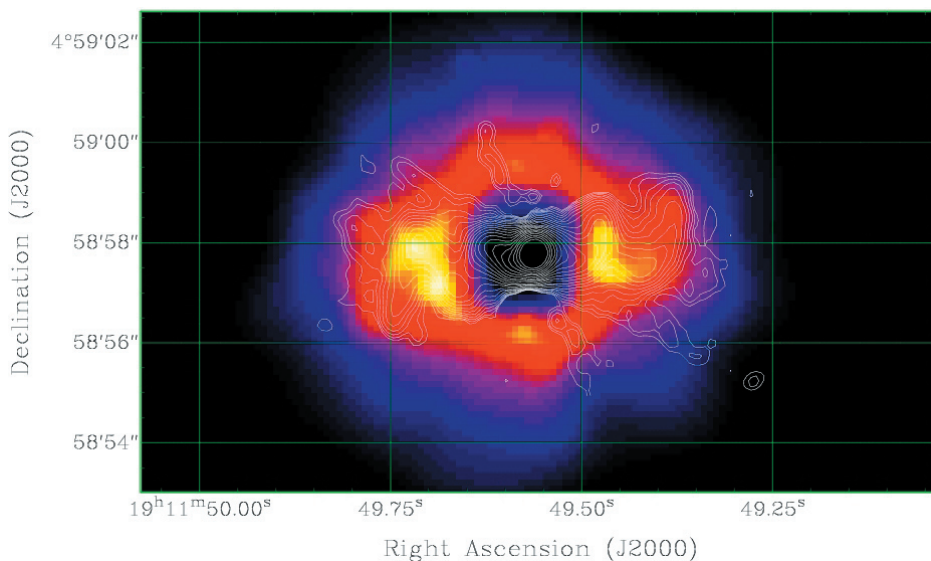


FIGURE 11: Colormap of the smoothed Chandra ACIS image of SS433 (2003 July), with simultaneous VLA radio contours superposed. There is clear evidence for extension of the X-ray source cospatial with the radio jets. Note the change in scale between this image and the HRC images, due to the larger PSF of the ACIS instrument.

6429. The spatial distribution of the events (~ 170 counts) clearly showed evidence for the presence of extended emission (see Figure 12), very likely an underlying Pulsar Wind Nebula, along with the point-source emission from the rapidly spinning ($P=166$ ms) neutron star. Accurate spin parameters from contemporaneous radio observations made the detection of the pulsed signal (pulsed fraction $40 \pm 12\%$) at X-ray energies possible (see Figure 13). This CXO observation demonstrates that with relatively small exposures crucial information on the X-ray characteristics can be derived for weak/dim, but energetic radio pulsars.

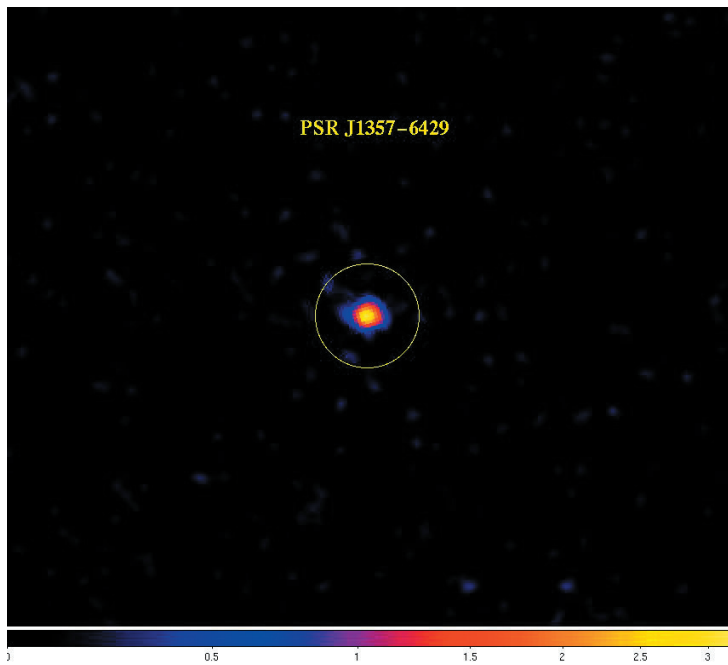


FIGURE 12: HRC-S image of PSR J1357-6429.

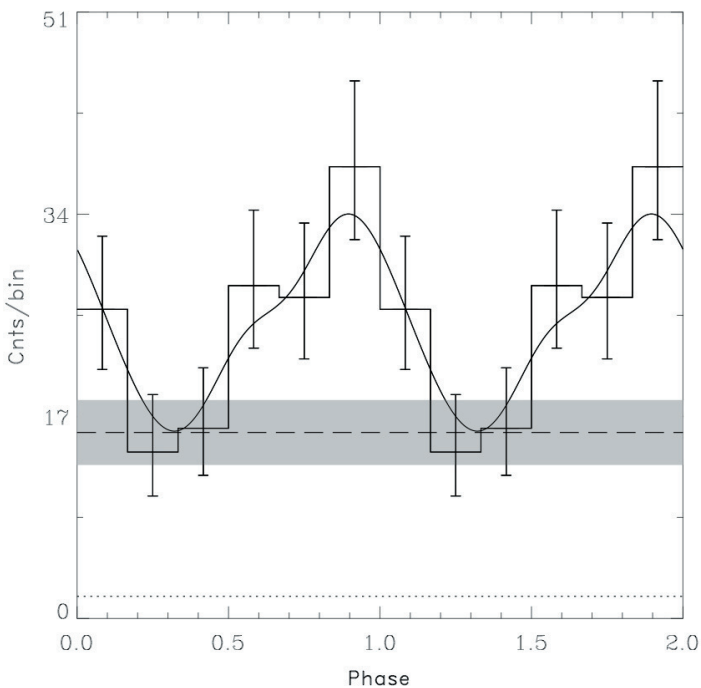


FIGURE 13: X-ray light curve of PSR J1357-6429. The period (166 ms) was determined from radio observations.

Ralph Kraft and Almus Kenter

Instruments: HETG

HETG Status and Calibration

The HRMA, HETG, and ACIS continue to perform superbly together since their memorable debut at the X-Ray Calibration Facility in Huntsville AL on 18 April 1997. There have been no new HETG-specific calibration changes in the past year. However small changes to the ACIS calibration which will show up in HETGS ARFs are present in the CALDB release 3.3.0, e.g., the frontside cosmic ray effect of order 2-to-4% and an improved Si-edge calibration. Attention is turning to cross-calibration of the *Chandra* instruments with other X-ray missions and instruments as described in the article by Herman Marshall in this issue.

High-Resolution Spectroscopy Workshop

A spectrum by any other wavelength would be as "Sweet!"

The *Chandra* X-ray Center is hosting a workshop 11-13 July 2007 entitled "X-Ray Grating Spectroscopy" [1]; one of the sub-themes is spectroscopic studies in conjunction with other wavebands. Across all wavebands high-resolution spectroscopy is sensitive to the geometry and kinematics of the source through Doppler and absorption effects. Likewise, the plasma state can be probed through line strengths and ratios from a variety of ions. For example, FUSE can measure O VI while current X-ray spectrometers include lines of O VII and O VIII ions. X-ray measurements of high-ionization states of Si in the SNR Cas A [2] can be compared with low-ionization Si seen with the Spitzer IRS [3] to study both shocked and "unshocked" SN material. As a final example, SN 1987A has been studied with HST-STIS [4], the *Chandra* HETG [5] and LETG [6], and with ground-based spectrometers that provide very high resolution ($E/dE \sim 5 \times 10^4$) over a full 2D field, e.g., the ESO/VLT-UVES [7,8]. Note that although optical wavelengths are involved, ionization states as high as Fe XIV can be measured and have relevance to the X-ray measurements, Figure 14. (This year further HETG and LETG observations of SN 1987A are planned.)

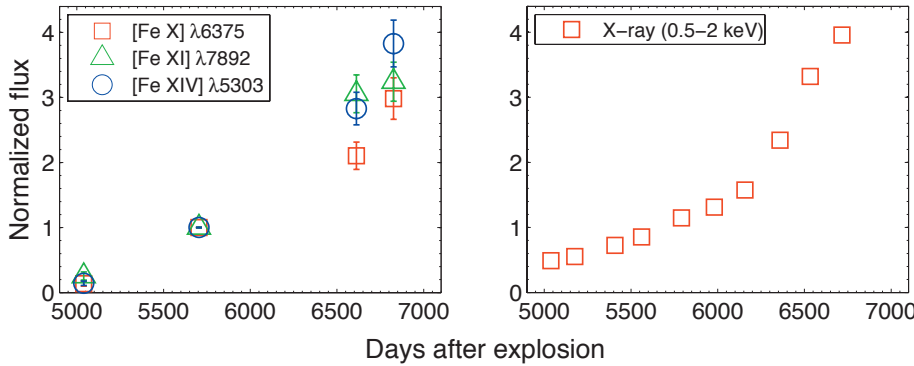


FIGURE 14: Ground-based measurements of “coronal” lines from SN 1987A. The growth over time of the optical Fe XIV flux (left, circles) shows a trend similar to that of the low-energy X-ray flux (right) which includes emission from Fe XVII lines (as shown in Kjaer et al. [7], from the detailed work by Gröningsson et al. [8].)

Not surprisingly, there is also a commonality across wavebands in the analysis and modeling challenges and techniques for high-resolution observations. These generally include 3D geometry and photon propagation modeling. The HETG group is involved in this domain through the Hydra project; for a sampling of the range of activity in this growing area see the list of related work by others on the Hydra web pages [9].

HETG Science: The Joy of Phase

We don’t usually get to view an astronomical source from other than a single direction but some systems, such as binaries, rotate on human timescales. Observing these systems at different orientations, orbital phases, helps us in getting a full 3D picture of the system. The following text and figures give a brief hint of some recent work which demonstrates the potential of multi-phase observations when combined with high-resolution spectroscopy.

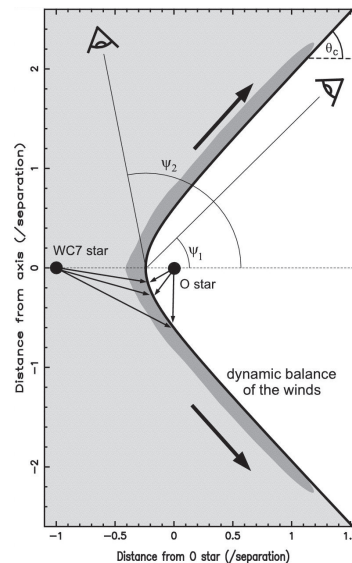
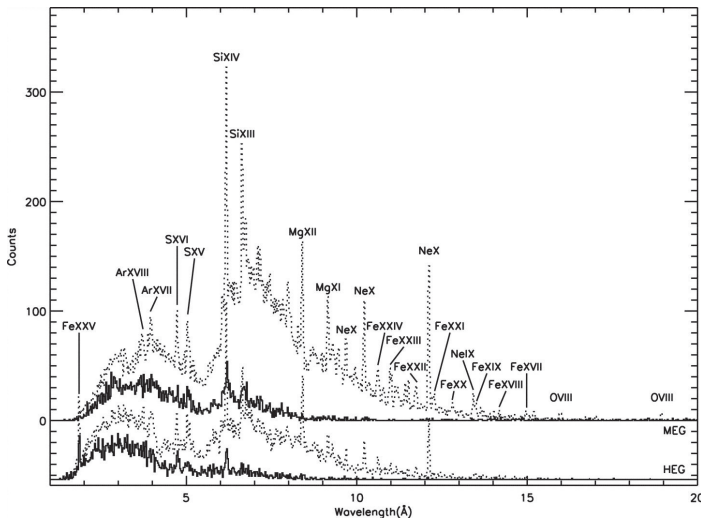


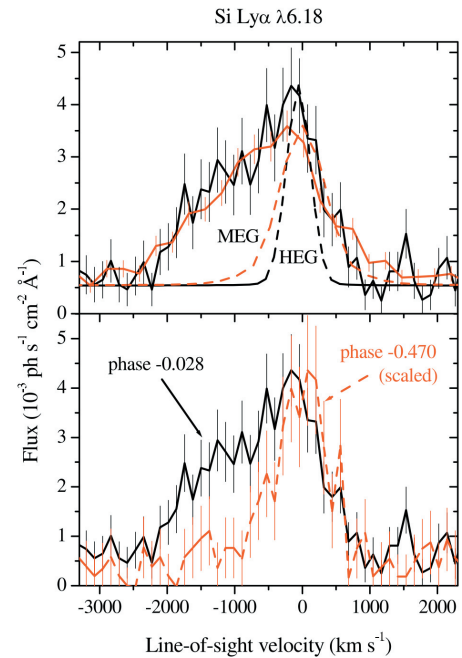
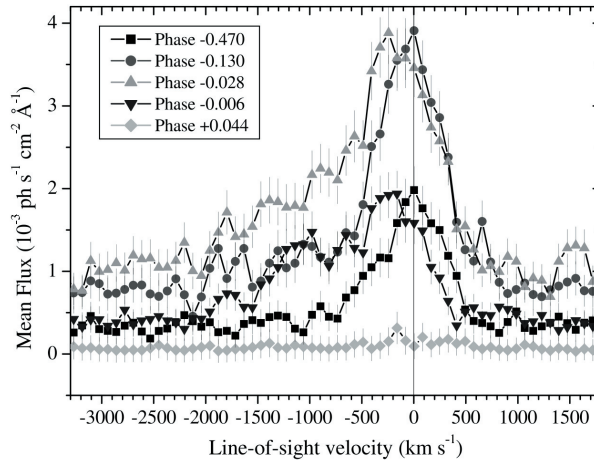
Figure 15: Emission from the colliding winds in WR 140. At left, HEG and MEG spectra are shown before (dotted) and after (solid) periastron. The change in viewing direction between these observations is indicated in the diagram at right. (From Pollock et al. [10].)

The massive stars in the system WR 140 are in a 7.94 year eccentric binary orbit and their stellar winds are in continuous collision. Work by Pollock et al. [10] shows clear changes in the amount of absorption with orbital phase, Figure 15. In addition, changes in the line profile of the Si XIV lines agree with the relative direction of the moving wind material at the different phases. Although the wind shock is ongoing and stationary, the shocked material is not in ionization equilibrium (instead, well fit with a vps shock model) and possibly includes nonthermal particle acceleration — basic physics similar to shocks in supernova remnants.

Eta Car consists of a 120 solar mass primary that is in “a phase of immense mass ejection” and in orbit with a companion in a 5.54 year binary period. Behar et al. [11] have taken a high-resolution look at archival HETG data on Eta Car, concentrating on the evolution of Si and S line shape versus phase near periastron (the binary components’ closest approach), Figure 16. At this phase they see enhanced high-velocity gas which they intriguingly suggest may be a “hot jet, or collimated fast wind”. Stay tuned for more data from the next periastron in January of 2009.

The Vela X-1 system consists of a neutron star (pulsar) orbiting a massive B supergiant companion with a period of 8.964 days. The companion’s wind is accreted onto the neutron star giving a bright X-ray emission which illuminates and photoionizes the stellar wind. The recent work by Watanabe et al. [12] com-

FIGURE 16: (left) Mean line profiles from the Eta Car system as seen with HETG observations. An outflow with velocities up to -2000 km/s dominates the line profile as the system approaches periastron (point-up triangles.) (From Behar et al. [11].) (right) Line profiles of the Eta Car system as seen with HETG observations. In the upper panel, the Si



XIV line profile at phase -0.028 is well resolved by - and consistent between - the HEG and MEG spectra. In the lower panel, comparison of the line profile at different phases shows that velocities up to -2000-km/s appear in the line profile (phase -0.028) as the system nears periastron. (From Behar et al. [11].)

bin detailed photoionization calculations with Monte-Carlo simulations of photon propagation to model the observed spectra at different orbital phases, Figure 17. Their results nicely confirm and give parameters for an ionized stellar wind and a cold cloud of material behind the neutron star. However, the model and data do not agree in the detailed line shapes, indicating that in places the wind speed is lower than expected. They show that this difference could be due to a reduced population of UV-absorbing ions in the wind caused by photoionization as the wind nears the neutron star. So, the next step is a “fully self-consistent 3D model including the X-ray photoionization”...

“Laissez les bons spectra rouler!”

Dan Dewey, for the HETG Team

References

- [1] Workshop web page: <http://cxc.harvard.edu/xgratings07>
- [2] Lazendic, J.S., et. al. 2006, ApJ 651, 250.
- [3] DeLaney, T., et al. 2007 to appear.
- [4] Pun, C.S.J., et al. 2002, ApJ 572, 906.
- [5] Michael, E. et al. 2002, ApJ 574, 166.
- [6] Zehkov, S.A., et al. 2005, ApJ 628, 127 and 2006, ApJ 645, 293.
- [7] Kjaer, K., et al. 2006, astro-ph/0612177 .
- [8] Groningsson, P., et. al. 2006, A&A 456, 581.
- [9] Hydra-related papers: <http://space.mit.edu/hydra/related.html>
- [10] Pollock, A.M.T., et al. 2005, ApJ 629, 482.
- [11] Behar, E., et al. 2006, astro-ph/0606251 .
- [12] Watanabe, S., et al. 2006 ApJ 651, 421.

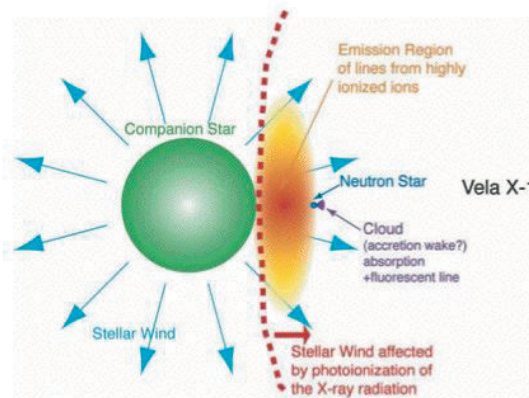
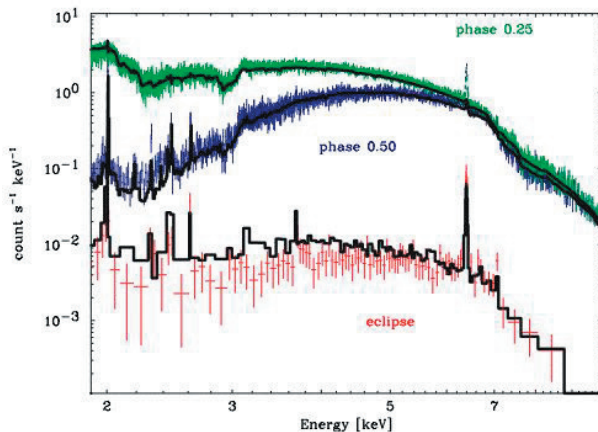


FIGURE 17: HETG observations of Vela X-1. At left HEG spectra at three phases are compared with simulated spectra from a detailed model of the photoionized stellar wind; this initial model does well, except at the Fe-K line in phases 0.25 and 0.5. This extra Fe-K emission is accounted for in the system (diagram at right) by reflection from the companion’s surface and photoionized emission from a small, cold cloud behind the neutron star, possibly an “accretion wake” (from Watanabe et al. [12]).

Instruments: LETGS

LETGS: Chandra's Stellar Evolution Spectrometer

The phrase “X-ray astronomy” generally conjures a picture featuring the more exotic aspects of the cosmos—black holes and neutron stars, accretion, relativistic jets, γ -ray bursts, supernovae and their remnants, all with a generous sprinkling of spicy multi-million degree plasmas that represent some of the extremes of behavior of galaxies and normal stars. It might then come as a bit of a surprise that *Chandra* is also making some significant contributions to a field as mature and firmly entrenched in the visible (and near infrared) as the evolution of stars of modest mass.

The first direct evidence that nuclear reactions actually occur in stellar interiors was the detection of the transition metal technetium in R Andromedae and other red giant variables by Merrill (1952). Of the three long-lived isotopes of Tc, only ^{99}Tc with a half-life of 200,000 yrs is expected to be produced in stable stars. The presence of Tc in stars thousands of times older than its half-life signals very recent production through s-process nucleosynthesis. The intervening 50 years or so has seen the development and refinement of the theories of stellar nucleosynthesis and evolution, and their confirmation in some detail by, for example, the direct observation of dredged-up products of nuclear burning at the surfaces of evolved stars. The weapon of choice brought to bear on this problem with such success in the 1970's and 1980's was high resolution spectroscopy in the visible (where here “high” means $\lambda/\Delta\lambda \gtrsim 50,000$) using efficient silicon detectors to record absorption lines of atomic and molecular forms of C, N and O.

In stellar evolution terms, the breakthrough of high resolution X-ray spectroscopy lies in the C and N (and to some extent O) lines that are found in the *Chandra* LETGS bandpass. The strongest are the n = 2-1 resonance transitions in H-like and He-like ions (C V $\lambda 40.27$, C VI $\lambda 33.74$, N VI $\lambda 28.79$ and N VII $\lambda 24.78$). It might at first sound absurd to a stellar spectroscopist working in visible light (I do, and it does) but the X-ray lines can offer a more accurate path to C and N abundances (particularly the C/N ratio) than high-quality ground-based spectra of photospheric features. Nitro-

gen abundances are quite tricky in the optical: atomic N features are few and weak, and the N abundance is often derived from CN lines and carries with it the additional uncertainty of the derived C abundance. Instead, the He-like and H-like X-ray lines are prominent, isolated, and theoretically well-understood. Moreover, in a coronal plasma the lines are optically-thin; radiative transfer complications that characterise the inhomogeneous, turbulent stellar photosphere problem are not an issue.

The C and N lines in some evolved and unevolved stars were examined by Schmitt & Ness (2002); the estimated C/N ratios are in qualitative agreement with the large body of earlier ground-based work and with stellar evolutionary models. At the time I was also looking at the C and N lines in a couple of objects difficult to observe from the ground: the late-type secondary of Algol, whose visible light is swamped by Algol A, and the K dwarf in the pre-cataclysmic system V471 Tau. The C/N ratios provided insights into the mass-transfer histories of these objects. Benevolently generous on-lookers in the field might consider these sorts of study a reasonable start. My own benchmark of the highest esteem for a piece of work is “wow, wish I had done that”. I thought exactly that when I first saw the results of the LETG observation of the planetary nebula BD +30°3639 at the 2006 October HEAD meeting. This in my opinion lifts the field to the next level.

The First High Resolution X-ray Spectrum of a Planetary Nebula: Probing the Gore of an AGB Star

In 2000, a team lead by Joel Kastner (Rochester Institute of Technology) found the first definitive evidence of extended X-ray emission from a planetary nebula in an ACIS-S observation of BD +30°3639. Planetary nebulae (PNe) are formed in the death throes of stars with mass $\sim 1-8M_{\odot}$ that have reached the end of their asymptotic giant branch evolutionary phase. The star ejects its envelope in a series of thermal pulses (see image on the back cover), and the hot, newly-exposed core bathes it in UV radiation to form an ionized nebula. The hot central stars of PNe are known from the Einstein and ROSAT era as very soft, thermal X-ray sources. However, their low-energy ionizing radiation field is thought to be supplemented by a much more vigorous wind that slams into the ejected envelope at up to $\sim 1000 \text{ km s}^{-1}$ – fast enough to produce an X-ray

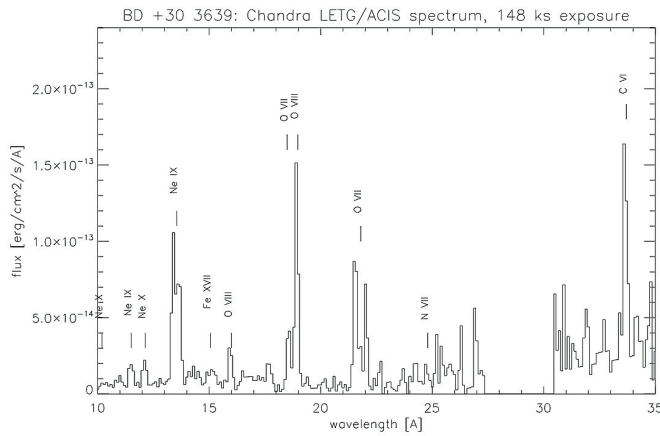


FIGURE 18: The first high resolution X-ray spectrum of a planetary nebula. BD+30 3639 was observed by LETG+ACIS-S in February and March of 2006. Note the relatively strong lines of C and the very weak Fe XVII resonance line at 15Å that are signatures of shell helium burning and the s-process on the AGB (from Kastner et al. 2006).

emitting shock and the extended emission first seen by Kastner’s group using ACIS.

The ACIS spectrum hinted at enrichment of the hot gas with nuclear burning products. Despite the object lying at perennially bad pitch for *Chandra*, Kastner and collaborators obtained the first grating spectrum of the PN in February and March of 2006. The LETG revealed clear signatures of modified abundances: C/O about 20 times the solar value with N/O less than solar, implying a C/N enhancement by a factor > 20 ; Ne/O ~ 4 times solar, but Fe/O only 1/10th solar—see the spectrum in Figure 18. The X-ray emission emanates from a layer originally deep within the stellar envelope, and the large C overabundance can be traced to the He-burning shell of the progenitor AGB star. Kastner and colleagues attribute the Ne enhancement to α -capture reactions on the nitrogen chain $^{14}\text{N}(\alpha, \gamma)^{18}\text{F}(\beta^+)^{18}\text{O}(\alpha, \gamma)^{22}\text{Ne}$, with $^{22}\text{Ne}(\alpha, n)^{25}\text{Mg}$ supplying neutrons for the s-process, probably along with $^{13}\text{C}(\alpha, n)^{16}\text{O}$; Fe seed nuclei are then depleted by neutron capture to form heavier elements such as the smoking gun, Tc, first found by Merrill.

The observed plasma temperature and spatial characteristics can also be combined with pre-PN AGB models to begin to understand better the specifics of the envelope ejection itself. It is already clear that the X-ray temperature of $2.5 \times 10^6 \text{K}$ is too cool based on the currently observed wind speed of $\sim 700 \text{km s}^{-1}$, possibly hinting at a slower wind in the recent past.

All in all, not bad for a star all dredged-up with nowhere to go.

RS Ophiuchus Explodes: The Brightest Supersoft X-ray Source

It takes about a thousand years to form a planetary nebula, and envelopes are ejected at very modest speeds of tens of km s^{-1} . If you want to watch things move a bit faster, nova explosions offer the “Stellar Evolution While You Wait” experience.

The symbiotic recurrent nova RS Ophiuchi (HD 162214) was found to be visible to the unaided eye on 2006 February 12 by Japanese amateur astronomers (Narumi et al 2006). It has previously undergone five known outbursts, in 1898, 1933, 1958, 1967, and 1985. RS Oph is the eponymous member of its subclass of binaries thought to comprise a white dwarf accreting from the wind of a red giant companion that does not fill its Roche lobe. About every 20 years, enough material from the red giant builds up on the surface of the white dwarf to produce a thermonuclear runaway. In less than a day, the otherwise quite dim white dwarf brightens to more than $100,000 L_{\odot}$.

This outburst was followed at different phases by several space-based facilities, including RXTE, Swift, HST, Spitzer, XMM-Newton and *Chandra*. Under the guidance of Julian Osborne (Leicester University) Swift has followed the X-ray evolution of the object from day 3.2 onwards; the lightcurve is shown in Figure 19. The X-ray flux declined steadily from day 4 onwards until day 29, when it was seen to rise strongly whilst undergoing wild variations. This was followed by a period of relative stability and then a slow decline.

The initial bright X-ray emission from RS Oph in the first few days of the outburst is thought to be caused by shock-heating of the ambient plasma of the extended wind of the red giant by the blast wave from the thermonuclear explosion. RS Oph presents one of the best examples of a momentum-conserving shock in an astrophysical source that evolves in a human lifetime. “In terms of stellar evolution,” as Mike Bode (Liverpool John Moores University) put it, “our current observations are enabling us to explore an analogue to a supernova remnant, but evolving over months, rather than millennia”.

RS Oph was first observed by the *Chandra* HETG at the end of the 13th day as a Directors Discretionary Time target of opportunity lead by Sumner Starrfield (Arizona State University). At that time, the bulk plasma velocities of the expanding blast wave were of order

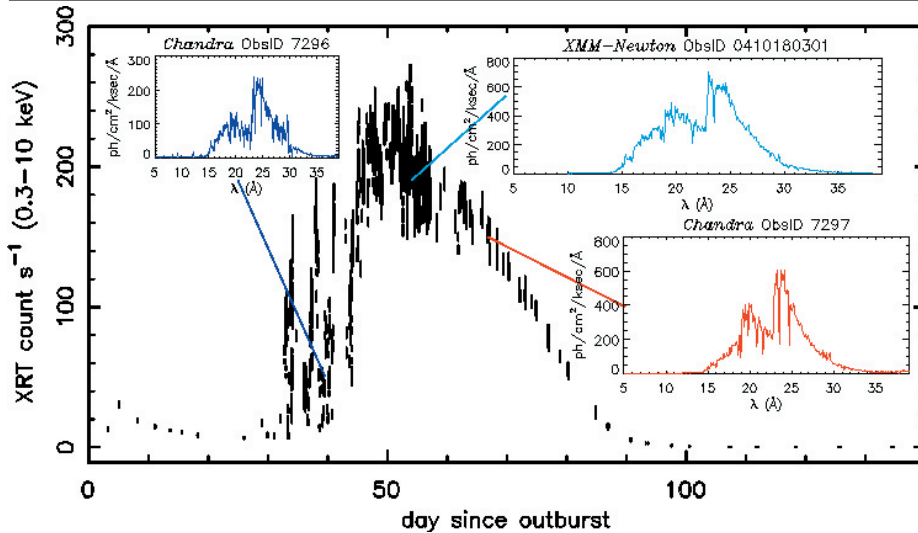


FIGURE 19: The impressive Swift XRT light curve of RS Oph from Osborne et al. (2006), with insets showing the times at which the LETGS and XMM-Newton RGS obtained high resolution spectra (Ness et al. 2007).

1700 km s⁻¹. The sharp rise in X-ray flux on day 29 ushered in the brightest Supersoft Source (SSS) phase that has ever been observed (Osborne et al. 2007): by then the envelope had thinned sufficiently to view the central star. The strong variability remains unexplained at present, but is possibly associated with either nuclear burning instability or absorption by patchy but thick condensations.

As shown in Figure 19, subsequent to the initial HETG observation of the blast wave *Chandra* LETG caught the SSS phase twice, and the first of these got a nibble of the strong variability at SSS onset. The LETG analysis, lead by *Chandra* Fellow Jan-Uwe Ness (Arizona State), shows a remarkable spectrum in which emission lines shortward of 15 Å due to H-like and He-like ions of Mg and Ne from the blast wave plasma are seen simultaneously with the hot (~680,000 K) absorbed, thermal SSS. Figure 20 illustrates spectra from the first observation during which RS Oph was entering its SSS phase while exhibiting violent variations in soft X-ray flux. Shown are spectra from relatively low and high flux states seen during the observation. The jagged coastline of the soft thermal component is not noise: close inspection shows the bumps and wiggles to correspond to absorption by abundant species, including O and N in He-like and H-like forms, and the neutral O edge and prominent 1s-2p resonance. This absorption has sculpted emission

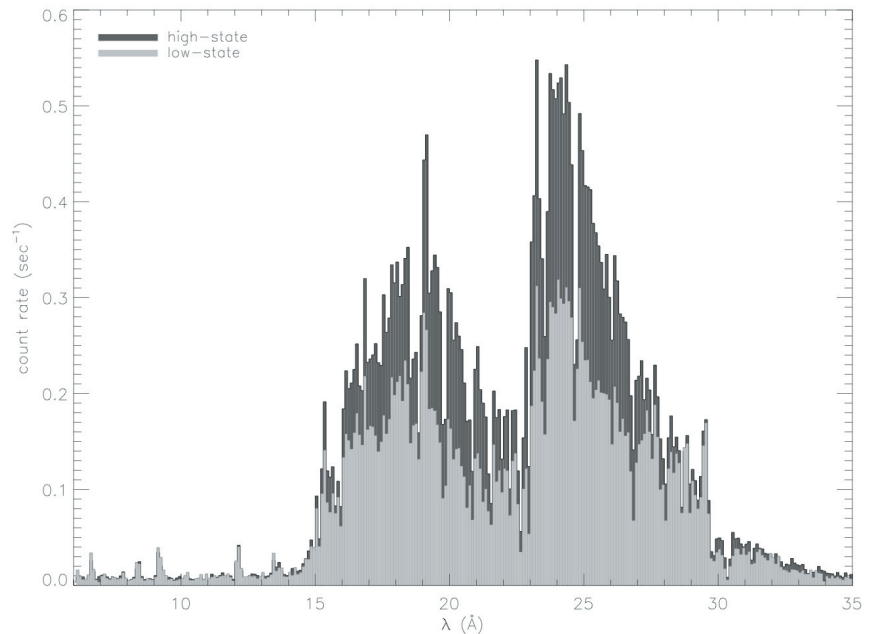


FIGURE 20: Comparison of LETGS spectra extracted from high-flux and low-flux intervals in ObsID 7296. The high and low states cannot be explained by a uniform variable absorption, and must instead be caused either by thick clumps with varying line-of-sight coverage, or by changes in the source luminosity such as through nuclear burning instability (from Ness et al. 2007).

to make a net gain of material with time, or whether its mass declines after each outburst event as a result of the explosion. The *Chandra* spectra of both the blast wave and SSS phases should in time help provide estimates of the accreted and ejected mass, and probe the site of thermonuclear runaway using the characteristics and chemical composition of the puffed-up atmosphere of the hot SSS.

LETG Programmatics

The LETG itself continues to perform flawlessly. Detectors are not so well-behaved. During the last few

lines sitting on the continuum into the P Cygni-like profiles shown in Figure 21; the absorption troughs formed in the expanding atmosphere are located ~1300 km s⁻¹ from the rest frame. In the later observation, these absorption troughs are seen to have slowed to 800 km s⁻¹.

One thorny issue with SNe Ia that currently form the basis for that minor backwater of modern astrophysics—the existence of dark energy—is that we don't really know which binary objects they come from. RS Oph is a possible SNe Ia progenitor. The key issue is whether or not it is able

years, we have noticed that the HZ43 LETG+HRC-S data show a steady drop in the QE, amounting to a ~5% decline at wavelengths longer than 50Å since launch. Superimposed on the monotonic drop are 1-2% fluctuations that are statistically significant. These effects are currently not well-understood and investigation is ongoing.

Recent activities of the instrument team also includes an updated HRC-S QE file with corrections near the O-K edge that should appear in the next CALDB release. This addresses problems that arose from the in-flight calibration using the primitive oversimplified edge structure of the ISM absorption previously avail-

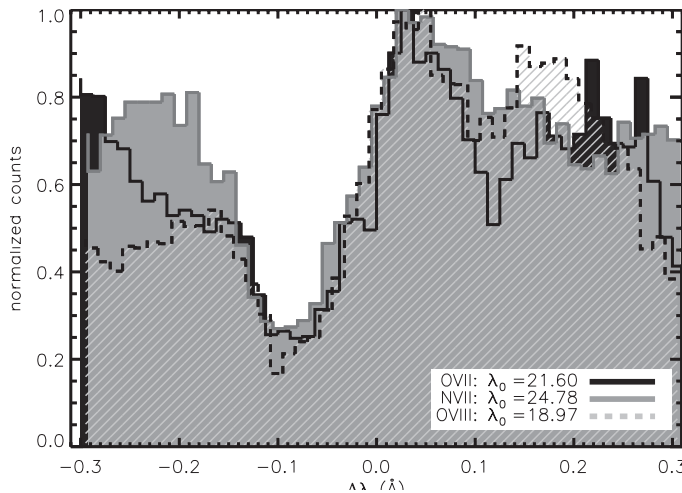


FIGURE 21: *P* Cygni profiles of *O* VII, *O* VIII and *N* VII lines seen during the SSS phase of the *RS Oph* 2006 outburst. The absorption troughs are superimposed on emission lines and are blue-shifted by 1300 km s^{-1} (from Ness et al. 2007).

able. The new QE was based on new R-Matrix computations of neutral and ionized ISM absorption structure published recently by Garcia et al (2005).

Future work will include revisions of the low-energy ($< 0.25 \text{ keV}$, $> 50\text{Å}$) HRC-S QE, a set of HRC-S gain correction files (one for each year) to account for secular gain trends observed, and further updates to the HRC-S degap correction coefficients table to improve empirical wavelength corrections from both line and continuum sources.

Bibliography

Kastner, J. H., Sam Yu, Y., Houck, J., Behar, E., Nordon, R., & Soker, N. 2006, IAU Symposium, 234, 169

Kastner, J. H., Soker, N., Vrtilik, S. D., & Dgani, R. 2000, ApJL, 545, L57

García, J., Mendoza, C., Bautista, M. A., Gorczyca, T. W., Kallman, T. R., & Palmeri, P. 2005, ApJs, 158, 68

Merrill, P., 1952, Science, 115, 484

Narumi, H., Hirosawa, K., Kanai, K., Renz, W., Pereira, A., Nakano, S., Nakamura, Y., & Pojmanski, G. 2006, IAUCirc, 8671, 2

Ness, J-U., et al, 2007, ApJ, submitted

Osborne, J., et al, 2007, Science, submitted

Schmitt, J. H. M. M., & Ness, J.-U. 2002, A&Ap, 388, L13

Jeremy Drake

Chandra Important Dates 2007	
Cycle 9 Proposals due	March 15, 2007
Users' Committee Meeting	April 25-26, 2007
Cycle 9 Peer Review	June 19-22, 2007
X-ray Grating Spectroscopy Workshop	July 11-13, 2007
Cycle 9 Budgets Due	September 13, 2007
Eight-Year Chandra Science Symposium	October 23-25, 2007
Cycle 9 EPO Electronic Deadline	October 19, 2007
Cycle 9 EPO Hardcopy Deadline	October 26, 2007
Chandra Fellows Symposium	October, 2007
Users' Committee Meeting	October, 2007
Chandra Fellowship Applications Due	November, 2007
Cycle 9 EPO Review	November, 2007
Cycle 9 Observations Start	December, 2007
Cycle 10 Call for Proposals	December, 2007

Chandra Calibration

ACIS

Most of the ACIS calibration efforts during the past year centered on developing cti-corrected (both parallel and serial) products for the BI chips S1 and S3 at a focal plane temperature of $T=-120^{\circ}\text{C}$. This was a large undertaking and required the development of new software, a restructuring of the calibration database as well as new calibration products. The cti-corrected products for the BI chips were released in CALDB 3.3 on Dec. 18, 2006 and included: new trap maps, QE uniformity maps appropriate for cti-corrected data, time-dependent gain corrections, and a matrix used to compute the spectral response at a given location on a given chip. With this version of the CALDB, all 10 chips on ACIS now have cti-corrected calibration products. The cti-uncorrected products are still required to analyze data taken in graded mode, which cannot be cti-corrected. The response of the BI chips is very uniform after applying the cti-corrections. These products were extensively tested with data from the ACIS external calibration source as well as several astronomical sources, in particular, the oxygen rich supernova remnant E0102-72. The 1σ uncertainty in the gain is 0.3% for cti-corrected data and is nearly independent of energy and location on the chips. This was actually the requirement imposed on the development of the cti-corrected products for both the BI and FI chips. Thus, all ACIS chips now have comparable gain uncertainties. The 1σ uncertainty in the FWHM of a spectral line after applying the cti-corrections is approximately 20 eV for the BI chips and is also nearly independent of energy and location on the chips.

Also released in CALDB 3.3 was a correction in the ACIS QE near the Si-K edge. Gratings data showed that there was a 4% residual over a 20eV energy band near the Si-K edge using the previous version of the ACIS QE. This residual was due to a simplifying assumption in the treatment of Si K- α escape peak in the ACIS model. The new ACIS QE applies to both BI and FI chips.

There now exists a complete, homogeneous, set of ACIS calibration products for TE data taken in faint or very faint mode at a focal plane temperature of -120°C , which comprises the bulk of ACIS observations tak-

en since launch. The primary ACIS calibration efforts at the present time are to improve CC mode calibration, graded mode calibration, and the calibration of data taken at a focal plane temperature of -110°C (data taken during the first 3 months after launch).

HRC

To further improve image reconstruction of HRC-I data, we performed a raster scan of Capella (twenty 5 ksec observations) on the inner portion of the detector in AO7. A complementary raster scan on the outer portion of the HRC-I will be carried-out in AO8. The observations acquired in AO7 were used to refine the HRC-I de-gap map which was released in CALDB 3.2.3 on Aug. 9, 2006. Reprocessing HRC-I data with the new de-gap map sharpens the PSF by about 5% relative to data processed with the earlier version of the HRC-I de-gap map. For example, reprocessing a long on-axis observation of AR Lac with the new HRC-I de-gap map produces 50% and 90% encircled energy radii of 0.41" and 0.93", respectively.

Prior to the release of CALDB 3.3, both the HRC-I and HRC-S only had a single time-independent gain correction file. A set of time-dependent gain correction files (one for each year since launch) was released for the HRC-I in CALDB 3.3. These new products can be used to generate consistent energy-invariant HRC-I hardness ratio images. Work is in progress to develop a set of time-dependent gain correction tables for the HRC-S. While detailed spectral analysis cannot be carried-out with HRC-I or HRC-S data, these detectors are capable of distinguishing between hard and soft sources (see Ch.7 of the POG). We have also released rmfs for both the HRC-I and HRC-S which can help with the interpretation of the hardness ratio images.

HRMA

The optics team has been actively engaged in porting the entire SAOsac raytrace software package to Linux. The initial motivation for this project was to produce a portable version of the raytrace code that could be used by *Chandra* observers to facilitate their data analysis. A preliminary version of this software was delivered to Data Systems in Jan., 2007 for testing and integration into Level III processing. Verification of this software is in progress.

Larry David for the Calibration Team

Cross-Calibrating Chandra and XMM-Newton

Overview

There has been an ongoing effort to compare results from *Chandra* and XMM-Newton and other X-ray astronomy missions. Results are available on a new dedicated web page, <http://space.mit.edu/ASC/calib/crosscal/> and were presented to the *Chandra* User's Committee (see http://cxc.harvard.edu/cdo/cuc/cuc-file06/oct06/Marshall_CUC_Oct06.pdf). Here, I summarize this work and some of the major results, uncertainties, and plans.

Due to the different angular resolutions of the telescopes involved, most cross-calibration observations have involved point sources. In order to avoid pileup and to check more components of the system, the transmission gratings on *Chandra* are inserted for most simultaneous observations. Because there are two grating assemblies that can be used and two detectors, the common combinations are usually implemented sequentially during cross-calibration campaigns. In other telescopes such as XMM, several instruments are used at the same time. Due to observing constraints that vary by observatory, cross-calibration campaigns are rare, usually performed once or twice per year. Observations of extended sources are also used in calibration, taking advantage of their unchanging fluxes and occasionally line-rich spectra.

Comparing Chandra and XMM-Newton Spectra

These results are summarized on web pages maintained by both the *Chandra* and XMM-Newton projects. See <http://space.mit.edu/ASC/calib/crosscal/> for the CXC web page and http://xmm.esac.esa.int/external/xmm_sw_cal/calib/cross_cal/index.php for the page developed by XMM-Newton ESAC scientists. See also the XMM-Newton technical document CAL-TN-0052 (available on-line at <http://xmm.esac.esa.int/docs/documents/CAL-TN-0052-3-0.ps.gz>).

There have been 10 successful cross-calibration campaigns to observe extragalactic targets with nearly featureless spectra using both XMM-Newton and *Chandra*. Three targets have been used: 3C 273, PKS

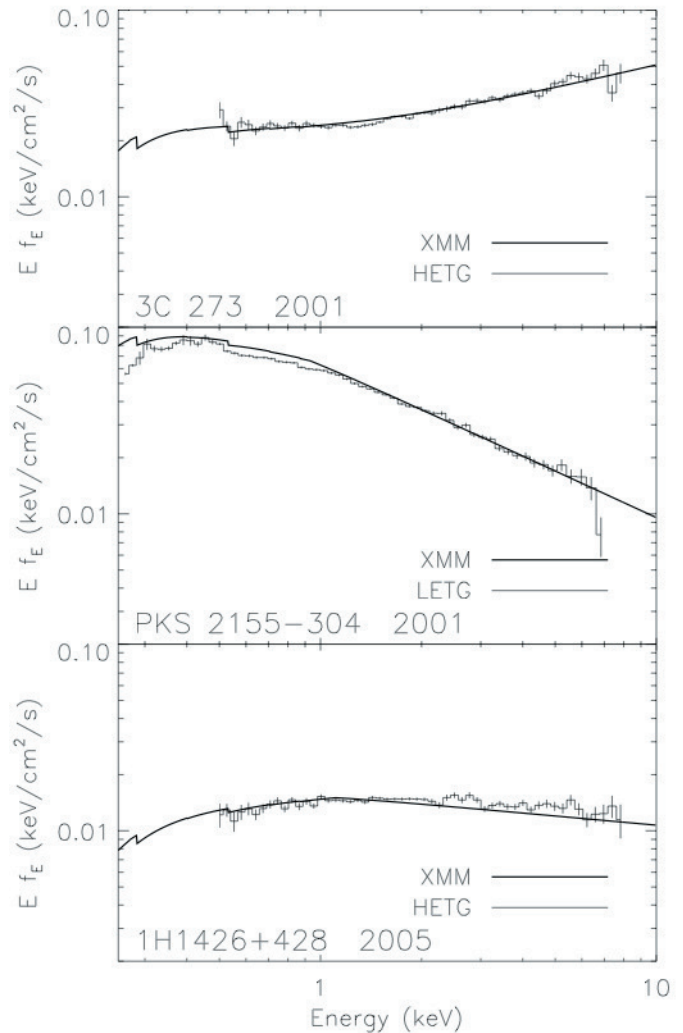


FIGURE 22: Shows three examples from figure 3 of the CXC cross-cal web page. The fluxes for the *Chandra* data were computed in energy bins 5% wide.

2155-304, and 1H1426+428. The *Chandra* configurations include the HETGS, the LETG with ACIS-S, and the LETG with HRC-S. Results are available at the aforementioned web sites for several of these campaigns.

The two projects have taken somewhat different approaches to comparing data. The ESAC web pages show joint spectral fits using XSPEC and give the spectral parameters derived. For example, fitting a broken power law model to the June 2005 observations of 1H126+428, the 1 keV normalization is 0.01493(6) (in $\text{ph}/\text{cm}^2/\text{s}/\text{keV}$) for the joint fit of all data, while the normalization is 0.0140(4) medium energy grating (MEG) portion of the HETGS. Fits to the XMM PN data alone gave a normalization of 0.01525(8). While these normalizations are formally inconsistent at the 3σ level, the difference is under 10% and the HETGS high energy grating (HEG) normalization, 0.0148(6), is within 1σ of that of the PN. Comparing spectral indices

gives a similar result: the high energy photon index ($E > 1$ keV) is 2.160(8) for the PN and 2.006(47) for the HEG. These are formally inconsistent while the low energy indices are almost identical: PN gives 1.893(7) and the MEG gives 1.892(53). All parameters from the fits to the August 2005 LETG/ACIS-S observation of PKS 2155-304 were within $1-2\sigma$ of the corresponding values from the PN fits and for the LETG/HRC-S observations of the same target and month, only the high energy photon index was discrepant at more than 3σ . More comparisons are being prepared.

On the CXC web page, the fits to the PN are compared directly to *Chandra* spectra in order to show more detail. Figure 22 shows three examples from figure 3 of the CXC cross-cal web page. The fluxes for the *Chandra* data were computed in energy bins 5% wide. These comparisons indicate that the XMM and *Chandra* spectra agree generally to better than 10% over a wide energy range. Some systematic differences are still apparent that aren't quite consistent between observations. These differences are still under investigation.

Comparisons of spectral fits to XMM-Newton PN data to coarsely binned Chandra grating spectra

The fluxes for the *Chandra* data were computed in energy bins 5% wide. These comparisons indicate that the XMM and *Chandra* spectra agree generally to better than 10% over a wide energy range. Uncertainties in the XMM spectral fits aren't shown but there may still be some systematic differences that aren't fully consistent between targets. These differences are still under investigation.

Comparing Fluxes in Specified Bandpasses

Another approach being used to compare XMM and *Chandra* results is to estimate fluxes in fixed bandpasses. This method gives a somewhat straightforward way of comparing XMM instruments and has now been applied to two of the simultaneous *Chandra*/XMM observations. For the December 2001 observation of PKS 2155-304, the LETG/ACIS fluxes in the 0.85-1.50, 1.50-4.00, and 4.0-10.0 keV bandpasses were consistent within 5% of the fluxes computed from model fits to PN data. The LETGS-derived flux in the 0.54-0.85 keV band was almost 10% lower than the PN value, which appears to be consistent with fluxes determined

from the XMM MOS detectors. Comparisons using the HETGS data from the June 2005 observation of 1H1426+428 give similar results: MEG and MOS fluxes are 7-13% lower than PN fluxes in the lowest band, within 3% in the 0.85-1.50 keV band, and 5-12% higher in the 1.5-4.0 keV band. In the highest energy band, the MOS is high by about 15% but the HEG flux is slightly lower but consistent with the PN flux. This work is continuing with the remaining targets from the cross-cal campaigns.

Cross-Calibration of Chandra and Suzaku

In May, 2006, PKS 2155-304 was observed by Suzaku, *Chandra*, and XMM-Newton.

Preliminary results from joint Suzaku-*Chandra* fits were presented by M. Ishida at the June 2006 international calibration meeting in Reykjavik, Iceland. The meeting was the first one for a newly formed group, called the International Astronomical Consortium for High Energy Calibration (IACHEC, see <http://www.iachec.org/>). Ishida showed that pure power law fits to the Suzaku XIS spectra gave normalizations consistent with the LETGS value to within 4% and that the photon indices agreed within uncertainties.

Summary

While the existing effective areas appear to be good to better than 10% over most of the *Chandra* energy range, we continue to work on ways to determine what systematic errors remain and to work jointly with other projects to improve the agreement among all X-ray observatories.

Herman L. Marshall

CXC 2006 Science Press Releases

See http://chandra.harvard.edu/press/press_release.html for more details.

Table 1 - Chandra 2006 press releases.

Date	PI	Objects	Title
01-10-2006	Thomas Statler	56 elliptical galaxies	NASA's <i>Chandra</i> Finds Black Holes Stirring Up Galaxies
02-03-2006	Kristian Pedersen	NGC 5746	Detection of Hot Halo Gets Theory Out of Hot Water
03-23-2006	Alan Stockton	4C37.43 and 3C249.1	NASA's <i>Chandra</i> Finds Evidence for Quasar Ignition
04-24-2006	Steve Allen	9 elliptical galaxies	NASA's <i>Chandra</i> Finds Black Holes Are 'Green'
06-01-2006	Bryan Gaensler	IC 443	The Case of a Neutron Star with a Wayward Wake
06-21-2006	Jon Miller	GRO J1655-40	Black Hole Paradox Solved by NASA's <i>Chandra</i>
08-08-2006	Max Bonamente	38 galaxy clusters	<i>Chandra</i> Independently Determines Hubble Constant
08-18-2006	Doug Clowe	1E 0657-56	NASA Finds Direct Proof of Dark Matter
09-18-2006	Jacco Vink	RCW 86	New Evidence Links Stellar Remains to Oldest Supernova Remnant
10-05-2006	Bill Forman	M87	<i>Chandra</i> Reviews Black Hole Musical: Epic but Off-Key
11-15-2006	Michael Stage	Cas A	<i>Chandra</i> Discovers Relativistic Pinball Machine
			Megan Watzke

Chandra Fellows for 2007

This year we had a record number of applications for Chandra Postdoctoral Fellowships. The list of Chandra Fellows for 2007 has just been finalized and is provided below. Keep an eye on our web pages for information about the Chandra Fellows Symposium (October 10, 2007) and the annual Fellowship competition (November 2007).

	PhD Institution	Host Institution
John Fregeau	MIT	Northwestern (yr1) KITP-USCB (yrs 2&3)
Jonathan McKinney	U. Illinois	
Ian Parrish	Princeton	Berkeley
Jesper Rasmussen	U. Copenhagen	Carnegie Obs.
Jerremy Schnittman	MIT	Johns Hopkins

Nancy Ramage Evans

Running Chandra

There were a number of discussions about *Chandra*, particularly behind the scenes operations presented at the SPIE Conference 6270, "Observatory Operations: Strategies, Processes, and Systems". Summaries of these discussions are presented here, but the full discussion can be found in Proc. SPIE v 6270 (2006).

Editor

Chandra Flight Operations Software Tools Improve Mission Execution

A full discussion of this topic is given in the SPIE Proc 6270, 2006

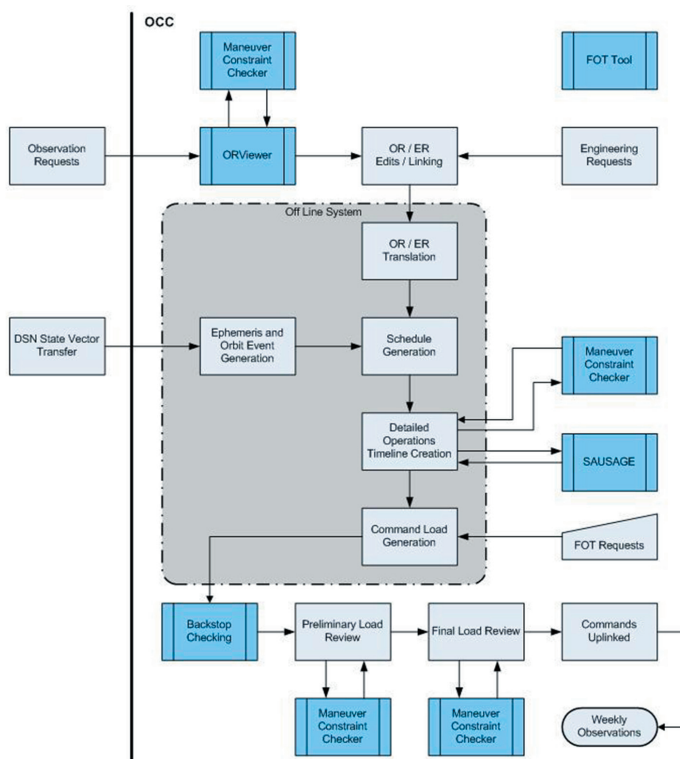


FIGURE 23: The Chandra Mission Planning process.

Over the first 6 years of the *Chandra* mission, the Flight Operations Team (FOT) has developed several ground software applications intended to help improve the efficiency of operating the Observatory. In May of 2006, a paper was presented at the SPIE As-

tronomical Telescopes and Instrumentation Conference in Orlando Florida highlighting these tools and way in which they've benefited the FOT. Several of these tools utilize commercial off the shelf software products such as Matlab, while others are completely home grown. The tools are introduced here but more fully discussed in the SPIE paper.

The FOT Mission Planning process (Figure 23) starts with the receipt of a weekly Observation Request (OR) list from the Science Mission Planning Team. This unordered OR list contains all of the information needed to schedule the individual observations during the planning week. After receipt of the OR list, the FOT Mission Planners add Engineering Requests and then start the process of ordering the observations into the most efficient possible schedule while at the same time ensuring that spacecraft and mission constraints are not violated.

This is a complicated process which has changed considerably since the beginning of the mission. The FOT has developed a set of software tools based on the Matlab scripting language to assist in this process. The ORViewer is utilized to assist the Mission Planners in optimally ordering observations. It is a graphical tool which shows the user different views of the observations and maneuver paths between observations. It works in conjunction with two other MP tools, the Maneuver Constraint Checker (MCC) and the SAUSAGE (the Simple AXAF User Selected Acquisition and Guide star Editor).

The MCC is another graphical tool which shows the Mission Planners all constraints which might affect the way in which the weekly schedule can be assembled. Some of these constraints include inertial constraints such as lunar, solar, and earth constraints. Others are temperature related and have to do with protecting spacecraft units. The MCC also allows users to view the predicted spacecraft momentum state, antenna views, and other important planning parameters.

Other FOT tools are used to support other aspects of operations such as real-time telemetry monitoring. One of the primary tools used by the FOT in telemetry monitoring is called GRETA. GRETA displays telemetry data in both a tabular layout and also in plots. Users may select any telemetry point to display. GRETA displays are used daily in operations to monitor the health and safety of all of the observatory systems. In addition to the display capabilities in GRETA, GRETA also monitors certain telemetry points to ensure that they do not exceed pre-specified limits. This limit monitoring process is the front line of Observatory protection. Any limit violation is immediately noticed and reported by the on-console operators to the engineering team for immediate response and analysis.

The final set of FOT tools which are utilized in nominal operations of the vehicle are web based tools such as the OCCWeb and the Integrated Flight Operations Timeline (IFOT). These tools are used to give users information to critical operations data. The OCCWeb is used to help individuals on the various operations team to find data about operations including how the spacecraft works, minutes from key meetings, ground stations status, etc. In addition, the OCCWeb provides an up to the minute snapshot of the mission including information such as current instrument in use, target name, altitude, and news and alerts. IFOT allows users to enter and query past mission events such as times of safing events, Deep Space Network communication passes, observations, etc. These tools are used by operations personnel to better conduct their day-to-day tasks.

FOT tools have been developed over a long time span and have been used to enhance operational efficiency and effectiveness. There are five primary reasons for the development of such tools. They are as follows.

- * Changing Requirements
- * Lack of visibility into complex processes
- * Need for more organized data management
- * Inefficiency in current processes
- * Reduction of errors

The FOT tools have helped in all of the areas to make the *Chandra* mission as successful as possible.

Dan Shropshire, Sabina Bucher, and Joe Rose

The Chandra X-Ray Observatory Mission Planning Process: Managing and Implementing Constraints

ABSTRACT

Planning an observation schedule for ground-based and space-based telescopes alike requires careful constraint management and implementation. Scientific constraints, which meet an observer's desire to maximize science returns, must be weighed against the physical constraints and capabilities of the telescope. Since its launch in 1999, the *Chandra* X-Ray Observatory (CXO) has provided excellent science in spite of evolving constraints, including the proliferation of constraint types and varying degrees of restriction. The CXO observation schedule is generated on a weekly basis, yet the mission planning process maintains the flexibility to turn around a target-of-opportunity (TOO) request within 24-hours. This flexibility is only possible when all personnel responsible for schedule generation-flight operations engineers, science operations personnel, and program office support - are actively involved in constraint management. A proper balance of software tools, guideline documentation, and adequate subjective judgment is required for proper constraint implementation. The decision-making process employed by mission planning personnel requires accurate, complete, and current constraint information.

This retrospective examines the existing constraint management process from a mission planning perspective. Topics include: introduction of constraints to the mission planning pipeline, the adaptivity of the mission planning process to constraint introduction, and the timing and efficiency of constraint implementation.

A full discussion of this topic can be found in Williams and Gage (2006, Proc SPIE, 6270),

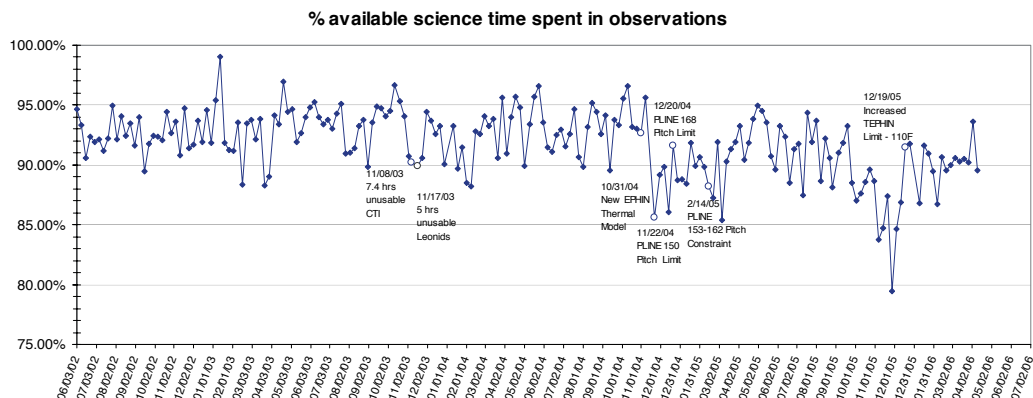


FIGURE 24: Based on the available science time (all time spent outside the radiation belts), the mission has regained efficiency above 90%. Significant events contributing to efficiency fluctuations are marked on the timeline.

INTRODUCTION

For nearly seven years, the *Chandra* X-Ray Observatory has provided world-class science, and was granted a prime-mission extension through 2009 (from the original 2004 end of prime). The observatory could easily transition to a reduced effort contract through 2014. While it is difficult to place a financial value on the science data provided by *Chandra*, the program continues to be a desirable public asset. As the program approaches its eighth annual observatory cycle, the oversubscription ratio continues to be large, and is a tangible metric of the scientific community's current needs. With the potential to exist as a useful observatory through at least 2014, careful constraint assessment and implementation can and will help manage vehicle limitations while still returning science data that meets the investigators' requirements and preferences.

CONSTRAINT INTRODUCTION PROCESS

There are two major pathways for spacecraft constraint introduction: discovery of an anomaly during real time operations, or by back-orbit analysis and trending. Trending might offer insight for detecting potential future constraints (i.e., approaching ACIS Power Supply & Mechanisms Controller (PSMC) thermal limits which might prohibit or limit forward sun pitch angles of 45-50 degrees). The entire process for discovering, analyzing and, if necessary, implementing an operational constraint is captured in the full SPIE article.

There is no standard-time for this process to complete, since each constraint is handled on a case-by-case basis. A short-term response may include placing a highly restrictive and conservative constraint on

operations until a more detailed and thorough analysis would allow a relaxation. Due to the varied complexity of analyses, it may take from two weeks through one full year for the guidelines to be optimized. Even an optimized guideline will need to be revisited as competing constraints add complexity to the mission-planning process.

IMPACT OF CONSTRAINTS ON EFFICIENCY

In spite of the proliferation of constraint changes and additions since launch, the CXO has easily maintained the Level 1 requirement for efficiency. However, efficiency has decreased an average of approximately 6% (Fig. 24). When comparing the trending data of schedule efficiency to major events in the constraint-change timeline, it is shown that the mission planning process is flexible enough to absorb individual constraints without too much decrease in efficiency. However competing constraints make scheduling even more difficult and will have a greater negative impact. Toward the end of 2005 (during perihelion), the recently added propulsion line thermal constraint competed with the EPHIN temperature limit. Only relatively short duration observations (~30ks) could be scheduled at a hot-pitch, because more efficient pre-cooling was impossible. The PLINE constraint also made it impossible to schedule a momentum desaturation with the Momentum Unloading Propulsion System (MUPS) because the thrusters could not get sufficiently cold without entering the newly constrained propulsion line pitch region.

Proposals which successfully pass the technical and peer review tollgates are still subjected to the evolving constraints and proposers are aware of this risk. There are caveats clearly stated in current revi-

sions of the POG and CfP describing the potential for observations to be segmented if updates to thermal models indicate an approved duration would violate a constraint.

To help mitigate the impact of an added constraint change (either a more restrictive change to an existing constraint, or the addition of a new constraint), the existing guidelines are reviewed and analyzed to look for flexibility. If a constraint can be relaxed without harming the longevity of the vehicle, it will only improve the chances for creating an efficient and safe schedule.

Brent S. Williams, Kenneth R. Gage

Chandra, Hardware and Systems: Keeping Things Running

A full discussion of this topic is given in the SPIE Proc 6270, 2006

<http://exc.harvard.edu/cda/SPIE/lpaton2006.ps>

System management for any organization can be a challenge, but satellite projects present their own issues. The systems group for the *Chandra* X-ray center provides the infrastructure for science data processing, mission planning, user support, archive support and software development.

Our challenge is to create a stable environment with enough flexibility to roll with the changes during the mission. To provide this we have selected mature technologies and stable hardware and software (Sun Solaris, Linux on Dell, MacOS X, Network Appliance, Cisco). We've limited the variety of systems used as much as possible to reduce administrative overhead. We deployed a high availability web cluster based on Central Dispatch from Resonate to ensure our critical web servers are always available. We run an enterprise class backup system from Syncsort with tapes archived to an off site location.

Our plans for the future include beowulf cluster support and methods for dealing with the explosive amount of data that needs to be managed.

Lisa Paton

Chandra Monitoring and Trends Analysis

The Monitoring and Trends Analysis (MTA) group is charged with providing data, tools, and analysis to assess telescope performance as it affects the science quality and efficiency of the Observatory in concert with the engineers, instrument experts, and scientists. This is an unique program to augment the purely health and safety, subsystem-specific approach of the Flight Operations Team engineering experts. Full discussion is provided in the SPIE (2007, Proc SPIE, 6270).

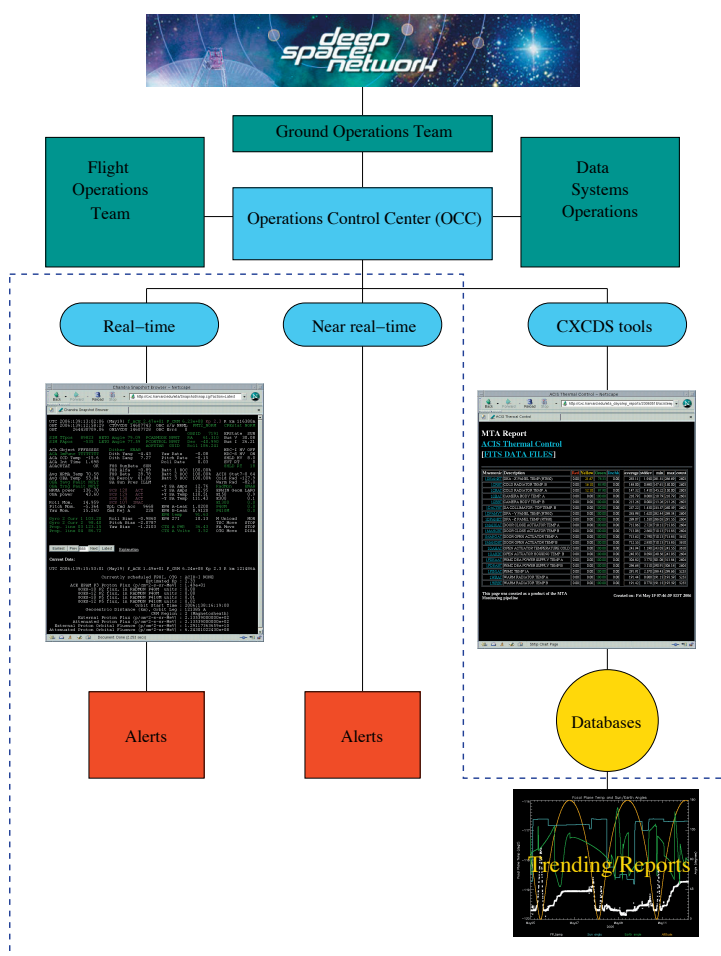


FIGURE 25: Data flow schematic from spacecraft to MTA products and services. The dotted line represents areas for which MTA is solely responsible.

We have created and maintain real-time monitoring tools capable of sending e-mail and pager alerts in the event of limit violations or unexpected spacecraft states detected on any of 40 critical parameters during 3 daily contact periods. The real-time telemetry stream is formatted for easy access through a web browser or wireless device. We also are responsible for monitor-

ing radiation data from other satellites (ACE, GOES) at all times. Eighty-two additional values are checked in near real-time including temperature and electronic hard limits and variable instrument configurations versus planned modes.

Approximately 1,500 parameters are averaged on 5-minute intervals and databased in 48 subsystem tables. This SQL database is used for long-term trending/modeling and is accessible to instrument and operations teams. An additional 24 higher order tables with 500 columns will capture key calibration and science data such as charge transfer inefficiency measurements and emission line detections. A separate database of point source properties for use in point spread function studies is under development.

Most MTA products are readily available on webpages, with, of course, some access restriction and password protection in certain areas. The homepage is <http://cxc.harvard.edu/mta/sot.html>. We also produce e-mail and pager alerts and wireless (WML) webpages. At this point, the primary MTA tasks are maintained automatically when possible, while long-term studies are expanded in response to life-limiting expectations and actual anomalies.

Brad Spitzbart, Scott Wolk,
Takashi Isobe

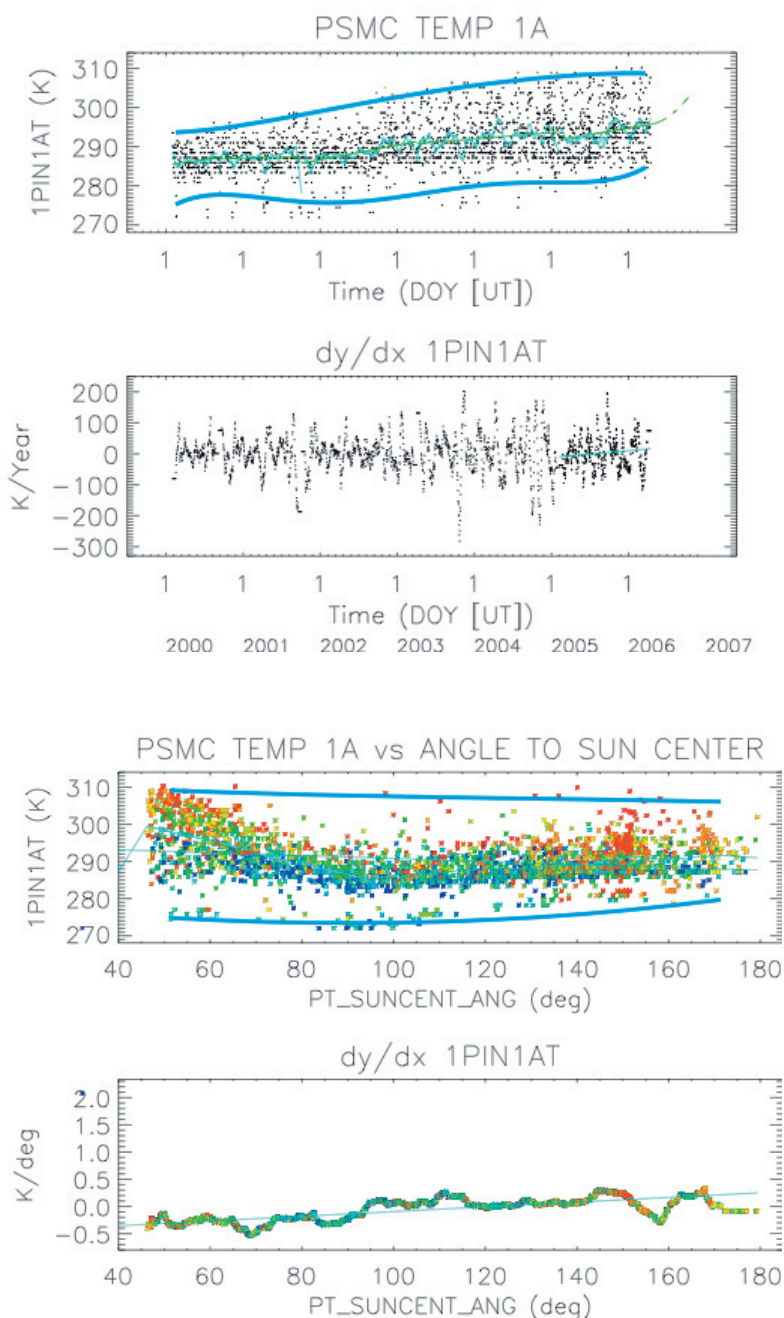


FIGURE 26: Examples of trending plots from the ACIS subsystem. The IDL code permits plots of mnemonic (MSID) versus time (top) or MSID versus another MSID (bottom). The top panel in each shows the 5-minute averaged data, a linear fit line, and a smoothed curve. The top and bottom blue lines are the envelopes. The bottom panels show the slopes between adjacent points on the smoothed curve and a linear fit, that is the second derivative. The data points in the lower plot are color-coded by date. Blue points are the earliest, from 1999; red are the most recent, from 2006.

A Historical Fluence Analysis of the Radiation Environment of the Chandra X-ray Observatory and Implications for Continued Radiation Monitoring

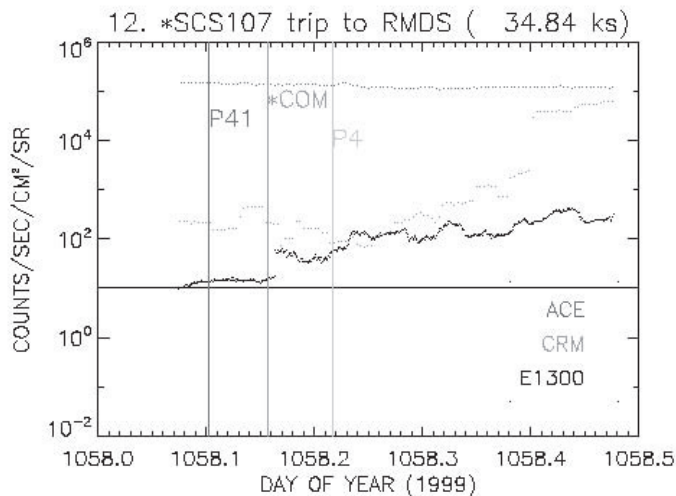


FIGURE 27: Sample data typical of that used in the analysis. The data shown from dark to light are EPHIN E1300 data, AdvancedCoronal Explorer (ACE) data, and Chandra Radiation Model (CRM) data. Vertical lines discussed in text.

A more complete discussion of this topic is provided in DePasquale et al. Proc. SPIE, “Observatory Operations: Strategies, Processes, and System”, v 6270.

<http://cxc.harvard.edu/cda/SPIE/depasquale2006.ps>

Now in operation for over 6 years, the *Chandra* X-ray Observatory has sampled a wide array of space environments. Its highly elliptical orbit, with a 63.5-h period, regularly takes the spacecraft through the Earth’s radiation belts, the magnetosphere, the magnetosheath and through the solar wind. Additionally, *Chandra* has weathered several severe solar storms during its time in orbit. Given the vulnerability of the CCDs to radiation damage from low energy protons, proper radiation management has been of prime concern for the *Chandra* team. A comprehensive approach utilizing scheduled radiation safing, in addition to both on-board autonomous radiation monitoring and manual intervention has proved successful at managing further

radiation damage. The future of autonomous radiation monitoring on-board *Chandra* faces a new challenge as the multi-layer insulation (MLI) on its radiation monitor, the Electron, Proton, Helium Instrument (EPHIN) continues to degrade leading to elevated temperatures. Operating at higher temperatures, the data from some EPHIN channels can become noisy and unreliable for radiation monitoring.

This paper explores the full implications of the loss of EPHIN to *Chandra* radiation monitoring by evaluating the fluences *Chandra* experienced during 37 autonomous radiation safing events from 2000 to 2005 in various hypothetical scenarios which include the use of EPHIN in limited to no capacity as a radiation monitor. Each safing event is evaluated in terms of the additional radiation fluence received on the spacecraft in the absence or limited use of the current radiation monitor. Figure 27 shows a sample “window” of just such an event. Plotted versus time in this figure are ACE P3 rates, *Chandra* Radiation Model (CRM) predicted rates, and EPHIN E1300 rates in counts/sec/cm²/sr. The data start at the time of the autonomous safing and extend until the nominal time of spacecraft shutdown prior to entering the Earth’s radiation belts. The times of an EPHIN P41, and P4 trip are included as vertical lines as well as the time while spacecraft controllers are in direct communication with the spacecraft (COM). We use these markers to calculate the additional fluence from the actual event to another EPHIN channel’s trip, or a communications pass. This analysis has shown that the additional fluence in the absence of any autonomous radiation monitoring would have been unacceptable. However, the spacecraft would have incurred only a minor increase in fluence from the loss of just the EPHIN E1300 channel which is currently degrading the most of any EPHIN channels.

This work was supported by NASA contract NAS8-39073.

J. M. DePasquale, P. P. Plucinsky,
D. A. Scwhartz

Eight Years of Science with Chandra

Preliminary announcement

We shall hold the symposium “Eight Years of Science with Chandra” on October 23-25, in Huntsville, Alabama. The fourth in a series, this meeting will highlight science results from the first eight years of operation of the Chandra X-ray Observatory, with emphasis on recent results.

Please visit <http://cxc.harvard.edu/>

X-ray Astronomy School

Preliminary announcement

We are in the process of organizing the 2007 X-ray Astronomy School, which will be held August 6-10th in Washington DC. This school is designed to assist graduate students, post-docs, and other researchers interested in learning both the physics and basic data analysis involved in X-ray astronomy. More information will be available shortly at: <http://xrayschool.gsfc.nasa.gov>.

Chandra Calibration Workshop

25 Oct 2007, Huntsville, AL

As in previous years, we will hold a Chandra Calibration Workshop (CCW) in conjunction with the 8 Years of Chandra Symposium. Abstracts are solicited on various aspects of Chandra calibration. Calibration related posters will be displayed all through the Symposium, and talks will be presented in an afternoon session on Thursday, October 25, at the conclusion of the Symposium. More information about the CCW, including registration and abstract submission instructions, will be available from the CCW website.

Please contact ccw@head.cfa.harvard.edu or see <http://cxc.harvard.edu/>

Useful Chandra Web Addresses

To Change Your Mailing Address:

<http://cxc.harvard.edu/cdo/udb/userdat.html>

CXC:

<http://Chandra.harvard.edu/>

CXC Science Support:

<http://cxc.harvard.edu/>

CXC Education and Outreach:

<http://Chandra.harvard.edu/pub.html>

ACIS: Penn State:

<http://www.astro.psu.edu/xray/axaf/>

High Resolution Camera:

<http://hea-www.harvard.edu/HRC/HomePage.html>

HETG: MIT:

<http://space.mit.edu/HETG/>

LETG: MPE:

<http://wave.xray.mpe.mpg.de/axaf/>

LETG: SRON:

<http://www.sron.nl/divisions/hea/Chandra/>

CIAO:

<http://cxc.harvard.edu/ciao/>

MARX simulator:

<http://space.mit.edu/ASC/MARX/>

MSFC: Project Science:

<http://wwwastro.msfc.nasa.gov/xray/axafps.html>

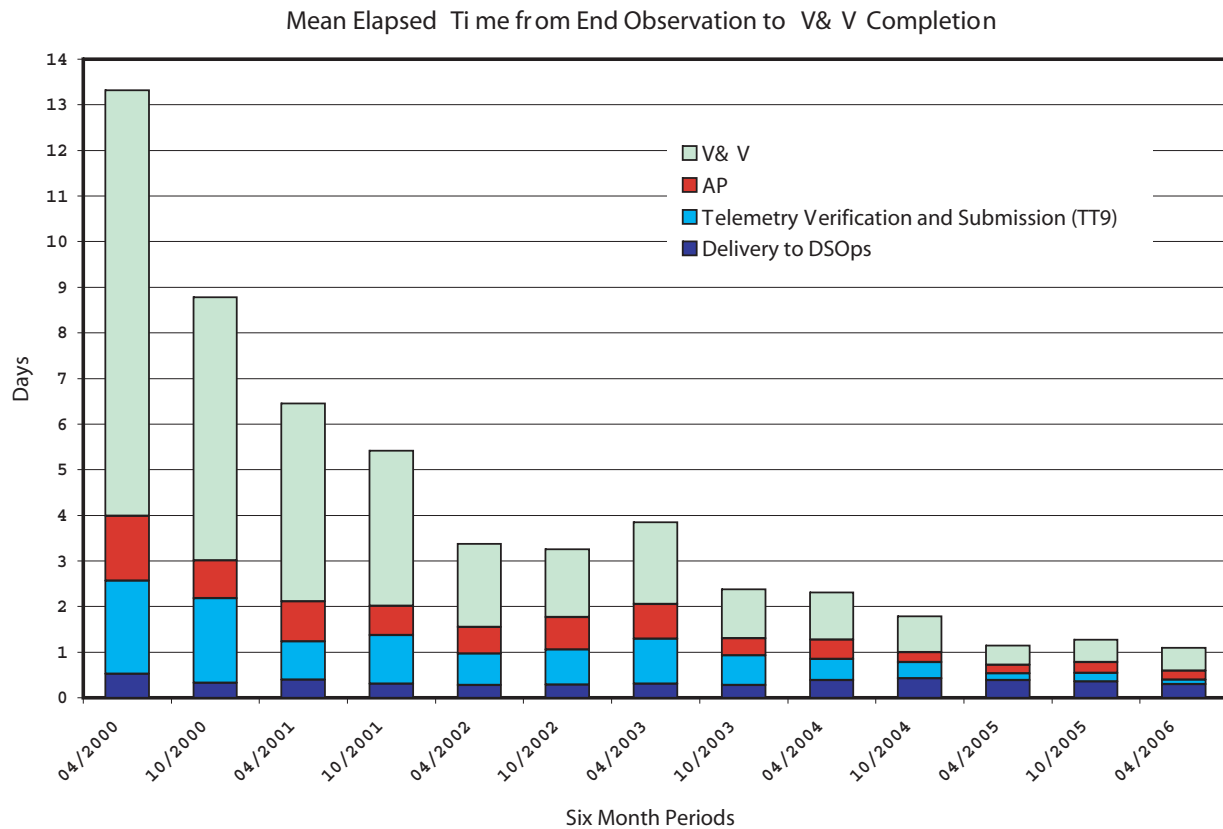


FIGURE 28: Mean elapsed time from end of observation to V&V completion

Chandra Data Processing: Lessons Learned and Challenges Met

A full discussion of this topic can be found in SPIE Proc, 6270, 2006

<http://cxc.harvard.edu/cda/SPIE/jnichols2006.ps>

There were several lessons learned and challenges met during the first six years of the *Chandra* mission by Data Systems Operations group. Incoming raw telemetry needed some form of quality control checks, quicklook images needed to be available to confirm target acquisition and early identification of instrument anomalies, and end to end tracking of observations through the data processing stages were all addressed shortly after launch and performed manually by operators.

Tools were developed to automate each task performed by operators and later integrated into one system called the Telemetry Tracker 9000 (TT9). TT9 consists of a database backend, daemon processes, and a GUI. TT9 has automated the raw telemetry quality con-

trol, quicklook processing, data submission to archival processing, and tracking of observations through the data processing system. By tracking each observation TT9 not only provides end to end visibility, but also estimates stages of processing for future observations, identifies data processing bottlenecks, and generates metrics for management reports.

J. Nichols, C. S. Anderson, P. J. Mendygral, D. L. Morgan, and G. Fabbiano

The Chandra Automated Processing System

(Adapted from a paper in the 2006 SPIE Proceedings (volume 6270), entitled “The *Chandra* automated processing system: challenges, design enhancements, and lessons learned” by David Plummer, John Grier, and Sreelatha Masters)

<http://cxc.harvard.edu/cda/SPIE/dplummer2006.ps>

Chandra standard data processing involves hundreds of different types of data products and pipelines. Pipelines are initiated by different types of events or notifications and may depend upon many other pipelines for input data.

The *Chandra* automated processing system (AP) was designed to handle the various notifications and orchestrate the pipeline processing. Certain data sets may require “special” handling that deviates slightly from the standard processing thread. Also, bulk reprocessing of data often involves new processing requirements.

Most recently, a new type of processing to produce the *Chandra* Source Catalog has introduced requirements not anticipated by the original AP design. Managing these complex dependencies and evolving processing requirements in an efficient, flexible, and automated fashion presents many challenges. The most significant of these challenges are described here along with highlights of the AP components designed to address them.

Pipeline Processing

A *Chandra* pipeline produces a set of archived data products. Pipelines (and data products) are divided into different levels. In general, higher level processing takes the lower level data products as inputs. The processing levels are defined as follows:

- **Level 0:** telemetry decommutation and ancillary data processing to produce FITS files
- **Level 0.5:** determine start and stop time of Observation Intervals and clean/format data for Level 1
- **Level 1:** data processed by Observation Interval (OBI) - calibrations and coordinates applied to science data; determination of Good Time Intervals (GTIs)
- **Level 1.5:** data processed for observations with gratings - determine grating coordinates and apply calibrations
- **Level 2:** data processed by Observation, possibly combining multiple OBIs; data from bad GTIs are screened out; sources are detected and other basic science analysis tasks are performed
- **Level 3:** data processed by source, possibly combining multiple observations to generate a *Chandra* Source Catalog

Pipelines are initiated by different events. Some pipes are run on a given data file with arbitrary start and stop times, for example, the EPHEM_L0 pipe pro-

cesses a raw ephemeris file. Some pipes are run on the observation interval boundary, like the ACIS/HRC Level 1 pipes. Some pipes need to wait till all the observation interval data is processed, like the ACIS/HRC Level 2 pipes. And some pipes need to wait till the proprietary period has expired, like the Level 3 pipes. All pipelines need to wait till the required input data products are available before they can run. The AP module that knows about data products and pipelines and kicks off the pipes at the appropriate time is called the “Observation Status Tracker” (OST).

Processing Registry

The OST manages some very complex pipeline processing requirements. To add to the complexity, these requirements often evolve with the mission (new Level 3 pipelines, for example). The OST would be a hopelessly complex program if all these requirements were incorporated directly into the software. Instead, we have taken a template driven approach and configured AP with a processing registry.

By abstracting the concept of a pipeline, the OST can be a simpler and more flexible application. Every pipeline is defined by a “profile” that lists the tools that are run, a notification that kicks it off, and a list of input and output data products. The details are captured in the ASCII Registry files and can be updated without a software release. The Registry contains template files for data products and pipelines:

Data Product registry files contain:

- File_ID
- file name convention (using regular expressions)
- method for extracting start/stop times
- archive ingest keywords (detector, level, etc.)

Pipeline registry files contain:

- Pipe_ID
- pipeline profile name (list of tools to run)
- pipeline parameters
- kickoff criteria
- input and output Data Products (by File_ID)
- method for generating the “root” part of output file names

Conclusion

Many of the concepts designed into the AP system were derived from excellent processing experience gained during the ground calibration of *Chandra*. For

example, during calibration (a 24/7 operation) the processing was driven by a hierarchy of shell scripts that were constantly in need of enhancements and updates; it was a stressful time. The current Registry/OST design is a direct result of that experience. Over the years, processing challenges and new requirements have resulted in other flexible modules being incorporated into the AP system. As a result, the latest project (the *Chandra* Source Catalog) required very few AP software enhancements to get Level 3 processing up and running.

Looking back at the evolution of the AP system and considering what has worked well and what has not worked well has been a useful exercise. It can help direct future enhancements and has also helped compile the following list of “lessons learned” over the years:

1. Designing a flexible template driven processing system is well worth the effort when dealing with complex processing requirements.
2. Keep modules loosely coupled to avoid processing bottlenecks and make error recovery easier.
3. Try to partition the processing modules in such a way that the parallel processing can begin as early as possible in the processing stream.
4. Look for places where a data cache could improve reliability and performance.
5. In certain circumstances the simpler “old” technology (like files) performs better than the “newer” technology (like UNIX IPC or CORBA).
6. Off-The-Shelf (OTS) software can sometimes be integrated into your system and save lots of development time even if the fit is not perfect. Look for a way to adapt the OTS software to fill a niche.
7. Do not assume external interfaces will be absolutely followed. You must make assumptions when designing your software, but make sure you add checks before passing data along. In other words, “Trust but verify”.
8. Consider good regression testing practices when designing your system.
9. Use the few extra bits of telemetry bandwidth to avoid clock counter roll-overs. It will eliminate untold complexity in the processing software.

David Plummer, John Grier,
and Sreelatha Masters

The Chandra X-ray Observatory Calibration Database (CALDB): Building Planning, and Improving

This article summarizes the SPIE paper “The *Chandra* X-ray Observatory Calibration Database (CalDB): Building, Planning, and Improving,” Dale E Graessle, Ian N. Evans, Kenny Glotfelty, X. Helen He, Janet D. Evans, Arnold H. Rots, Giuseppina Fabbiano, and Roger J. Brissenden, Smithsonian Astrophysical Observatory, in *Observatory Operations: Strategies, Processes, and Systems*, Proceedings of the SPIE, vol. 6270, p. 62701X-1, 2006.

<http://cxc.harvard.edu/cda/SPIE/dgraessle2006.ps>

The *Chandra* X-ray Observatory (CXO) is the most precisely and minutely calibrated X-ray telescope to date, and it stands to reason that it should have the largest and most detailed calibration database of any space-borne X-ray mission yet flown. The *Chandra* Calibration Database (CalDB) comprises over 550 datasets and in excess of 300 FITS files, each individually and uniquely specified in its six index files. (These figures are current as of the release of CalDB 3.3.0 in December 2006.)

The *Chandra* CalDB conforms to the HEASARC CalDB specifications, version 1.1. It employs the CALTOOLS subset of the FTOOLS software for index maintenance and dataset selection. The software interface is the tool quzcif, with its associated library functions. For the CXC pipeline software and the CIAO analysis software, the UNIX-wrapped routine quizcaldb employs the quzcif library structure to select calibration data in their respective environments.

A typical CalDB call for either the data systems (DS) or CIAO tools is illustrated in Fig. 29 where three examples are included. Example A illustrates a CalDB call for an ACIS gain file (codename “DET_GAIN”). Example B is for a grating efficiency (“GREFF”) file selection, and Example C is for an effective area file to be used to populate the PIMMS count rate calculator for a particular CXO observing configuration. In all three cases currently, the accessing program interface (API) has hard coded in the tolls the full index specification

for each and every required dataset to be accessed from CalDB. Hence, the datasets may be upgraded within the same data structure specification without requiring any software upgrades to accommodate it. When a new calibration parameter is introduced, then the software must be modified to add this new parameter specification to get a unique and appropriate dataset.

These CalDB specifications are reasonable and ordinarily very stable for the maintenance of existing software in a non-evolving or archival mission. However, this data and index structure may be found rather awkward and constrained when dealing with a new or developing X-ray mission, whose spacecraft and telescope configurations may vary greatly from the older mission models.

In particular, if newer, alternative configurations, which are better described by different keywords than are found in the current index (CalDB version 1.1) file specification, are to use the CalDB structure, additional standard index columns are required. Furthermore, the existing index column structure may be inapplicable, and an essentially new index specification is warranted. However, backward compatibility with preexisting mission CalDB structures is essential to the HEASARC archival database model. Hence, a flexible indexing system is required to continue the use of the HEASARC CalDB with both new and old missions. Furthermore, the development of mission-independent analysis software requires some degree of hand-shaking between the various CalDB structures that will result from this flexible index implementation, and the software that will require these calibration data. Therefore, a new CalDB software interface is required to deal with these challenges.

The CXC Data Systems team is engaged in this new development currently, with promising results for *Chandra*, and possibly for many future missions. The new CalDB dataset selection model being developed is illustrated in Fig. 30. Here, we illustrate the same three examples as in Fig. 29. However, in the new interface design, the API is not expected to have the full CalDB specification hard-coded into each CalDB call, but instead simply to expect that there will be some specification necessary, and to be able to load the required information once determined from CalDB into a second level CalDB query. The required parameters are to be determined from the first level CalDB query, and the parameter specifications are to be loaded from the headers of the observation datasets being analyzed,

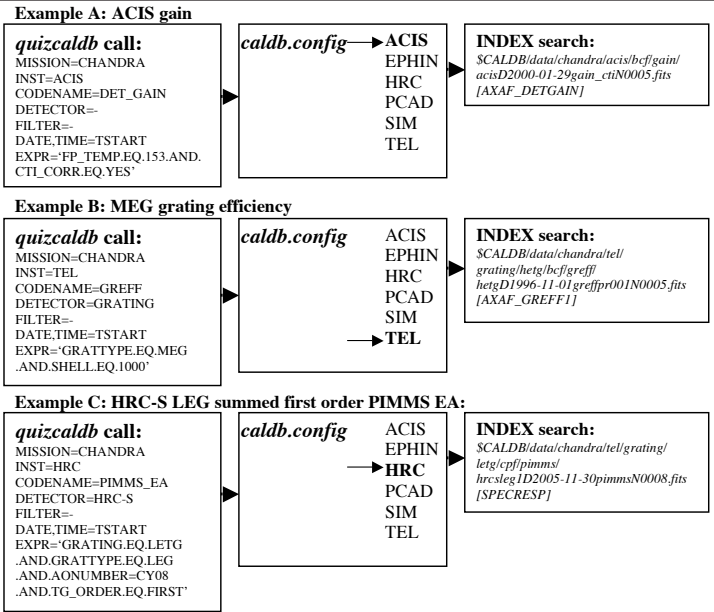


FIGURE 29: Example of Chandra CalDB calls with quizcaldb, for ACIS gain, HETG (MEG) grating efficiency, and HRC-S/LETG summed first order PIMMS effective area. Specific knowledge of the CalDB index listings is necessary to obtain a unique filespec.

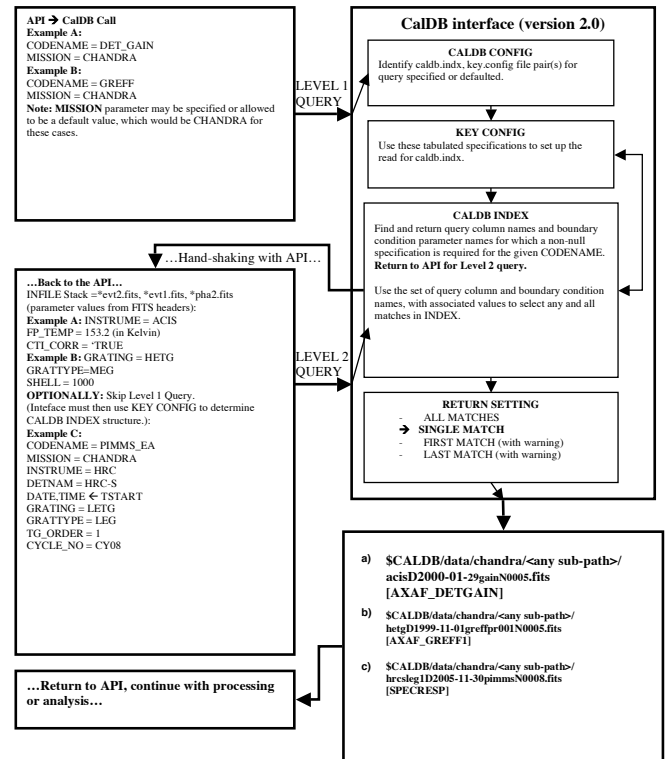


FIGURE 30: Illustration of the two-level CalDB/CIF version 2.0 query with hand-shaking, using three example code-names and configurations. These are the same examples as used in Figure 29.

and/or from the user-specified information if needed. Note that Fig. 30 example C, for the PIMMS effective area file, illustrates that it is still possible in this new interface to specify all the required information if it

is known, and skip the first level query, if this method is optimal. Hence, full backward compatibility with CalDB index specification version 1.1 is maintained with the new design.

We anticipate installing and testing the new CalDB building and querying tools (CalDB index specification version 2.0) with the development of both CIAO 4.0Beta and *Chandra* CalDB release 4.0.0, within the coming year.

Dale E Graessle, Ian N. Evans, Kenny Glotfelty, X. Helen He, Janet D. Evans, Arnold H. Rots, Giuseppina Fabbiano, and Roger J. Brissenden

Chandra Data Archive Operations: Lessons Learned

A full discussion of this topic can be found in SPIE Proc, 6270, 2006

<http://cxc.harvard.edu/cda/SPIE/mccollough2006.ps>

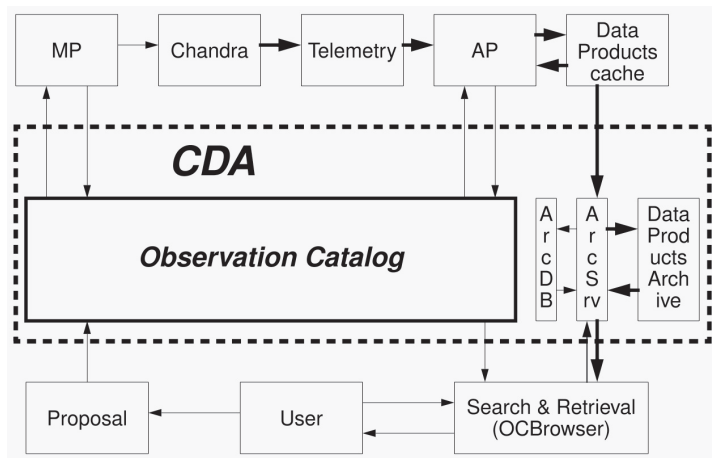


FIGURE 31: The figure shows schematically the CDA. The sizes of the boxes in the CDA say nothing about the data volume, but the thickness of the arrows indicates whether the data transfer volume is heavy or not. Data Products is the data warehouse, ArcDB is the data products database, and ArcSrv is the interface server. The MTA databases are not shown.

In the full published paper we present a review of the development of the archive in the context of the *Chandra* mission. This includes an overview, preparations for launch, operations, and the unexpected developments. We discuss the lessons learned in terms of data standards, archive integration, necessary requirements, operations, the realities of launch, user interfaces, new tasks, and the management of the archive.

Overview of the Archive: The *Chandra* Data Archive (CDA) has a central position in the operation of the CXC. Its dual role is the support of mission operations and storage and distribution of all data products including those that users of the observatory need to perform their scientific studies using *Chandra* data. In this paper we specify the various functional components of the CDA (Fig. 31). We also detail the various clients of the archive and what services need to be provided to these groups.

Preparations for launch: We examine the early history of archive and the establishment of the archive operations group (arcops). The various issues that had to be addressed before launch are reviewed and decisions made to address problems are noted.

Operations: The operations of the CDA since launch are reviewed. We discuss initial issues which had to be addressed, the evolution of the operational environment, and the importance of addressing operational software issues.

Unexpected developments: As the mission proceeded we encountered a variety of unexpected (new archive related projects and tasks) and unfinished (projects known about but not full scoped or finished) projects. We review the major tasks encountered and the actions taken on them.

Lessons Learned: A summary of the major lessons:

Data Format Standards: We note how crucial it is to determine them in the early stages of the project.

Integration of the Archive: We emphasize how early decisions need to be made on the integration of the archive into the entire operational system.

Requirements: We discuss how development of the archive is driven by requirements and how their formulation needs to be explicit.

Operations: We review a series of operations concerns which need to be addressed before going live with the mission.

Managing Proprietary Data: We review our approach to handling proprietary data. This includes how and when data becomes public.

How to Handle Unfinished Business (from Launch): We review what must be done to address the issues which are not completed by the time the mission becomes active.

User Interface: We review how various users will retrieve data from the archive and how this is expected to evolve during the mission.

New Tasks: We note how old tasks will change and new tasks will present themselves.

Management and Team Organization: We finally review some of our thoughts on the optimal management and team structure that will facilitate a smooth running archive.

After over seven years of operations we have gained considerable experience in the construction and operating of an archive for a major NASA project. It has been taken from concept to a fully functional archive serving international clientele. We have presented a range of lessons we have learned in the process of creating and running the CDA.

Michael L. McCollough, Arnold H. Rots, and Sherry L. Winkelman

CIAO: Chandra's Data Analysis System

A more complete version of this topic appears in 2006, Proc SPIE, 6270.

During the recent SPIE Conference in Orlando Florida, the CIAO software team took the opportunity to present, for the first time, an overview paper about the *Chandra* data analysis system.

The CIAO (*Chandra* Interactive Analysis of Observations) software package was first released in October 1999, following the launch of the *Chandra* X-ray Observatory and is used by astronomers across the world to analyze *Chandra* data as well as data from other telescopes. From the earliest design discussions, CIAO was planned as a general-purpose scientific data analysis system optimized for X-ray astronomy, and consists mainly of command line tools (allowing easy pipelining and scripting) with a parameter-based interface layered on a flexible data manipulation input-output library (the "Data Model" library). The same code is used for the standard *Chandra* archive pipeline, allowing users to recalibrate their data in a consistent way.

In the paper - which can be retrieved on the CIAO web site (<http://cxc.harvard.edu/ciao/> scroll to "Citing CIAO in a Publication") - we discuss the lessons

learned from the first six years of the software's evolution. Our initial approach to documentation evolved to concentrate on recipe-based "threads" which have proved very successful. A multidimensional abstract approach to data analysis has allowed new capabilities to be added while retaining existing interfaces. A key requirement for our community was interoperability with other data analysis systems, leading us to adopt standard file formats and an architecture which was as robust as possible to the input of foreign data files, as well as re-using a number of external libraries. We support users who are comfortable with coding themselves via a flexible user scripting paradigm, while the availability of tightly constrained pipeline programs are of benefit to less computationally-advanced users. As with other analysis systems, we have found that infrastructure maintenance and re-engineering is a necessary and significant ongoing effort and needs to be planned into any long-lived astronomy software.

Data analysis tools, data files, graphical user interfaces (GUIs) and modelling, fitting and plotting applications (Sherpa and Chips) are all described in detail with an eye on future development and redesign. The reasons and choices made for the introduction in CIAO of a scripting language for more advanced and scriptable task are also illustrated. The scientific and functional testing process of CIAO is briefly summarized. And finally the last section is devoted to the large body of documentation which accompanies the software, ranging from website, to command-line help to data analysis threads and more.

Since the paper was published, a new version of the software and several patches have been released. Currently CIAO version 3.4 (plus two patches to support Mac OS X users) is available for download from <http://cxc.harvard.edu/ciao/download/>.

The CIAO software is available for a number of different platforms which have evolved during the years: currently it is offered for Solaris, Mac OS X and several Linux flavors. The source code for the entire software system is distributed along with the binary files, through a GNU General Public License (GPL).

As we acknowledge in the paper, we would like to repeat here that the CIAO software package is the product of many years of work on the part of very numerous people: the authors of the paper, all current or recent members of the CXC Science Data System group (SDS) are purely reporters on behalf of a much larger group of contributors.

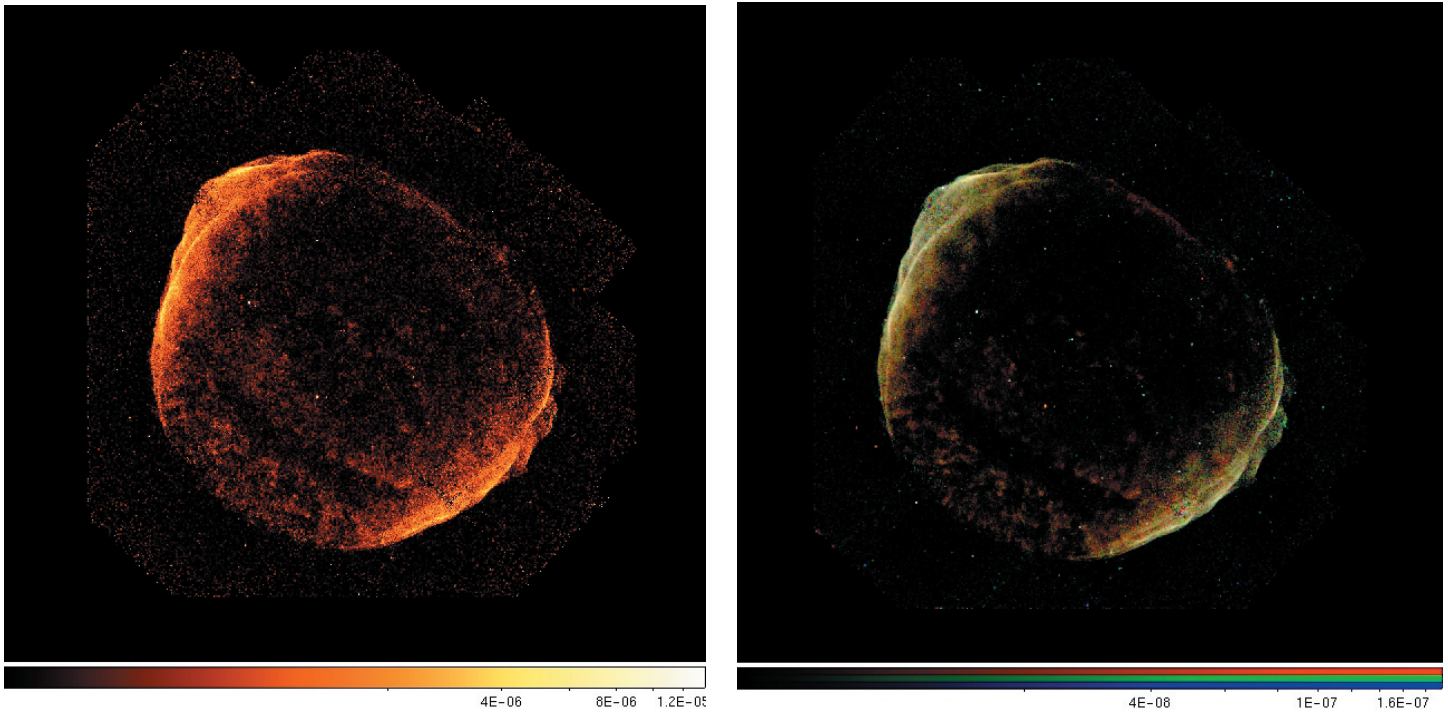


FIGURE 32: An exposure-corrected composite mosaic image from 11 separate Chandra ACIS observations of the supernova remnant SN1006. In the right panel the image is displayed in “true” colors (where color correlates with energy) obtained from the ACIS energy bands. Blue represents non-thermal emission above 2.5 keV while red represents thermal emission below 1.5 keV. Several CIAO tools were used to create these images and in particular the tools `reproject_image_grid` and `reproject_image` which allow a user to project images to common coordinate systems and `aconvolve` and `dmimg2jpg` used to create the smoothed three-color image.

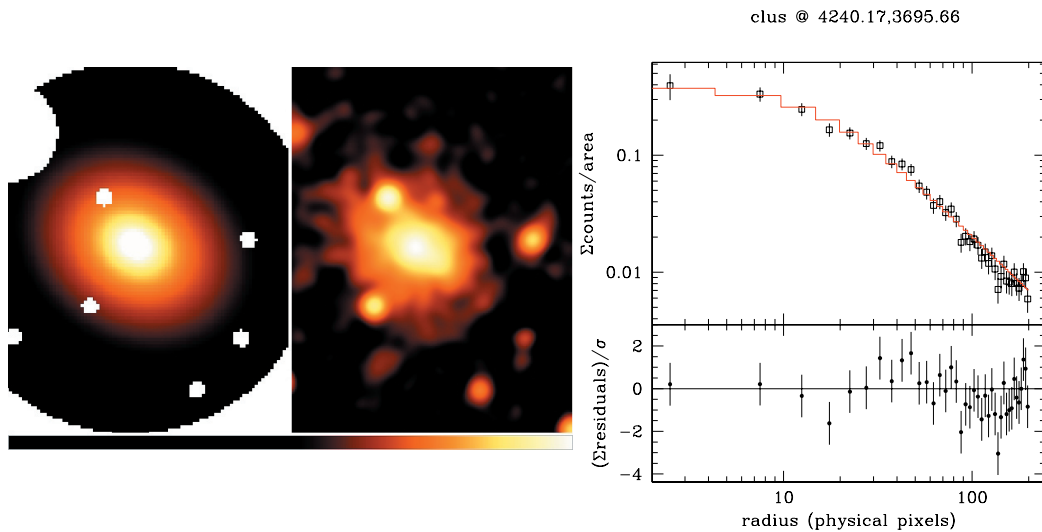


FIGURE 33: An example of a 2D modeling and fitting and a radial profile extraction and fitting performed on a X-ray cluster using the Sherpa application. The left panel shows the best-fit 2D model (a two-dimensional version of $f(r) = A \times [1 + (r/r_c)^2]^{(3\beta+0.5)}$ which includes ellipticity). The “null” values are regions, corresponding to point sources, excluded from the fit. The data (smoothed using the CIAO tool `aconvolve` for illustration purposes) is shown on the middle panel. Note however that the fitting has been performed to the un-smoothed data using the Cash statistics to account for the low count rate. The right panel represents a radial profile of best-fit 2D model (solid line) superimposed on the radial profile of the raw data. The profiles were generated within the Sherpa application with ellipticity and position angle taken from the best-fit values, rather than circular annuli

In particular we would like to acknowledge the valuable contributions from past members of the SDS group: David Davis, Adam Dobrzycki, Holly Jessop, Joel Kastner, Casey Law, Eric Schlegel, and Jennifer West.

None of the CIAO design and development would have been possible without the expertise and hard work of the members of the CXC Data System (DS) group and in particular Giuseppina Fabbiano, Janet DePonte Evans, Ian Evans, Mark Cresitello-Dittmar, Stephen

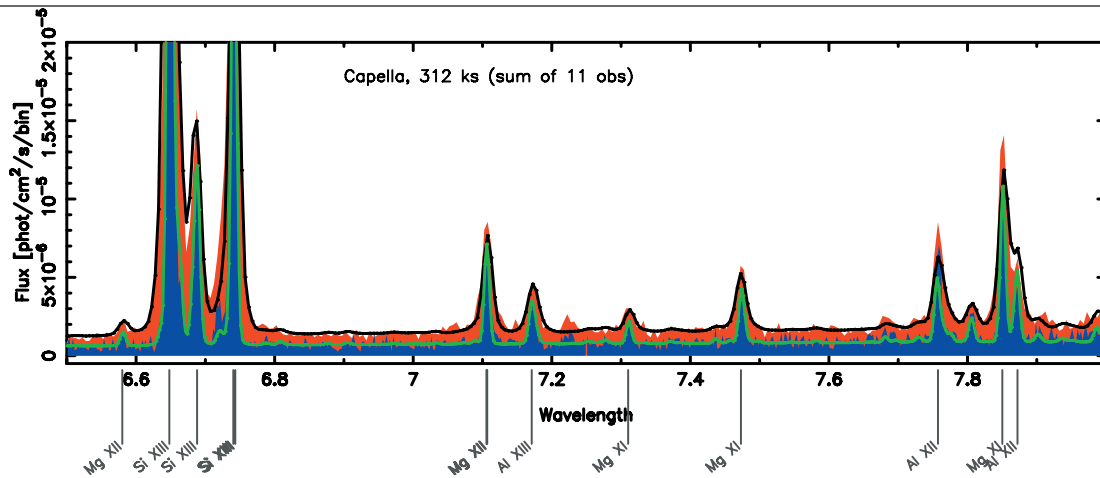


FIGURE 34: This shows a small portion of the High Energy Transmission Grating Spectrometer (HETGS) flux-calibrated spectrum of the star Capella, from the sum of 11 observations. The upper filled region (red) is from the Medium Energy Grating (MEG), and the lower (blue) is from the High Energy Grating (HEG) (HEG and MEG have different spectral resolutions and sensitivities). The solid lines outlining each region (black and green) are models derived from the atomic database (APED) convolved with the instrument responses. Line identifications are shown below the spectrum. Each individual observation and calibration were computed with standard CIAO tools, velocities and wavelength shifts computed with custom S-Lang programs, and spectra were combined and displayed with ISIS.

Doe, Gregg Germain, Kenny Glotfelty, Tom Calderwood, Judy Chen, Roger Hain, Helen He, Janine Lyn, Joseph Masters, Warren McLaughlin, Robert Milaszewski, Joe Miller, Dan Nguyen, Jim Overly, Brian Refsdal, Chris Stawarz, Michele Wilson plus numerous past members of the DS group.

A sample of the *Chandra* data prepared with CIAO software is illustrated in Figs. 32-34.

Support for development of CIAO is provided by the National Aeronautics and Space Administration through the *Chandra* X-ray Center, which is operated by the Smithsonian Astrophysical Observatory for and on behalf of the National Aeronautics and Space Administration under contract NAS 8-03060.

Antonella Fruscione, Jonathan C. McDowell, Glenn E. Allen, Nancy S. Brickhouse, Douglas J. Burke, John E. Davis, Nick Durham, Martin Elvis, Elizabeth C. Galle, Daniel E. Harris, David P. Huenemoerder, John C. Houck, Bish Ishibashi, Margarita Karovska, Fabrizio Nicastro, Michael S. Noble, Michael A. Nowak, Frank A. Primini, Aneta Siemiginowska, Randall K. Smith, Michael Wise

Status of the Chandra Source Catalog Project

Over the past year, significant progress has been made in the development of the scientific algorithms, “Level 3” pipeline software, and associated infrastructure needed to generate the first release of the *Chandra* Source Catalog (CSC).

For those who are unfamiliar with the CSC project, the CSC will be the definitive catalog of all X-ray sources detected by the *Chandra* X-ray Observatory. The catalog will include fields of all Galactic latitudes, and sources from the entire detector field of view, although the first catalog release will be restricted to imaging data only (i.e., no grating spectroscopy or ACIS continuous clocking data). For each detected X-ray source, the catalog will list the source position (accurate to ~ 1 arcsec), and a detailed set of source properties, which will ultimately include aperture and model fluxes in multiple bands to construct X-ray colors, source extent estimates, and spectral fits for bright sources. In addition to these traditional catalog elements, other file-based data products will be included for each source individually from each observation in which a source is detected. These data products, which can be manipulated interactively by the user, include images, event lists, light curves, and spectra.

An estimate of the eventual size of the catalog can

be obtained by projecting forward from the sky coverage to date. Observations obtained during the first 6 years of the *Chandra* mission covered about 160 square degrees on the sky (including ~ 80 square degrees down to a flux level of 1.0×10^{-14} ergs cm^{-2} s^{-1}), with an estimated 150,000 detectable sources containing at least 10 counts. These numbers will continue to grow as the mission continues, with a 15 year prediction of $\sim 400,000$ sources distributed over ~ 400 square degrees, or $\sim 1\%$ of the sky.

Catalog Releases and User Interface

The catalog construction process will be carefully controlled, to ensure that each catalog release is a reliable, robust, and well characterized product to maximize the usefulness to the user community. A detailed statistical characterization of the source properties will accompany each release, including studies of astrometric and photometric accuracy, limiting sensitivity, completeness, and false source rates. Characterization requirements have been established, and a detailed characterization plan has been developed to meet these requirements.

User access to the catalog will be through a web-based browser interface in the first instance, with future support for a scripting language interface and virtual observatory workflows. High level requirements for the user interface have been developed, and detailed functional requirements are currently being evolved by studying a set of science “use cases”.

Level 3 Pipelines, Software, and Algorithms

Prototype source detection and source properties Level 3 pipelines have been developed and tested. A test set of roughly 60 observations have been processed through the prototype pipelines. The results of these runs are providing valuable feedback aimed at improving the scientific integrity of the source analyses by identifying deficiencies in the current algorithms, and highlighting areas where pipeline operations could be improved. Scientific development of a new local background algorithm — one of the major missing components for the source detection pipeline that is essential to minimize the false source rate — is nearing completion, and is expected to be incorporated into the pipeline in the next few weeks. This algorithm combines a low-spatial frequency background component comput-

ed using a Poisson mean with a high spatial-frequency component that accurately identifies the ACIS read-out streaks associated with bright sources in the field of view. A few weeks ago the CXC calibration team provided a beta version of the SAOTrace ray-trace software that is capable of running directly on our Level 3 operations Beowulf cluster. This will alleviate a processing bottle-neck by allowing point spread function models to be generated directly in the source properties pipelines, taking advantage of the parallel processing capabilities of the Beowulf cluster, rather than processing serially on a Sun platform.

The first version of the science requirements for the remaining Level 3 pipeline was completed just before Christmas, and is presently being coded for testing. This “merge” pipeline matches each detected source in an observation with detections of the source in any other observations, and determines the “best estimates” of the source properties by combining data from all observations in which the source was detected. This process is complicated because of the spatially variable PSF (the source may be present at different off-axis angles in the observations), differing detector responses, and source time variability.

Hardware and Infrastructure

The algorithms required to build the CSC are very computationally intensive. To ensure that the catalog can be constructed in a reasonable time, a 15 node Linux Beowulf cluster has been installed for Level 3 pipeline operations, together with 3 Terabytes of scratch space. The automated processing infrastructure that runs the pipelines has been enhanced to manage pipeline processing on this cluster, and is being used to run the prototype pipelines. A recent upgrade to the third party Beowulf cluster software has addressed some early stability issues with the hardware, and the production platform now seems to be stable. Performance estimates based on the observed processing efficiency indicate that a production run of all the public observations to date will take of order 4 months using this cluster.

Ian Evans, for the *Chandra* Source Catalog Project Team

Chandra Data Archive

There are a few developments of note this year in the archive area.

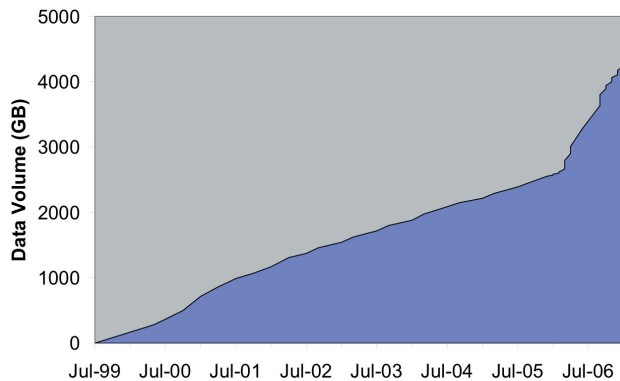


FIGURE 35: Chandra Data Archive: Data Volume

Provisional Retrieval Interface versus RetrieVER

The Provisional Retrieval Interface (PRI) that was put into service shortly after launch has finally been retired. We had not meant it to be around for this long, but it provided the only public means through which instrument teams could retrieve data products associated with Engineering Requests (ERs), pseudo observations without science data, such as CTI measurements, that provide information on spacecraft performance. It finally became too much of a burden to maintain this interface and we have replaced it with RetrieVER, a light-weight web interface that specifically (and exclusively) allows browsing and retrieval of ER data. There is a link on the CDA web page.

Archive Mirrors

Some users may discover that at times they are directed to different servers to download their retrieval packages. In those cases the downloads are routed through one of our archive mirrors which hold copies of the current version of all primary and secondary data products for all observations that have become public. The objective is to provide optimum download speed.

Downloads of Proprietary Data

Once in a while we get an inquiry from a PI who, to his or her distress has discovered that it is possible to download data pertaining to observations that are still proprietary through an utterly public interface. The an-

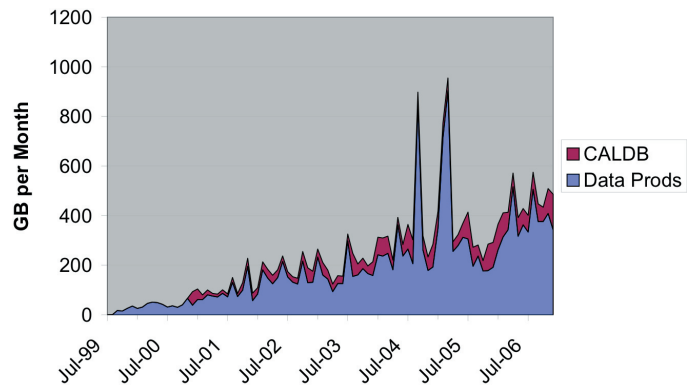


FIGURE 36: Chandra Data Archive Downloads

swer is: yes, one can, but if you look inside the tar file you will discover that the files with proprietary information are not included. The data products for proprietary observations are divided into public and proprietary products. The latter will only be included in the retrieval package if the client is logged into an account that authorizes access to those data.

Reprocessing III

As reported elsewhere, the third reprocessing run is still underway. At the beginning of February all data in the archive for observations made since 2001 have been reprocessed and form a homogeneous set as far as processing software and calibration are concerned. In the following months we expect the arrival of reprocessing products for the observations made in 2000, after the drop in the focal plane temperature to -120°C in January 2000.

Bibliography Database

Now that it has become feasible to scan the bodies of papers in the ADS, we have started to collect various bits of interesting information from the articles and we would like to encourage all users to include acknowledgements to software packages (CIAO, Sherpa, ChiPS) and grant numbers. Of course, we continue to appreciate your including ObsIds and Dataset Identifiers (see the link on the CDA web page).

Archive Statistics

In the accompanying two figures we present some basic archive statistics. The first figure (Figure 35) shows the growth of the archive (only the primary operational archive, excluding additional copies at CfA and mirror sites). The two periods of increased slope (2000/2001 and 2006) correspond to the two major reprocessing runs. The second figure (Figure 36) presents

the monthly download volume (only data downloads directly from the archive and CalDB; Quicklook and prepackaged data are excluded, but very minor). At this time, a typical number is 350 GB per month for data and 100 GB per month for CalDB. This means that every month roughly half of the volume of all primary and secondary data products is downloaded. Additional information shows that the observations that are downloaded are fairly evenly distributed over the life of the mission; i.e., people are equally interested in old, as well as in recent, observations. The prominent spikes betray (multiple) downloads of the entire archive by certain organizations.

Arnold Rots, for the *Chandra* Data Archive
Operations team
arcops@head.cfa.harvard.edu

Absolute Time Calibration for the *Chandra* X-Ray Observatory

Abstract

We performed an absolute time calibration of the *Chandra* clock through simultaneous observations by *Chandra* and the Rossi X-ray Timing Explorer (RXTE) of the millisecond pulsar PSR B1821-24. Using an updated clock correlation file, we find that the error in the *Chandra* clock, with respect to the RXTE clock, is $4 \pm 3 \mu\text{s}$. Considering that the uncertainty in the RXTE times is typically $2 \mu\text{s}$ and taking into account other sources of error, we conclude that *Chandra* time is off by $4 \pm 4 \mu\text{s}$. We add two caveats to this. First, this is only a single snapshot measurement; although we feel confident about the stability of the *Chandra* clock, we cannot entirely exclude the possibility of random or systematic variations in this offset. Second, first-version standard production data are typically run by CXC with an extrapolated clock correlation; in this particular case the error in the extrapolated clock correlation was $3 \pm 1 \mu\text{s}$, but that is not necessarily a typical value. The final conclusion is that with careful processing we may reasonably have confidence that *Chandra* absolute time can achieve an accuracy of $4 \mu\text{s}$.

Introduction

An accurate absolute time calibration of the *Chandra* X-ray Observatory is particularly important for observations made with the HRC in Timing Mode which affords a timing resolution of $16 \mu\text{s}$. In 2003, the precision of the time stamps in *Chandra* data was improved considerably after Northrop-Grumman personnel associated with the *Chandra* FOT derived an instrumental correction of $284.4 \mu\text{s}$ (reported by W. S. Davis¹) and A. H. Rots confirmed that this produced correct absolute times within about $50 \mu\text{s}$, on the basis of observations of the Crab pulsar²; to be precise, the offset was determined to be $35 \pm 12 \mu\text{s}$. However, the peak of the Crab pulse is sufficiently wide to preclude a very accurate timing determination and in retrospect we must conclude that the error was underestimated. Nevertheless, this result yielded an order of magnitude improvement in the precision of the *Chandra* time stamps.

What is needed for a precise measurement of the absolute clock error, allowing another order of magnitude improvement, is a celestial observation of a pulse that can be timed accurately and that has a width of no more than a few tens of μs . This can be achieved by simultaneous observations with *Chandra* and the Rossi X-ray Timing Explorer (RXTE) of the millisecond pulsar PSR B1821-24 which has a very sharp component in its X-ray pulse profile.

Observations and Analysis

The 3 millisecond pulsar PSR B1821-24 was observed on 27 May 2006 for 41 ks by *Chandra* (HRC timing mode) and for 16 ks by RXTE (GoodXenon event mode). The time range of the RXTE observation was fully covered by the *Chandra* observation. *Chandra* data are routinely processed with only past clock correlation information, extrapolated to the date of observation. This *Chandra* observation was reprocessed with a clock correlation file that was based on clock correlation data obtained before and after the observation. The RXTE time stamps can be corrected during analysis through the use of a fine-clock-correction file, tdc.dat.

Paul Demorest and Donald Backer (UC Berkeley) kindly provided us with an accurate timing ephemeris of the pulsar for this epoch, based on radio monitoring observations.

Both X-ray observations were analyzed using the program faseBin, that bins the individual events using orbit ephemeris, timing ephemeris, and clock

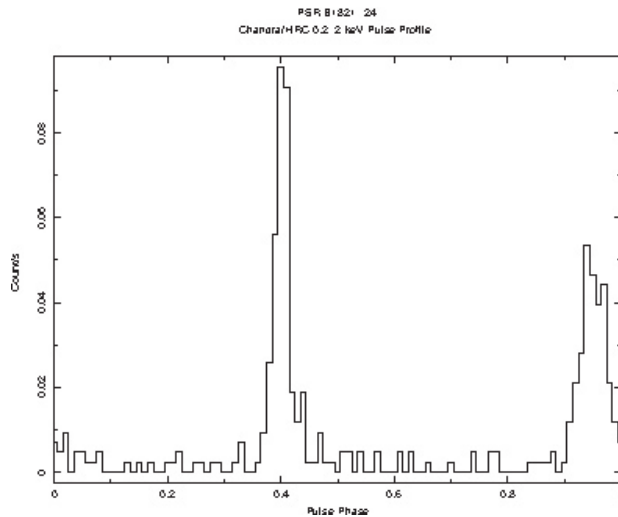


FIGURE 37: PSR B1821-24 Chandra/HRC 0.2-2.0 keV Pulse Profile

corrections. The resulting pulse profiles are shown in Figs. 37 and 38. We have some doubts about the zero-phase point of the timing ephemeris, but since the ephemeris was applied to both observations any such term would vanish.

Results

The offset between the two pulse profiles was measured by cross-correlating the profiles and fitting a Lorentzian to the cross-correlation function. We conclude from this fit that the *Chandra* time stamps in the present observation are $4 \pm 3 \mu\text{s}$ too late.

We performed the same analysis comparing the standard *Chandra* data with the data derived from the improved clock correlation and found the difference to be $3 \pm 1 \mu\text{s}$.

There are seven other sources of error:

- RXTE orbit ephemeris $< 0.2 \mu\text{s}$
- RXTE timing calibration error $< 2 \mu\text{s}$
- Chandra* orbit ephemeris $< 0.5 \mu\text{s}$
- Chandra* random clock variations unknown
- Chandra* relativistic orbital variations $< 1 \mu\text{s}$
- Chandra* clock correlation error $1.8 \mu\text{s}$
- Chandra* clock correlation extrapolation $12 \pm 12 \mu\text{s}$

The large unknowns here are random variations in the *Chandra* clock that we know nothing about and the error resulting from the extrapolation of the clock correlation data. The latter can actually run anywhere from 3 to $25 \mu\text{s}$, depending on the time elapsed since the last correlation used.

Our recommendation is to have observations that are very time-critical reprocessed using an improved

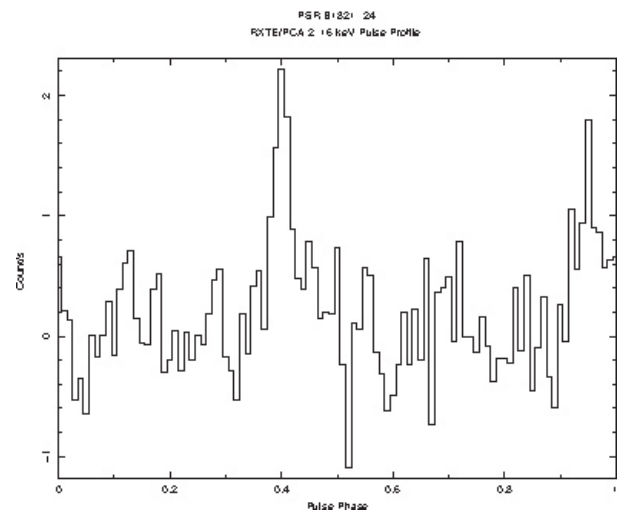


FIGURE 38: PSR B1821-24 RXTE/PCA 2-16keV Pulse Profile

clock correlation file; this is already the case for all observations performed prior to 15 November 2005. We also recommend that the CXC consider whether to adjust the present standard clock correction in Standard Data Processing from 284.4 to $280.4 \mu\text{s}$. These recommendations should result in an absolute time accuracy of about $4 \mu\text{s}$, unless there are random variations in the *Chandra* clock of the same order or larger. The only way to get a direct handle on that error is to repeat these coordinated observations several times. Absent such observations, one may infer from the dispersion of deviations between adjacent clock correlations ($1.8 \mu\text{s}^3$) that such variations are likely to be smaller. Hence, we feel that, if these recommendations are followed, one may reasonably have confidence that the *Chandra* absolute time stamps are accurate to about $4 \mu\text{s}$.

Acknowledgments

I gratefully acknowledge the help that I received from Donald Backer, William Davis, Paul Demorest, Ian Evans, Dong-Woo Kim, Craig Markwardt, Gail Rohrbach, Jean Swank, and CXC and RXTE Mission Planning.

(Footnotes)

¹ See <http://cxc.harvard.edu/ccw/proceedings/03/proc/presentations/davis/>

² See <http://cxc.harvard.edu/ccw/proceedings/03/proc/presentations/rots/Clock.html>

³ I. Evans 2006, CXC-DS ECR 06-005

The Results of the Cycle 8 Peer Review

Chandra is now in its 8th observing cycle! Cycle 7 observations are very close to completion and Cycle 8 started in the Fall 2006 with substantial overlap of the two cycles in order to efficiently fill the observing schedule.

The Cycle 8 observing and research program was selected as usual, following the recommendations of the peer review panels. The peer review was held 20-23 June 2005 at the Hilton Boston Logan Airport. 110 reviewers from all over the world attended the review, sitting on 13 panels to discuss 725 submitted proposals (Figure 39).

In addition, *Chandra* time was allocated to several joint programs by the proposal review processes of Hubble XMM-Newton and Spitzer (2,3,4 proposals respectively). Similarly the *Chandra* review accepted joint proposals with time allocated on Hubble (6), XMM-Newton (3), Spitzer (3), VLA (10, 1 with VLBA), NOAO (4) and RXTE (3). The Target Lists and Schedules area of our website lists the various approved programs, including abstracts.

The *Chandra* review panels were organized as follows:

Topical Panels:

Galactic

Panels 1,2:

Normal Stars, WD, Planetary Systems and Misc

Panels 3,4:

SN, SNR + Isolated NS

Panels 5,6,7:

WD Binaries + CVs, BH and NS Binaries,

Galaxies: Populations

Extragalactic

Panels 8,9:

Galaxies: Diffuse Emission, Clusters of Galaxies

Panels 10,11,12:

AGN, Extragalactic Surveys

Big Project Panel: LP and VLP proposals

The over-subscription rate in terms of observing time for Cycle 8 was 6.0, very similar to previous cycles (Figure 40), with the total time request being ~100 Msecs, steady for the past 4 cycles (Figure 41). As is our standard procedure, all proposals were reviewed and graded by the topical panels, based primarily upon their scientific merit, across all proposal types. The topical panels produced a rank-ordered list along with detailed recommendations for individual proposals where relevant. The topical panels were allotted *Chandra* time to cover the allocation of time for GO observing proposals based upon the demand for time in that panel. Other allocations made to each panel were: joint time (for those facilities which were over-subscribed), Fast and Very Fast TOOs, time constrained observations and money to fund archive and theory proposals. Many of these suffer from small number statistics in individual panels so allocations were made based on the full peer review over-subscription ratio. In some cases panel allocations were modified in real time during the review as some panels did not use all their allocation while others requested more. Large and Very Large Projects were discussed by the topical panels and ranked along with the rest, and the recommendations of these panels were recorded and passed to the Big Project Panel.

Following the deliberations of these topical panels, the Big Project Panel discussed and recommended Large and Very Large Projects to be included in the Cycle 8 science program. For the first time this year we allowed additional time in the BPP schedule for both reading and meeting with appropriate panel members to allow coordination for each subject area. The meeting extended into Friday morning for the additional discussion and the rank-ordered list to be finalized.

The resulting observing and research program for Cycle 8 was posted on the CXC website three weeks later, 14 July 2006. This wait time (longer than the two weeks in past cycles) was due to the complexities added by the strict limit on constrained observations. Not all passing-ranked proposals which requested time constrained observations could be approved. Effort was made to ensure that the limited number of constrained observations were allocated to the highest-ranked proposals review-wide. All post-review decisions were discussed with the relevant panel chairs before the recommended target list was posted.

Letters detailing the results and providing a report from the peer review were mailed to each PI in early August. PIs of proposals with US collaborators were

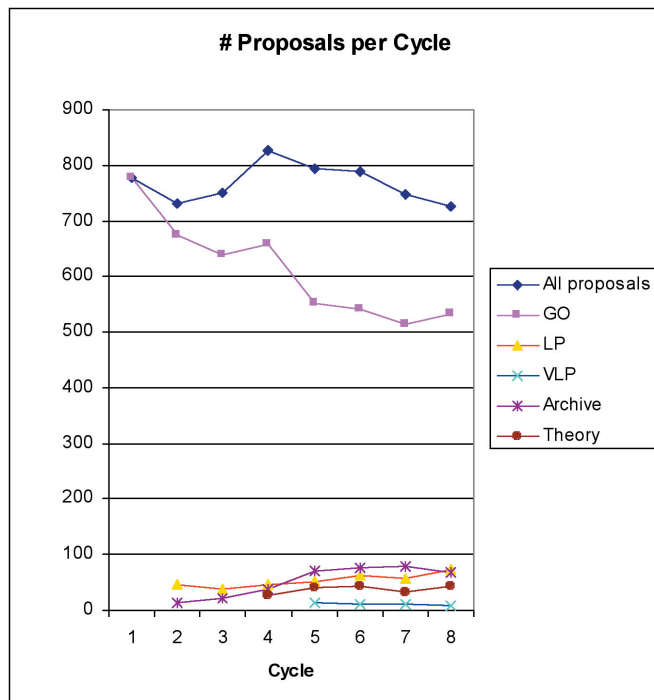


FIGURE 39 (left): The number of proposals submitted of each proposal type (e.g. GO, LP, Archive etc.) as a function of cycle. Since more proposal types have become available in each cycle, the number classified as GO has decreased as other types increase. The total number of submitted proposals is remarkably constant.

invited to submit a Cost Proposal, due by 14 Sep 2006 at SAO. These proposals were reviewed by a subset of the science peer reviewers and the results were announced in early December, in good time for the official start of Cycle 8 on 1 Jan 2007.

Statistics on the results of the peer review can be found from the “Statistics” link for a given cycle, linked from the “Target Lists and Schedules” area of our website. We present a subset of these statistics: Figure 42 shows the percentage of proposals accepted in each category; Figures 43, 44 show the percentage of time allocated to each science category and to each instrument combination. To the right is a list of proposals according to their country of origin.

TABLE 3: Proposals by Country

Requested Country	# Proposals	Time	Approved # Proposals	Time
AUSTRALIA	4	659.80		
BELGIUM	2	35.00		
BRAZIL	1	50.00		
CANADA	5	700.00	1	80.00
CHINA	2	132.00		
FINLAND	1	55.50		
FRANCE	4	500.00	3	430.00
GERMANY	17	3097.00	4	202.00
GREECE	2	90.00		
INDIA	1	139.40	1	30.00
ISRAEL	1	150.00		
ITALY	29	4172.00	6	650.00
JAPAN	12	1725.00	3	220.00
NETH	18	3660.00	6	392.00
RUSSIA	3	123.00		
S AFRICA	1	80.00		
SPAIN	9	915.00	2	100.00
SWEDEN	1	130.00		
SWITZ	10	1031.00	4	125.00
TURKEY	1	550.00		
UK	50	7496.70	12	1260.00
USA	551	77355.85	142	13768.00
Total Foreign	174	25491.40	42	3489.00

Oversubscription in Time

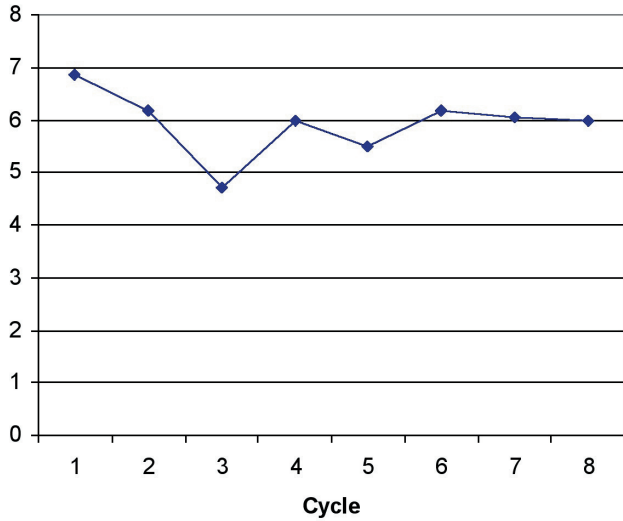


Figure 40: The over-subscription in observing time based on requested and allocated time in each cycle. Again the numbers are remarkably constant.

Time Requested per Cycle

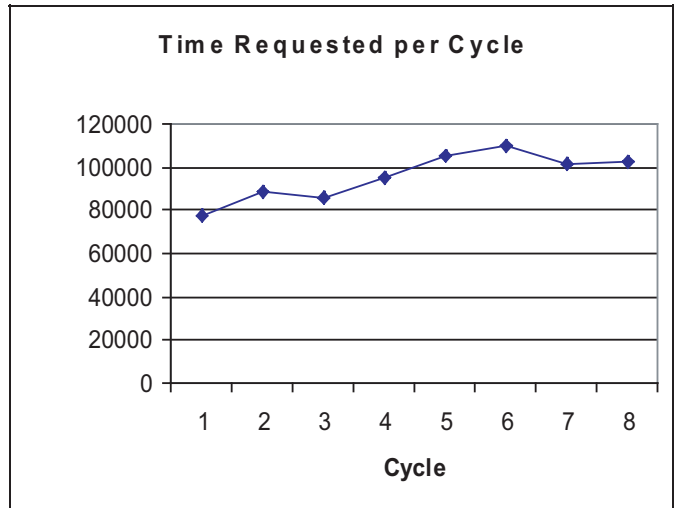


Figure 41: Requested time as a function of cycle in ksecs.. This has slowly increased, the largest effect being the introduction of VLPs in Cycle 5.

(figures continue on next page)

Percent Proposals Accepted

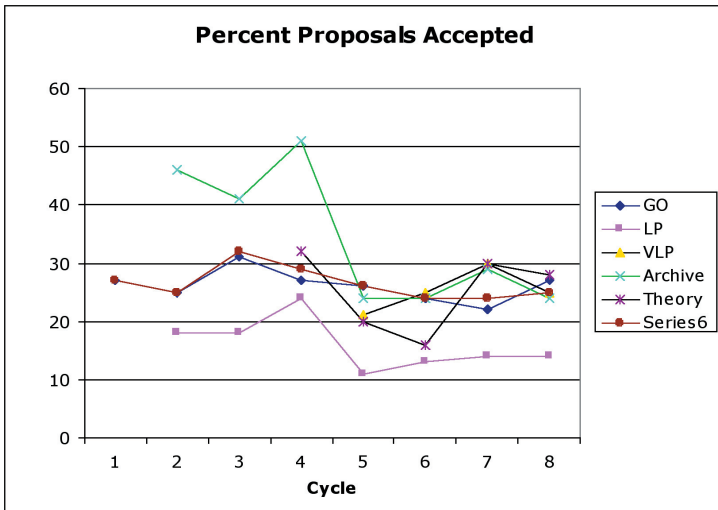


Figure 42: The percentage of proposals accepted, all or in part, for each category as a function of cycle. Please note that some of the fluctuations are due to small number statistics (e.g. Theory proposals).

Chandra-Related Meetings Planned for the Next Year

Keep an eye on the CXC Webpage:
<http://cxc.harvard.edu> for further information

Chandra Users' Committee Meeting
 April 25-26 2007
<http://cxc.harvard.edu/cdo/cuc/index.html>

Workshop: X-ray Grating Spectroscopy:
 Kinematics and Conditions in Hot Gas
 July 11-13, 2007
 Cambridge MA

X-ray Summer School
 August 2007
 Washington, D.C.

Chandra Fellows Symposium
 October 2007
 Cambridge, MA
<http://cxc.harvard.edu/fellows/>

Eight Years of Science with Chandra
 October 23-25, 2007
 Huntsville, AL
http://cxc.harvard.edu/symposium_2007

Chandra Calibration Workshop
 October 25 2007
 Huntsville, AL
<http://cxc.harvard.edu/ccw/>

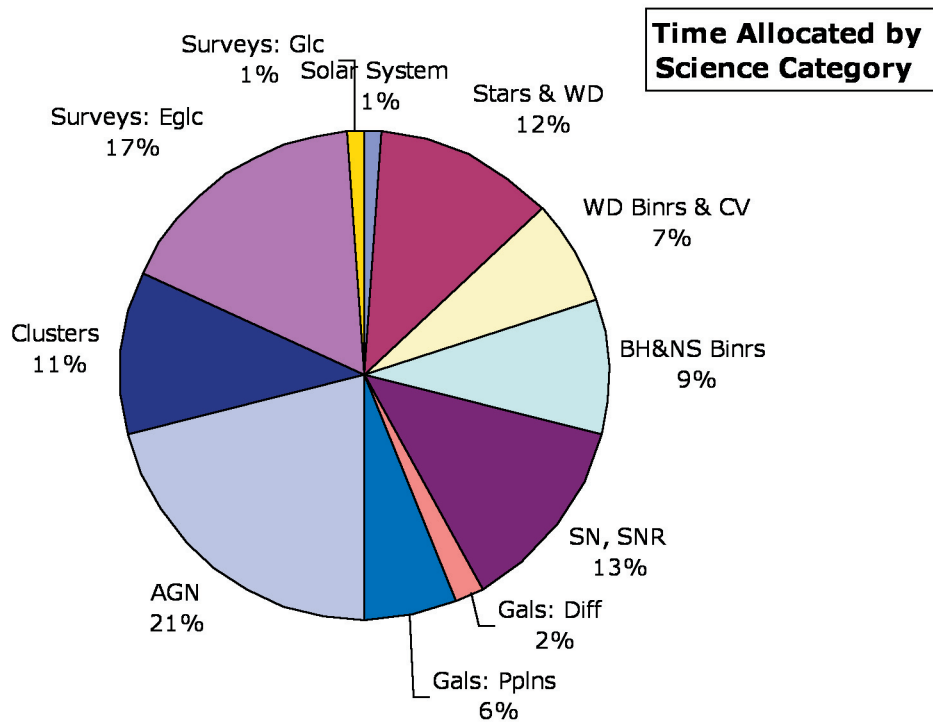


Figure 43: Pie chart indicating the percentage of Chandra time allocated in each science category. But note that the time available for each category is determined by the demand.

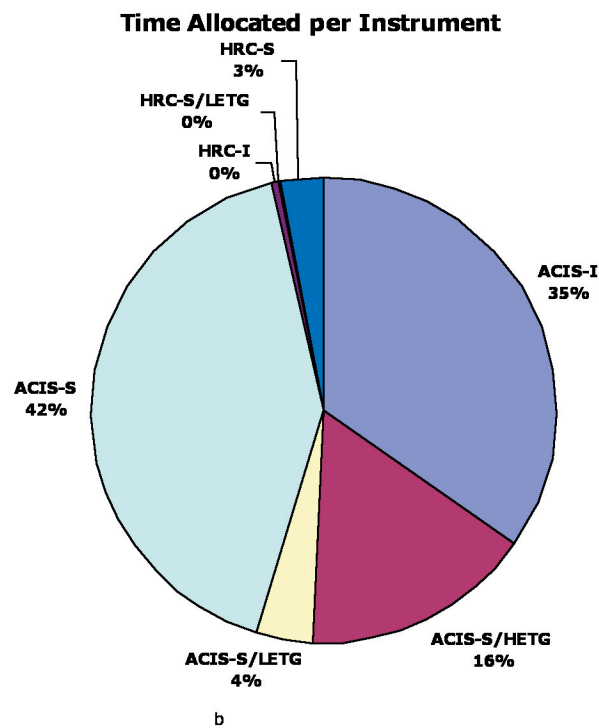


Figure 44: A second pie chart, shows the percentage of Chandra time allocated to observations for each instrument configuration.

Monte-Carlo Processes for Including Chandra Instrument Response Uncertainties in Parameter Estimation Studies

A longer discussion of this topic was published in *Observatory Operations: Strategies, Processes, and Systems.*, David R. Silva and Rodger E. Doxsey, Editors, *Proceedings of SPIE Vol. 6270*, p. 49.

Modern X-ray observatories, such as *Chandra* and XMM-Newton, frequently acquire data for which photon counting statistics are not the dominant source of error. The photon noise is easily assessed and is routinely included in “fitting engine” approaches ubiquitous to analyses of low resolution X-ray spectra. Instrument response uncertainties are instead almost universally ignored.

Such dramatic (over) simplification of the problem is prompted mostly by analytical and computational expedience: uncertainties in the response of a typical X-ray telescope and detector system are not independent and easily incorporated into a typical analy-

sis. They are correlated in complicated ways that are often not easy to specify in precise mathematical terms. Likewise, uncertainties in source models, such as those used to model hot, optically-thin astrophysical plasmas, might be subject to a very complex set of uncertainties involving an extensive assemblage of atomic data, all correlated through the plasma ionization balance, atomic level populations and element abundance. There is no standard set of procedures for incorporating complicated correlated systematic uncertainties in non-linear parameter estimation: the approaches used for treating independent errors simply do not apply. The problem presents a daunting prospect for analytical solution and suggests instead the use of Monte Carlo techniques.

This paper presents a method to treat instrument response uncertainties in a reasonably realistic way and applies this to an investigation of the limiting accuracy of *Chandra*’s ACIS-S instrument for the study of sources characterized by blackbody, powerlaw and optically-thin thermal spectra. The method essentially involves an iterative application of parameter estimation using a slightly modified instrument response at each iteration.

Instrument responses are constructed by perturbing existing calibration quantities – HRMA effective area, or CCD quantum efficiency, for example – within reasonable limits of uncertainty, guided by our current knowledge of the errors of these quantities. Iterative fitting was accomplished using version 12.2.0 the XSPEC program driven by a Perl module to control the Monte Carlo aspects of response perturbations and data I/O.

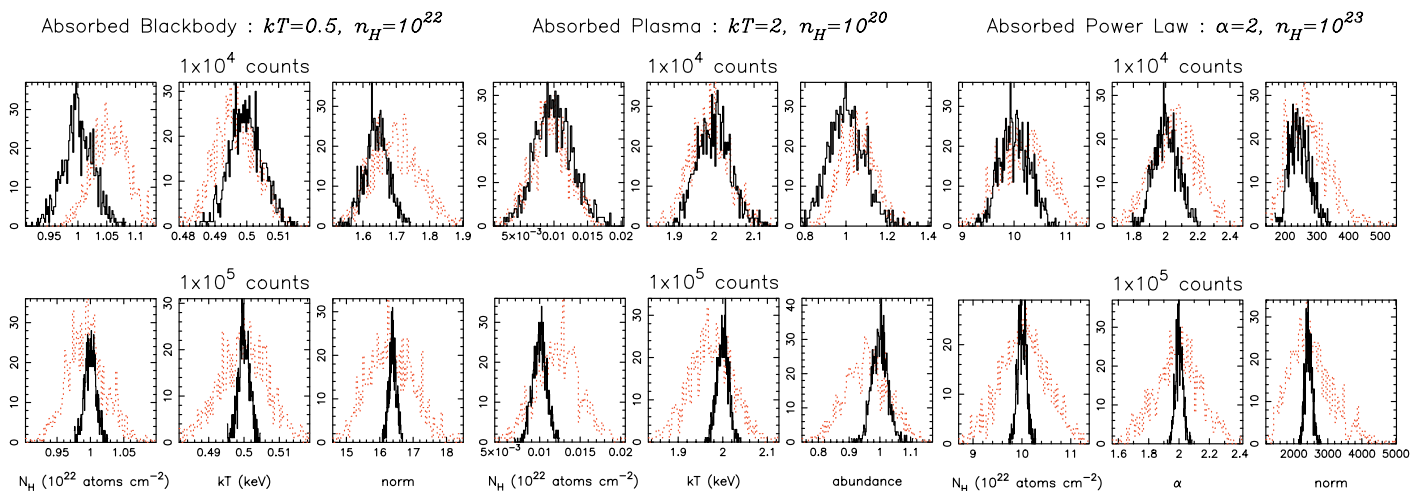


FIGURE 45: Frequency distributions of best-fit parameters obtained for typical blackbody, thermal plasma and powerlaw models from XSPEC for synthetic data sets containing 10^4 (upper panels) and 10^5 (lower panels). Black histograms are distributions resulting from 1000 Monte Carlo samplings of the synthetic data allowing Poisson noise variations alone. Red histograms are the distributions of parameters resulting from fits to a single synthetic data set using 1000 Monte Carlo-generated effective areas and response matrices.

The XSPEC parameter estimation procedure consists of two steps: (i) generation of a synthetic data set using the spectral model of interest and a nominal effective area; (ii) repeated parameter estimation using a different effective area and response matrix each time. The distributions of the model parameters found from step (ii) can then be compared with those resulting from photon noise alone. For consistency, we assess this by examining the distribution of best-fit parameters obtained for a large sample of synthetic data sets identical except for variations due to Poisson noise.

Models investigated were: typical absorbed blackbodies with parameters temperature, neutral H column density nH , and normalization; optically-thin thermal plasmas with solar composition and parameters temperature, metallicity, nH , and normalization; and power laws with parameters slope α , nH , and normalization. The computations were repeated for synthetic ACIS-S3 spectra containing 10^4 and 10^5 counts; the former represents the signal in a typical observation of reasonable quality, while the latter probes the case in which photon noise is negligible. Typical distributions of parameters resulting from calibration uncertainties and Poisson noise are illustrated in Figure 45.

Based on our assessments of the current uncertainties in effective area, gain and pulse height distributions, it appears that the limiting accuracy of *Chandra* is reached in spectra containing about 10^4 counts. This is diagnosed from the similarity between uncertainties due to the instrument response (red distributions) to those due to Poisson noise alone (black). Beyond $\sim 10^4$ counts, errors in best-fit parameters due to calibration uncertainties will dominate those due to photon noise.

Jeremy J. Drake, Peter Ratzlaff, Vinay Kashyap,
Richard Edgar, Rima Izem, Diab Jerius
Aneta Siemiginowska, and Alexey Vikhlinin

Chandra Education and Public Outreach

Two activities of the Education and Public Outreach (EPO) group are discussed here: I. the new EPO proposals selected in Cycle 8 and II. new EPO products.

I. Education and Public Outreach Proposals Selected in Cycle 8

The Cycle 8 *Chandra* EPO Peer Review, conducted by the CXC, was held in Cambridge MA on Dec. 6-8, 2006. A panel representing science, education, museum, Forum, and NASA mission and management perspectives reviewed 13 proposals. Five individual and 8 institutional proposals were submitted. Of the 13 PIs, 10 had not proposed prior to this cycle. Three individual and 6 institutional proposals were selected for funding. An overview of the selected proposals by type follows, alphabetically in order of PI last name.

Individual Proposals

1. Using Simple Ball and Stick Models to Explain Stellar Size Scales and Magnetic Fields in Vocational High Schools

PI: Stanley Owocki/U. Delaware

owocki@bartol.udel.edu

EPO Co-I: Asif ud-Doula

asif@bartol.udel.edu

EPO Partner: New Castle County Vocational Technical School District, DE

The partner school district consists entirely of vocational schools. Students will construct a series of scale models of main sequence stars for use as an aid in the teaching of the relative sizes, luminosities, temperatures, masses and lifetimes of stars as well as the structures of magnetic fields. Students and vocational teachers will be given science explanations necessary to build the models. Science teachers will be given background for use of the models in the classroom. Students and teachers will be informed about the role that *Chandra* X-ray Observations have played in furthering our knowledge about stars. Completed projects will be presented at an Astronomy Night at Mt. Cuba Observatory.

2. Refining the Beyond Einstein Explorers Program

PI: Christopher Reynolds/U.MD

chris@astro.umd.edu

EPO Co-I: Anita Krishnamurthi

anitak@milkyway.gsfc.nasa.gov

EPO Partner: DC Children and Youth Investment Trust Corp.

This project will refine an existing after school astronomy program to serve solely a middle school

audience. The program is designed as an introduction to astronomy and objects in the Universe beyond the solar system. The focus of the refinements will be the sessions on black holes, stellar evolution, and galaxies. These topics were of most interest to past participants but materials were aimed at the high school level. The revised program will be released in the summer of 2007.

3. Stretching the Rainbow: Engaging Prospective and Practicing Educators in Multi-Wavelength Astronomy

PI: Joseph Shields/Ohio U
shields@phy.ohio.edu

EPO Co-I: Mangala Sharma
sharma@ohio.edu

EPO partner: South East Ohio Center for Excellence in Mathematics and Science (SEOCEMS)

This project will provide immersive experiences in multi-wavelength astronomy for pre- and in-service high school teachers in Appalachian Ohio through two workshops and an astronomical observing experience. In the workshops, the educators will learn astronomical concepts, use standards-aligned, inquiry-based NASA education material that can be readily incorporated into their classrooms, design an observing program, and analyze data using student-friendly software. The program will culminate in optical observations with the 1.3-m at MDM, and radio observations on the education telescope at Green Bank. The workshops will emphasize the unique capabilities of NASA's great observatories in studying normal galaxies, black holes, and AGN.

Institutional/Team Proposals

1. *Chandra* Astrophysics Institute

PI: Dr. Frederick Baganoff/MIT Kavli Institute for Astrophysics and Space Research
fkb@space.mit.edu;

EPO Co-I: Dr. Irene Porro
iporro@mit.edu

EPO Partners: John D. O'Bryant School of Mathematics and Science, Boston, MA;
Lynn Public School District, Lynn MA;
Rutgers Astrophysics Institute, Piscataway NJ.

This program will continue and expand the *Chandra* Astrophysics Institute (CAI). The goal of the CAI is to provide an opportunity for students underrep-

resented in STEM to build the background and skills necessary to understand how research science is done, by actually doing it. Students practice these abilities during a 5 week summer session at the MIT Kavli Institute for Astrophysics and Space Science Research (MKI) that emphasizes mastery of the background needed to undertake a range of projects. They then apply these skills during the school year to undertake research projects in X-ray astronomy that are developed with and mentored by the MKI *Chandra* researchers.

2. Penn State's Astronomy Program for In-Service Educators

PI: Professor Niel Brandt/Penn State
niel@astro.psu.edu

EPO Co-I: Dr. Christopher Palma
cpalma@astro.psu.edu

EPO Partners: Pennsylvania Space Grant Consortium, University Park PA; Penn State Center for Science and the Schools, University Park PA

This program will fund tuition and materials for teachers from the targeted audience of rural and urban under served districts to attend week-long summer workshops at Penn State on space science topics. The professional development offerings will expose educators to inquiry-based, peer-reviewed astronomy activities produced by NASA. Workshops are designed to improve the educator's ability to address both national and state science education standards. Participants receive two Penn State graduate credits.

3. The Invisible Universe: Video Conference Field Trips for Grades 6-10

PI: Dr. Edward Brown/Michigan State
ebrown@pa.msu.edu

EPO Co-I: Dr. Megan Donahue
donahue@pa.msu.edu

EPO Partner: Michigan State University Museum, East Lansing MI

This program will develop science content around the theme "The Invisible Universe" primarily for an on-going teleconferencing project distributed to Michigan middle schools, and secondarily for an interactive science site called "Science Buzz". The teleconferencing system (Learning and Developing Distance Education Resources in Sciences - LADDERS) is a currently active mode of outreach to remote Michigan middle schools. This program will develop video con-

tent and activities supporting the theme of light exploration that directly address state and national science education standards. The full program, supported by the MSU Museum, includes local and remote teacher workshops, video production, kit development for in-class use, and the development of specific lesson plans. Additional dissemination will be provided via the Science Buzz site in collaboration with the Science Museum of Minnesota.

4. Kids Question the Cosmos

PI: Professor Deepto Chakrabarty/MIT Kavli Institute for Astrophysics

and Space Research

deepto@space.mit.edu

EPO Co-I: Dr. Irene Porro

iporro@mit.edu

EPO Partners: Citizen Schools, Boston MA; Smithsonian Astrophysical Observatory MicroObservatory program, Cambridge MA; Amateur Telescope Makers of Boston

Kids Question the Cosmos is an astronomy apprenticeship for middle-school students developed for, and in partnership with the Citizen Schools (CS), a leading national initiative in out-of-school time education. CS operates in primarily low-income, minority neighborhoods in communities around Massachusetts, as well as Northern CA, TX, NJ, and NC. It is expected to grow its network to approximately 92 sites in 8-10 states by 2012. Through the CS partnership, this program will contribute to the development of astronomy resources specifically certified for use in after school settings. The intent is to provide the opportunity for quality science learning to youth from underserved communities and from groups traditionally under-represented in STEM. The program will provide an 11-week apprenticeship in astrophotography through the use of the MicroObservatory program. Once the curriculum is certified by CS, it will be disseminated locally in partnership with the Amateur Telescope Makers of Boston, and nationally in collaboration with the CS, Night Sky Network and the Astronomical Society of the Pacific.

5. Black Holes and Galaxy Evolution Museum Component

PI: Dr. Martin Elvis/Smithsonian Astrophysical Observatory

elvis@cfa.harvard.edu

EPO Co-I: Dr. Simon Steel

sjsteel@cfa.harvard.edu

EPO Partners: Science Education Department, CfA, Cambridge, MA;

Association of Science-Technology Centers, Washington D.C.

The Science Education Department at the CfA is creating The Black Hole Experiment Gallery (BHEG), a 2500 sq. ft. national travelling exhibition that will use the demonstrated popularity of black holes to engage visitors in active learning about the frontiers of astronomical discovery and the nature of scientific investigation. This program will augment the BHEG exhibition through the research and development, prototyping, formative evaluation, and production of an interactive, multi-media component, the Black Holes and Galaxy Evolution station. The station will provide interactive visualization and computer-based investigations that visitors can actively explore. The BHEG exhibition will include professional development opportunities for host-site museum staff and is geared to medium-sized museums which typically lack the resources to develop up-to-date exhibitions, or to keep existing ones up to date on current research topics.

6. Development of a Model Teacher/Student Workshop Program for Ohio Middle Schools

PI: Dr. Smita Mathur/Ohio State

smita@astronomy.ohio-state.edu

EPO Co-I: Dr. Donald Terndrup

terndrup@astronomy.ohio-state.edu

EPO Partner: COSI Columbus, Columbus Ohio

This project will develop and test a new model of field trips for middle school students during which the students will participate in inquiry-based lessons on astronomy while their teachers engage in professional development activities that parallel the student content. Content will focus on the fundamental concepts used in teaching and learning about gravity, with reference to *Chandra* science results where appropriate. The content and goals will be tied to Ohio standards for middle-school science education. The program will bring together scientists from Ohio State University and education professionals from COSI Columbus, an internationally known science center. The anticipated direct audience is 2400 students and 120 teachers. Ohio State will provide participating teachers with continuing education credits. The new concept-building material developed for this program will also be disseminated on CD-ROM to other science centers and Ohio school districts with support from COSI.

II. New EPO Products and Resources

We continue to produce *Chandra* podcasts (with video). Eight episodes have been released. These can be downloaded from the *Chandra* public web site at the link on the front page. *Chandra* podcasts have risen to no. 25 on the itunes science→natural sciences list and have also been selected for listing in the special features section. They can also be accessed through YouTube, and the NASA and Smithsonian podcast pages.

We have produced a beta version of a DVD based on the *Chandra* podcasts with additional video content. Two main uses are envisioned. The first is content for museum kiosks and public stations. The second is classroom use where self-contained, short topical episodes about *Chandra* and its science results can be used to initiate discussion. The beta DVD can be requested by e-mail to the EPO group at cxcpub@cfa.harvard.edu. Requestors will later be surveyed to provide input to the final version of this product.

Also linked from the top page of the public web site is a 2007 month-by-month calendar featuring larger scale *Chandra* and composite images. It can be downloaded for printing.

Kathleen Lestition
Education & Outreach Coordinator

Constellation X-ray Mission Update

Over the past year, the *Constellation-X* mission design has gone through several studies which have resulted in a new, streamlined configuration. This new configuration is estimated to save \$500M to \$600M in end-to-end costs over the original 4-satellite configuration. All of the science goals envisioned in the 2000 Decadal Survey and subsequent Con-X science papers (i.e., *Science with Con-X*, May 2005) are fully enabled by this configuration. This new, lower mass configuration is depicted below, and can be launched on a single Atlas-V launcher. The previous single satellite version depicted in the March 2006 newsletter required the more expensive and higher capacity Delta IVH launcher.

We had a very productive and lively Facility Science Team (FST) meeting at GSFC in December, with approximately 100 people attending. The first day of the meeting was dedicated to discussion of the various options to enhance the low and high energy capabilities of Con-X, and the next 2 days covered the science that would be done with a Con-X configuration including these enhancements. One result of this input from the FST was a slight revision in the top level requirements. The field of view of the XMS has been expanded to 5x5 arcmin from the original 2.5x2.5 arcmin, and now the goal is 10x10 arcmin. The energy resolution requirement is now 1250 at 0.3-1.0 keV, up from the baseline of 300. These changes will enhance our ability to study

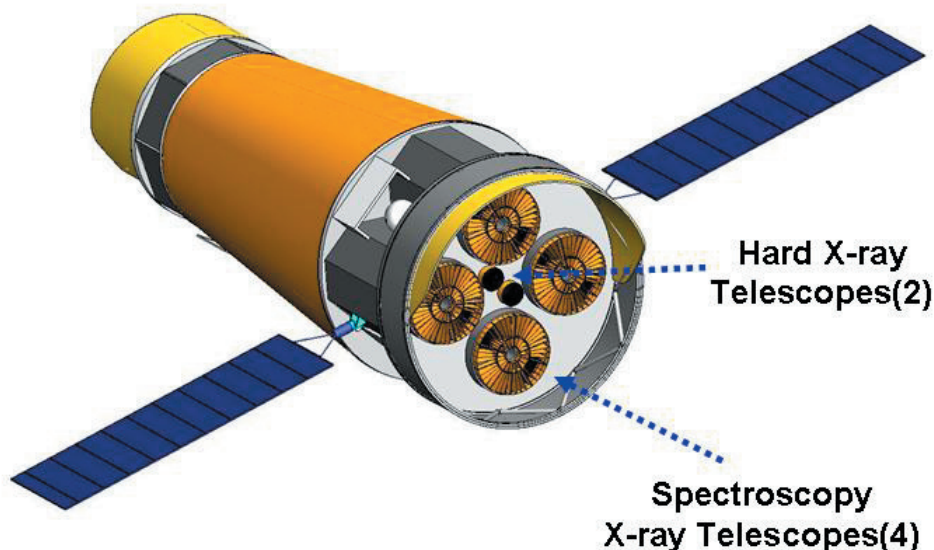


FIGURE 46: The streamlined Con-X configuration which is light enough to be launched on a single Atlas V launch vehicle. The science outlined in the 2000 Decadal Survey and updated in 'Science with Constellation-X' (May 2005) are fully enabled with this configuration.

clusters and the WHIM, respectively.

The *Constellation-X* budget, along with all of Beyond Einstein, took a significant hit this year. Half way through FY06 the budget allocation was cut in half, resulting in significant reductions in the staffing levels at GSFC and many other labs and Universities that have been supporting the project. The project has continued to be funded in FY07 at the same modest level established in FY06. By the time you read this article, the FY08 budget request will have been submitted and we will know the requested levels for Con-X in FY08.

All of the Beyond Einstein missions have devoted substantial effort preparing for a review by the National Academy (National Research Council) requested by NASA and DOE. The charge to the committee is to choose ONE Beyond Einstein mission to go first, utilizing a funding wedge which is planned in FY09. The Beyond Einstein Program Assessment Committee (BEPAC) has met twice in order to receive input from the missions, and plans 2 more meetings. The final report is due Sep 8 2007. In order to collect input from the community at large, the BEPAC is holding a series of Town Hall type meetings. Next meetings are Feb. 12 in Cambridge, March in Baltimore (registration Deadline March 5) and April in Chicago (registration deadline March 26). Details can be found at <http://www7.nationalacademies.org/ssb/BeyondEinsteinPublic.html>.

Michael Garcia, for the Con-X team

Mission Planning under Bill Forman

The Science Mission Planning team at the CXC is responsible for working with *Chandra* observers, instrument specialists, Flight Operations engineers and schedulers, and the Director's Office to carry out the hard-won science observations for *Chandra* users. The process is a delicate balance of observation constraints, spacecraft restrictions, schedule reviews, and process replans in response to Targets of Opportunity or spacecraft anomalies. Deadlines are deadlines; if command loads with science observations are not ready when needed, a truly precious resource — *Chandra* observing time — is at risk.

The road to success for *Chandra* Mission Planning was laid during the preparation of the proposal



FIGURE 47: Bill Forman demonstrates the masterful balance required for *Chandra* Mission Planning.

for what would become the *Chandra* X-ray Center: the plans were put into the hands of Bill Forman. As the Group Leader for the Science Operations Mission Planning team, Bill had his hand in the development of plans for virtually every aspect of the process by which Observer's requests are turned into successful science observations. From co-chairing the AXAF Mission Planning Working Group in the crucial development phase of the mission, to assembling a team of scientists and data aides that has performed at an incredibly high level throughout the operation of *Chandra* (Bill has the unique gift of being able to identify, almost on sight, people who are sharp, dedicated, and somehow require less than half the normal amount of sleep for humans), he has served the CXC and the entire X-ray community well by making the observing process such a success.

At the end of 2006, Bill transitioned from his position on the *Chandra* team to pursue other areas of interest in the High Energy Astrophysics Division at SAO - particularly his research program on Galaxy Groups and Clusters. At that time, I was selected to follow Bill as the new group leader for the Mission Planning team. Having been with the group from the beginning, I look

forward to this new role. I extend my thanks, along with those from our colleagues, for Bill's work in this area. His passion for *Chandra* Mission Planning continues to be evident: he has continued to support meetings for our group, and I interpret this to mean, in part, that he is not yet ready to give up those midnight phone calls about Targets of Opportunity. Accordingly, we have hard-wired his phone number permanently in our TOO alert software...

Pat Slane

HELPDESK

Questions can be sent to the CXC by using the HelpDesk facility. The HelpDesk is reached from a link on the header of the CXC web pages (i.e., at <http://cxc.harvard.edu>). The information entered into the form is passed into our HelpDesk Archive; we can easily track pending items with this tool. An introduction to the HelpDesk system is available from this same link.

Questions can also be sent to the HelpDesk staff using email (cxchelp@cfa.harvard.edu), but we prefer submissions through the web.

Chandra Users' Committee Membership List

The Users' Committee represents the larger astronomical community. If you have concerns about *Chandra*, contact one of the members listed below.

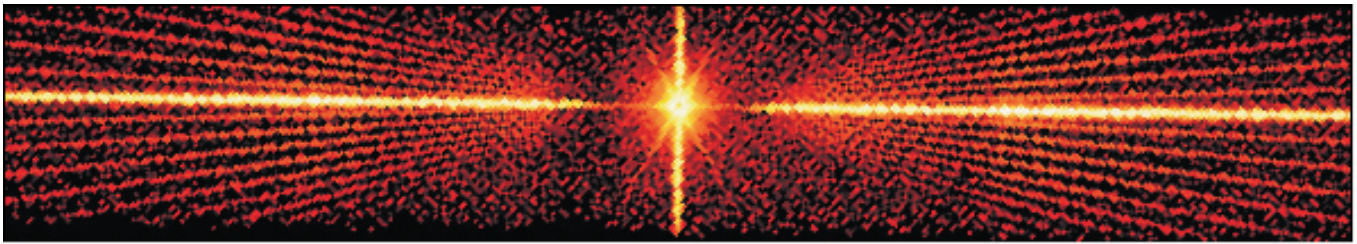
<u>Name</u>	<u>Organization</u>	<u>Email</u>
Mark Dickinson	NOAO	med@noao.edu
Vassiliki Kalogera	Northwestern	vicky@northwestern.edu
Nobuyuki Kawai	Tokyo Tech, Japan	nkawai@phys.titech.ac.jp
Smita Mathur	OSU	smita@astronomy.ohio-state.edu
Chris Mauche	LLNL	mauche@cygnus.llnl.gov
Chris Reynolds (Chair)	University of Maryland	chris@astro.umd.edu
Maria Santos-Lleo	XMM	msantos@xmm.vilspa.esa.es
Lisa Storrie-Lombardi	Spitzer Science Center	lisa@ipac.caltech.edu
Leisa Townsley	PSU	townsley@astro.psu.edu
Randal Smith	GSFC	rsmith@milkyway.gsfc.nasa.gov
Henry Ferguson	STScI	ferguson@stsci.edu

Ex Officio, Non-Voting

Alan Smale	NASA HQ	Alan.P.Smale@hq.nasa.gov
Wilt Sanders	NASA HQ	wsanders@hq.nasa.gov
Allyn Tennant	NASA/MSFC	allyn.tennant@msfc.nasa.gov
Martin Weisskopf	NASA/MSFC	martin@smoker.msfc.nasa.gov

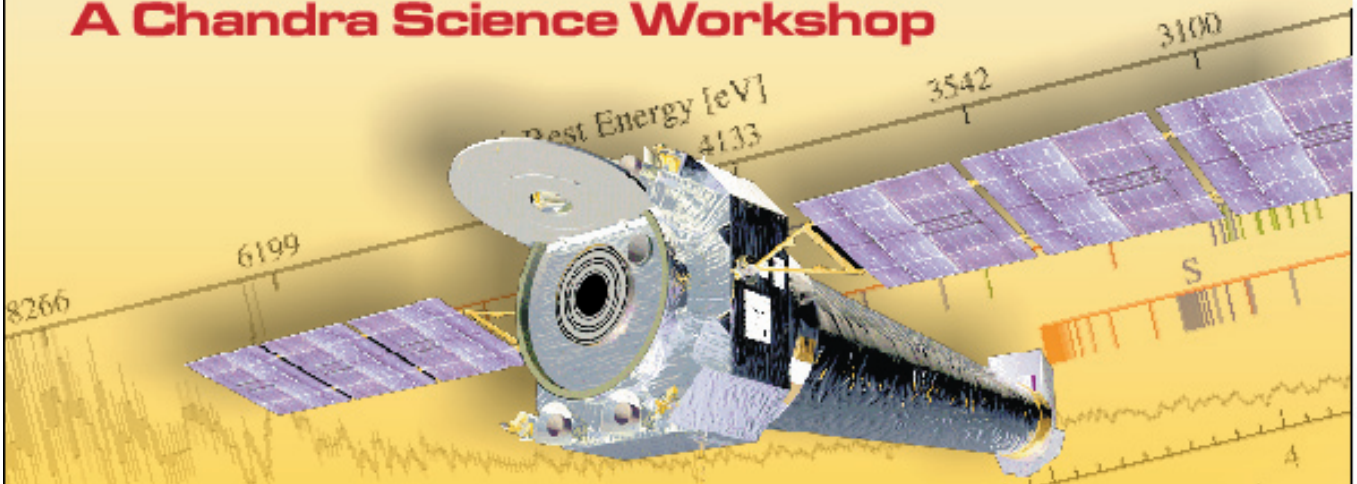
CXC Coordinator

Belinda Wilkes	CXC Director's Office	belinda@head.cfa.harvard.edu
----------------	-----------------------	--



X-ray Grating Spectroscopy: Kinematics and Conditions in Hot Gas

A Chandra Science Workshop



July 11-13, 2007 Cambridge, MA

Workshop Goals:

- ✦ Review progress afforded by X-ray grating spectroscopy of extragalactic and galactic sources
- ✦ Compare/contrast physical conditions in X-ray emitters/absorbers
- ✦ Review and compare available atomic data and codes
- ✦ Provide a forum for discussion of:
 - Controversial or unexpected new results
 - Potential new strategies for Chandra/XMM grating observations
 - The future of X-ray spectroscopy

Scientific Organizing Committee:
Chair - Jane Turner (GSFC)
Vice Chair - Nancy Brickhouse (SAO)

Local Organizing Committee:
Chair - Paul Green

Contact: xgratings07@cfa.harvard.edu

<http://cxc.harvard.edu/xgratings07>

Mz 3, BD+30°3639, Hen 3-1475, and NGC 7027: Planetary Nebulas - Fast Winds from Dying Stars

This article is taken from the Chandra Public Photo Album. The figure in discussion is Figure 48 on the next page. Text and images can be found here: <http://chandra.harvard.edu/photo/2006/pne/>. See also the discussion of BD+30°3639 in the LETG article.

Planetary nebulas - so called because some of them resemble a planet when viewed through a small telescope - are produced in the late stages of a sun-like star's life. After several billion years of stable existence (the sun is 4.5 billion years old and will not enter this phase for about 5 billion more years) a normal star will expand enormously to become a bloated red giant. Over a period of a few hundred thousand years, much of the star's mass is expelled at a relatively slow speed of about 50,000 miles per hour.

This mass loss creates a more or less spherical cloud around the star and eventually uncovers the star's blazing hot core. Intense ultraviolet radiation from the core heats the circumstellar gas to ten thousand degrees,

-Editor

and the velocity of the gas flowing away from the star jumps to about a million miles per hour.

This high speed wind appears to be concentrated into opposing supersonic funnels, and produces the elongated shapes in the early development of planetary nebulas (BD+30°3639 appears spherical, but other observations indicate that it is viewed along the pole.) Shock waves generated by the collision of the high-speed gas with the surrounding cloud create the hot bubbles observed by *Chandra*. The origin of the funnel-shaped winds is not understood. It may be related to strong, twisted magnetic fields near the hot stellar core.

CXC Contact Personnel

Director:	Harvey Tananbaum	Calibration:	Christine Jones
Associate Director:	Claude Canizares	Development and Operations:	Dan Schwartz
Manager:	Roger Brissenden	Mission Planning:	Bill Forman
Systems Engineering:	Jeff Holmes	Science Data Systems: Deputy:	Jonathan McDowell Mike Nowak
Data Systems:	Pepi Fabbiano	Director's Office:	Belinda Wilkes
Education & Outreach:	Kathy Lestition	Media Relations:	Megan Watzke

Note: E-mail address is usually of the form: <first-initial-lastname>@cfa.harvard.edu
(addresses you may already know for nodes head.cfa.harvard.edu or cfa.harvard.edu should work also)

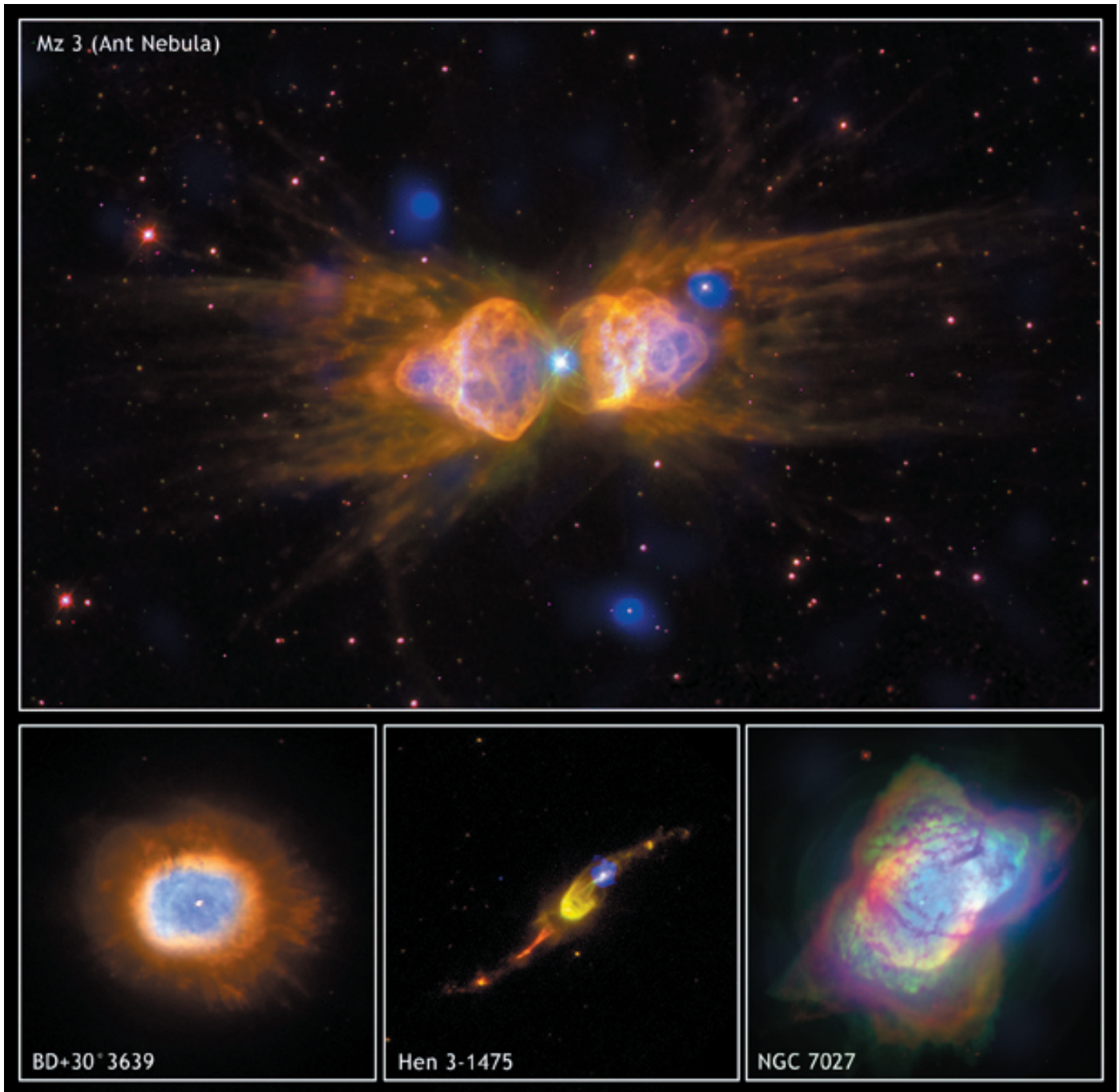


FIGURE 48: This panel of composite images shows part of the unfolding drama of the last stages of the evolution of sun-like stars. Dynamic elongated clouds envelop bubbles of multimillion degree gas produced by high-velocity winds from dying stars. In these images, Chandra's X-ray data are shown in blue, while green and red are optical and infrared data from Hubble. (See article on page 55)

Credit: X-ray: NASA/CXC/RIT/J.Kastner et al.; Optical/IR: BD +30 & Hen 3: NASA/STScI/Univ. MD/J.P.Harrington; NGC 7027: NASA/STScI/Caltech/J.Westphal & W.Latter; Mz 3: NASA/STScI/Univ. Washington/B.Balick

The Chandra Newsletter appears approximately once a year. We welcome contributions from readers. Nancy Remage Evans edits "Chandra News", with editorial assistance and layout by Tara Gokas. Comments on the newsletter and corrections and additions to the hardcopy mailing list should be sent to: chandranews@cxc.harvard.edu